University College London

PHASM201 Project

Department of Physics and Astronomy

Entropy Production in Small Systems

A Study of the Jarzynski Equality

Author:
Robert Eyre

Supervisor:
Professor Ian Ford

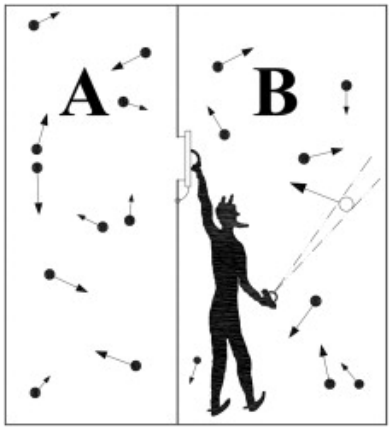

October 2012 - March 2013

Abstract

Within this investigation we have considered the Jarzynski equality and its generalisations to both systems with feedback control and to non-isothermal systems. To explore and confirm all results, we have modelled the system of a single classical particle, in one dimension trapped in a harmonic potential and in thermal contact with an overdamped langevin heat bath, undergoing a cyclic work process of a step up and step down in spring constant. For feedback control systems, we considered the maximisation of the efficacy parameter within the Sagawa-Ueda generalisation of the Jarzynski equality, where the feedback for our system involves either changing or not changing the spring constant of the potential dependent on what the position of the particle is at the start of the process. We have found that changing the spring constant for a longer amount of time allows for a greater value in the efficacy parameter. Also, we have confirmed the expected result that the greater the error in the measurement that the feedback is based on, the lower the efficacy parameter becomes. Lastly for this generalisation, we considered the characteristics of the optimal value in spring constant to change to: specifically, an increase for position close to the centre of the potential, a decrease when far from the centre, and remaining the same otherwise. Numerical results from modelling these characteristics indeed show an increase in the value of the efficacy parameter. Finally, we have shown that, for the same cyclic step process, the Jarzynski equality takes on a different generalisation in terms of Tsallis q-exponentials when considering non-isothermal systems. Numerical results confirm this new equality. We have also examined the Tsallis distributions that arise in the process for non-isothermal systems, and shown how the Crooks work relation can also be generalised in this case when considering a simple single step process. Numerical modelling implies a correlation to the theoretical prediction in this case, but further numerical confirmation is required.

Acknowledgements

First and foremost, thanks must go to my supervisor Ian Ford for allowing me to be involved in his research and supplying me with an interesting and involving project that has allowed me to learn a great deal about not just areas of statistical physics I have not been exposed to before but also about the methods of scientific research itself. Thanks must also go to Janet Anders for agreeing to be my second supervisor, and, alongside Professor Ford, for correcting various misconceptions and gaps in my knowledge that I possessed. Further thanks must go to Andrew Gormanly for allowing me access to a department machine so that I could run the code quicker, and for being very helpful in fixing various problems I had with the machine. Last but not least, thanks goes to my wife May for listening tirelessly to me as I talked about this project to her for six months straight.

Contents

Figure on title page taken from figure 3 of [1].

Chapter 1

Introduction

The laws of Physics and their consequences are often frought with controversies. Certainly one of the oldest of these is the second law of thermodynamics and the irreversible nature of processes that arises as a consequence of it. The second law stated in its most general and applicable form is that there exists an extensive quantity called entropy, which we shall label S, that never decreases for any process [2]. Mathematically, this can be stated as

$$\Delta S \geq 0 \tag{1.1}$$

where the equality only occurs for reversible (i.e. quasistatic) processes.

The second law is considered by many to be the strongest of the physical laws. Many quotations can be found to echo that of Eddington, who stated "The law that entropy always increases ... holds, I think, the supreme position among the laws of Nature." (from P74 of [3]). However, this often prevalent opinion has not prevented the creation of many challenges to the second law. One such challenge, principally directed at Boltzmann's H-theorem, is Loschmidt's paradox [4] [5]. This paradox is concerned with the existence of irreversibility, which results from the second law as any process tracing a path through phase space that involves an increase in entropy, cannot be time-reversed to follow that path back as it would involve a decrease in entropy. The paradox essentially states that it does not make sense for irreversible behaviour to arise from microscopic dynamics that are deterministic and therefore must be reversible. The laws of deterministic dynamics are, after all, symmetric in time.

Boltzmann himself, as well as others, formulated arguments defending the second law against this paradox. However, in the last few decades, relations acting as statements of the second law have emerged that reconcile the second law with the contents of this paradox. These are the fluctuation theorems. In their most general form, the fluctuation theorems act as expressions detailing the likelihood of observing time-reversed trajectories in phase space which therefore violate the second law [6]. The nature of their derivations brings reconciliation with Loschmidt's paradox, and their forms as analytical expressions shine new light on the second law itself. They also serve an immense practical purpose, as they are some of the few relations which are valid arbitrarily far from equilibrium.

One particular fluctuation theorem of great importance is the Jarzynski equality. This equality acts as a strict statistical statement of the second law for work processes. Not only does it allow for greater exploration of the nature of entropy production for small systems undergoing these processes, but it also serves immense practical purpose due to the type of process it concerns. The purpose of this report and the investigation it details is to consider the Jarzynski equality, and to explore theoretical generalisations of this equality in various different circumstances, comparing all results against numerical modelling.

The second section of this report will introduce the fluctuation theorems by considering a formal derivation, before deriving the Jarzynski equality itself. We will then proceed to define the system upon which all our considerations and modelling takes place, which is that of a classical particle trapped in a harmonic potential and in thermal contact with a langevin heat bath. Lastly, for this section we will then show how the Jarzynski equality with respect to this system can be modelled, and compare the results of such modelling to the theoretical prediction.

In the third section of this report, we will consider another challenge to the second law: the famous Maxwell's demon [7] [8]. A pictoral representation of the demon is present on the title page for this report. In essence, Maxwell's demon states that by introducing an intelligence to the system, the demon, that is aware of what is happening in the system and makes changes to the system based in this awareness, we can decrease the entropy of the system. The solution to this problem has been found, and Maxwell's demon manages to strengthen the second law. However, it is still a worthy subject to consider, as it

will be shown that, through the application of Maxwell's demon through feedback control, the Jarzynski equality takes on a generalised form involving a constant known as the efficacy parameter which allows us to explore the relations between information from the demon's measurements on the system and the free energy within the system. Thus, section three is concerned with exploring this form further and comparing all theoretical results against those of numerical modelling. We build on work already completed to explore the effect that specific changes in the system, errors in the measurements, and changing the time for which changes are applied have on the efficacy parameter. By doing so, we lay a theoretical and numerical grounding for experimental work into these kinds of systems, allowing for greater efficiency in the application of feedback control by maximising the efficacy parameter.

Finally, in section four we will show that, when considering non-isothermal systems, we can derive a new generalisation in a form involving very different statistics to the traditional Maxwell-Boltzmann distributions. As with all other cases, we will also look into numerical work in an effort to confirm the new relation. Then we finish by exploring further the unusual statistics of the system and how they apply to another fluctuation theorem related to the Jarzynski equality: the Crooks work relation.

Chapter 2

The Jarzynski Equality

2.1 The Fluctuation Theorems

To give a better understanding of the fluctuation theorems it is informative to consider the derivation of one of the most general of them. What follows will be a slightly simplified version of the derivation found in [9]. Alternate versions of this same style of derivation, alternate styles of derivations entirely, and derivations of other less general fluctuation theorems can be found in [9], [6], [10], [11], and [12].

We consider a path $X(t)$ through phase space, under a protocol $\lambda(t)$ defining the process occuring between times $t = 0$ and $t = \tau$. We define a time reversal operator $\hat{T}$. For instance, for position x, momentum p, and protocol λ, we would have operations $\hat{T}x = x$, $\hat{T}p = -p$, and $\hat{T}\lambda = \lambda$. For our path and protocol, we then define the time reversal quantities as

$$\bar{X}(t) = \hat{T}X(\tau - t) \tag{2.1}$$
$$\bar{\lambda}(t) = \lambda(\tau - t) \tag{2.2}$$

where we indicate the time reversal values with a bar, and note that time reversal does not change the form of the protocol.

We can define a measure of the irreversibility $I[X]$ of the path as

$$I[X] = \ln\left[\frac{P^F[X]}{P^R[\bar{X}]}\right] \tag{2.3}$$

where $P^F[\ldots]$ is the probability dependent on the forward protocol, and $P^R[\ldots]$ is the probability dependent on the reverse protocol. We can see from the form of the irreversibility that it becomes increasingly positive as the forward trajectory becomes more likely, increasingly negative as the reverse trajectory becomes more likely, and equals zero when both are equally likely.

Defining the probability of being at the start of the path $X(0)$ as $P_{\text{start}}[X(0)]$ and the probability of the path given the starting point $X(0)$ as $P^F[X(\tau)|X(0)]$, we can write

$$P^F[X] = P_{\text{start}}[X(0)]P^F[X(\tau)|X(0)]. \tag{2.4}$$

We can consider the process as a Markovian process, such that at any given point in time the process has no dependency on the history of what has happened up to that point, exhibiting stochastic behaviour [13] [14]. We can then approximate it as a series of jump processes occuring over discrete time jumps, and apply the Markov property to get

$$P^F[X] = P_{\text{start}}[X_0]P[X_1|X_0, \lambda(t_1)] \times \ldots \times P[X_n|X_{n-1}, \lambda(t_n)] \tag{2.5}$$

where $t_0 = 0$, $t_n = \tau$, and therefore $X_0 = X(0)$ and $X_n = X(\tau)$.

Defining $P_{\text{end}}[\bar{X}(0)]$ as the probability of being at the end of the path, and applying the same logic gives

$$\begin{aligned} P^R[\bar{X}] &= \hat{T}P_{\text{end}}[\bar{X}(0)]P^R[\bar{X}(\tau)|\bar{X}(0)] \\ &= P^R_{\text{start}}[\bar{X}(0)]P^R[\bar{X}(\tau)|\bar{X}(0)] \\ &= P^R_{\text{start}}[\bar{X}_0]P[\bar{X}_1|\bar{X}_0, \bar{\lambda}(t_1)] \times \ldots \times P[\bar{X}_n|\bar{X}_{n-1}, \bar{\lambda}(t_n)]. \end{aligned} \tag{2.6}$$

According to (2.1) and (2.2), this is

$$\begin{aligned} P^R[\bar{X}] &= P^R_{\text{start}}[\hat{T}X_n]P[\hat{T}X_{n-1}|\hat{T}X_n,\lambda(t_n)]\times\ldots\times P[\hat{T}X_0|\hat{T}X_1,\lambda(t_1)] \\ &= P_{\text{end}}[X_n]P[\hat{T}X_{n-1}|\hat{T}X_n,\lambda(t_n)]\times\ldots\times P[\hat{T}X_0|\hat{T}X_1,\lambda(t_1)] \end{aligned} \tag{2.7}$$

where we have used $P^R_{\text{start}}[\hat{T}X_n] = \hat{T}P_{\text{end}}[\hat{T}X_n] = P_{\text{end}}[X_n]$.

We now see that

$$\begin{aligned} \ln\left[\frac{P^F[X]}{P^R[\bar{X}]}\right] &= \ln\left[\frac{P_{\text{start}}[X(0)]}{P_{\text{end}}[X(\tau)]}\right] + \ln\left[\frac{P^F[X(\tau)|X(0)]}{P^R[\hat{T}X(0)|\hat{T}X(\tau)]}\right] \\ &= \ln\left[\frac{P_{\text{start}}[X_0]}{P_{\text{end}}[X_n]}\prod_{i=1}^{n}\frac{P[X_i|X_{i-1},\lambda(t_i)]}{P[\hat{T}X_{i-1}|\hat{T}X_i,\lambda(t_i)]}\right]. \end{aligned} \tag{2.8}$$

To gain an understanding of the physical meaning of $I[X]$, we can consider a certain model. Namely, the Ornstein-Uhlenbeck process described by the langevin equation [13] [14]

$$\dot{v} = -\gamma v + \beta\xi(t) \tag{2.9}$$

where the process describes a particle with velocity v subject to a deterministic dissipative friction term with coefficient γ and a random fluctuative noise term with coefficient β. The noise is characterised as an idealistic gaussian white noise with

$$\langle\xi(t)\rangle = 0 \tag{2.10}$$

$$\langle\xi(t)\xi(t')\rangle = \delta(t-t') \tag{2.11}$$

where $\langle\ldots\rangle$ is the expectation value, $\delta(t-t')$ is the Euler delta distribution, and (2.11) means that the noise has no autocorrelation in time.

According to the fluctuation-dissipation relation, $\beta^2 = 2k_BT\gamma/m$, where T is the temperature of the langevin heat bath, m is the mass of the particle, and k_B is Boltzmann's constant. This relation results from comparing the stationary state probability distributions of the process to the Maxwell-Boltzmann velocity distribution. We therefore have

$$\dot{v} = -\gamma v + \left(\frac{2k_BT(t)\gamma}{m}\right)^{1/2}\xi(t) \tag{2.12}$$

where we are allowing the temperature to vary with time.

The evolution in time of the probability densities $p(v,t)$ for the process are given by the Fokker-Planck equation, which for this process is

$$\frac{\partial p(v,t)}{\partial t} = \frac{\partial(\gamma v p(v,t))}{\partial v} + \frac{k_BT(t)\gamma}{m}\frac{\partial^2 p(v,t)}{\partial v^2} \tag{2.13}$$

which, for some initial condition $v = \delta(v-v_0)$ at initial time t_0, has time-dependent solution given by the Ornstein-Uhlenbeck transition probability density

$$p^T_{OU}(v,t|v_0,t_0) = \sqrt{\frac{m}{2\pi k_BT(t)\left(1-e^{-2\gamma(t-t_0)}\right)}}\exp\left(-\frac{m\left(v-v_0e^{-\gamma(t-t_0)}\right)^2}{2k_BT(t)\left(1-e^{-2\gamma(t-t_0)}\right)}\right). \tag{2.14}$$

(2.14) corresponds to the probability of an Ornstein-Uhlenbeck process ending at value v at time t occuring given it started at v_0 at time t_0. Note that, without any loss of generality, we may substitute probability densities and their associated infinitessimal volumes into (2.8) and cancel the infinitessimal volumes to give $I[X]$ for continuous stochastic behaviour.

We now need to consider this system with given forward and reverse processes dictated by the protocol. To do this, we consider that the temperature varies with the protocol, and that the protocol is simply a step change such that

$$T(\lambda(t_i)) = T_j \qquad t_i \in [(j-i)\Delta t, j\Delta t] \tag{2.15}$$

for integer j where $1 \leq j \leq N$ with $N\Delta t = \tau$. The path is then a combination of Ornstein-Uhlenbeck processes characterised by (2.14), and we can consider the continuous langevin behaviour at fixed temperature to be the limit $dt = (t_{i+1} - t_i) \to 0$ of the discrete jump process, so that the path probability over one such step change is

$$\begin{aligned} &\lim_{dt\to 0} \prod_{t_i=(j-1)\Delta t}^{t_i=j\Delta t} P[v_i|v_{i-1}, \lambda(t_i)] = p_{OU}^T\left(v(j\Delta t)|v((j-1)\Delta t)\right)\, dv(j\Delta t) = \\ &\left(\frac{m}{2\pi k_B T_j\left(1-e^{-2\gamma\Delta t}\right)}\right)^{1/2} \exp\left(-\frac{m\left(v(j\Delta t) - v((j-1)\Delta t)e^{-\gamma\Delta t}\right)^2}{2k_B T_j\left(1-e^{-2\gamma\Delta t}\right)}\right) dv(j\Delta t). \end{aligned} \tag{2.16}$$

Applying the Markov property, the total path probability density over N step changes is then

$$\begin{aligned} &p^F(v(\tau)|v(0)) = \\ &\prod_{j=1}^{N}\left(\frac{m}{2\pi k_B T_j\left(1-e^{-2\gamma\Delta t}\right)}\right)^{1/2} \exp\left(-\frac{m\left(v(j\Delta t) - v((j-1)\Delta t)e^{-\gamma\Delta t}\right)^2}{2k_B T_j\left(1-e^{-2\gamma\Delta t}\right)}\right). \end{aligned} \tag{2.17}$$

For the reverse process, note that $\hat{T}v = -v$, so that

$$\begin{aligned} &p^R(-v(0)|-v(\tau)) = \\ &\prod_{j=1}^{N}\left(\frac{m}{2\pi k_B T_j\left(1-e^{-2\gamma\Delta t}\right)}\right)^{1/2} \exp\left(-\frac{m\left(-v((j-1)\Delta t) + v(j\Delta t)e^{-\gamma\Delta t}\right)^2}{2k_B T_j\left(1-e^{-2\gamma\Delta t}\right)}\right). \end{aligned} \tag{2.18}$$

If we write $v(j\Delta t) = v_j$, and take the logarithm of the ratio of these probability densities, we see the second term of (2.8) becomes

$$\ln\left[\frac{p^F(v(\tau)|v(0))}{p^R(-v(0)|-v(\tau))}\right] = -\sum_{j=1}^{N}\frac{m}{2k_B T_j}\left(v_j^2 - v_{j-1}^2\right). \tag{2.19}$$

This is equal to the sum of negative changes of the kinetic energy of the particle, i.e. a negative flow of heat $-\Delta Q$, scaled by k_B and the environment temperature. As our system is a closed system composed of a particle and an environment, there must therefore be an associated heat flow ΔQ_{med} into the environment such that $\Delta Q_{\text{med}} = -\Delta Q$. The Langevin equation describes the idealisation of a particle subject to a large equilibrium Langevin heat bath, so that $\Delta Q_{\text{med}} = T\Delta S$, where ΔS is the entropy change of the bath. In this case, N step changes in temperature can be seen as equivalent to letting the particle come in to thermal contact with N different equilibrium heat baths, each with entropy change ΔS_j. Therefore

$$\begin{aligned} k_B \ln\left[\frac{p^F(v(\tau)|v(0))}{p^R(-v(0)|-v(\tau))}\right] &= \sum_j \frac{\Delta Q_{med,j}}{T_j} \\ &= \sum_j \Delta S_j \\ &= \Delta S_{\text{med}} \end{aligned} \tag{2.20}$$

where ΔS_{med} is the total change in entropy for the environment, or medium.

Writing the first part of (2.8) in terms of the probability density solutions to (2.13), we find

$$\begin{aligned} \ln\left[\frac{P_{\text{start}}[v(0)]}{P_{\text{end}}[v(\tau)]}\right] &= \ln\left[\frac{p(v,0)}{p(v,\tau)}\right] \\ &= -\left(\ln p(v,\tau) - \ln p(v,0)\right). \end{aligned} \tag{2.21}$$

Defining the mean entropy S_{sys} of the particle, or system, as a time dependent Gibbs entropy

$$\begin{aligned} \langle S_{\text{sys}}\rangle &= \int S_{\text{sys}} p(v,t)\, dv \\ &= S_{\text{Gibbs}} \\ &= -k_B \int p(v,t)\ln p(v,t)\, dv \end{aligned} \tag{2.22}$$

we see that $S_{\text{sys}} = -k_B \ln p(v,t)$ so that

$$k_B \ln \left[\frac{P_{\text{start}}[v(0)]}{P_{\text{end}}[v(\tau)]} \right] = \Delta S_{\text{sys}}. \tag{2.23}$$

Substituting all our relevant expressions into (2.8) gives $k_B I[X] = \Delta S_{\text{sys}} + \Delta S_{\text{med}}$. However, as our system is a closed system composed of just the system and the environment, this is

$$\Delta S_{\text{tot}}[X] = k_B I[X] \tag{2.24}$$

so we see that the irreversibility has physical meaning in being related to the change in total entropy S_{tot} over the process. Also, note how the change in entropy is dependent on the path and can therefore be both positive and negative, a fact that we will come back to later.

Further arguments can also be used to show that $k_B I[X]$ is indeed the total entropy production, and that this relation is a general result within stochastic thermodynamics. The reader is referred to [9] for these arguments.

Returning to the case of a general path X, from (2.24) we see

$$\Delta S_{\text{tot}}[X] = k_B \ln \left[\frac{p_{\text{start}}(X(0)) p^F(X(\tau)|X(0))}{p^R_{\text{start}}(\bar{X}(0)) p^R(\bar{X}(\tau)|\bar{X}(0))} \right]. \tag{2.25}$$

We can construct the probability distribution of entropy production over the forward process as

$$p^F(\Delta S_{\text{tot}}[X] = A) = \int dX \, p_{\text{start}}(X(0)) p^F(X(\tau)|X(0)) \delta(A - \Delta S_{\text{tot}}[X]). \tag{2.26}$$

We can define a new functional

$$R[X] = k_B \ln \left[\frac{p^R_{\text{start}}(X(0)) p^R(X(\tau)|X(0))}{p_{\text{start}}(\bar{X}(0)) p^F(\bar{X}(\tau)|\bar{X}(0))} \right] \tag{2.27}$$

which evaluated over the reverse path is

$$\begin{aligned} R[\bar{X}] &= k_B \ln \left[\frac{p^R_{\text{start}}(\bar{X}(0)) p^R(\bar{X}(\tau)|\bar{X}(0))}{p_{\text{start}}(X(0)) p^F(X(\tau)|X(0))} \right] \\ &= -\Delta S_{\text{tot}}[X]. \end{aligned} \tag{2.28}$$

We can also construct a probability distribution for this over the reverse process

$$p^R(R[\bar{X}] = A) = \int d\bar{X} \, p^R_{\text{start}}(\bar{X}(0)) p^R(\bar{X}(\tau)|\bar{X}(0)) \delta(A - R[\bar{X}]). \tag{2.29}$$

Therefore

$$p^R(R[\bar{X}] = -A) = \int d\bar{X} \, p^R_{\text{start}}(\bar{X}(0)) p^R(\bar{X}(\tau)|\bar{X}(0)) \delta(A + R[\bar{X}]). \tag{2.30}$$

We now note that $dX = d\bar{X}$ as the Jacobian is unity so the path integrals are equivalent, that (2.25) gives the substitution

$$p^R_{\text{start}}(\bar{X}(0)) p^R(\bar{X}(\tau)|\bar{X}(0)) = p_{\text{start}}(X(0)) p^F(X(\tau)|X(0)) e^{-\Delta S_{\text{tot}}[X]/k_B}, \tag{2.31}$$

and that $R[\bar{X}] = -\Delta S_{\text{tot}}[X]$, so that we have

$$\begin{aligned} p^R(R[\bar{X}] = -A) &= \int dX \, p_{\text{start}}(X(0)) p^F(X(\tau)|X(0)) e^{-\Delta S_{\text{tot}}[X]/k_B} \delta(A - \Delta S_{\text{tot}}[X]) \\ &= e^{-A/k_B} \int dX \, p_{\text{start}}(X(0)) p^F(X(\tau)|X(0)) \delta(A - \Delta S_{\text{tot}}[X]) \\ &= e^{-A/k_B} p^F(\Delta S\text{tot}[X] = A). \end{aligned} \tag{2.32}$$

This gives the Transient Fluctuation Theorem

$$\frac{p^F(\Delta S_{\text{tot}}[X] = A)}{p^R(R[\bar{X}] = -A)} = e^{\frac{A}{k_B}} \tag{2.33}$$

which is fundamental and holds for all protocols and initial conditions. This is our most general fluctuation theorem, but is abstract enough to prevent us from seeing the physical implications of the fluctuation theorems, which is the purpose of this section.

To gain a physical interpretation, we can define an entropy production functional $\Delta S^R_{\text{tot}}[\bar{X}]$ for the reverse process by comparing the probability for a path under protocol $\bar{\lambda}(t)$ starting from an initial distribution $p^R_{\text{start}}(\dots)$ which evolves to a final distribution $p^R_{\text{end}}(\dots)$ to the probability of a path starting from $\hat{T}p^R_{\text{end}}(\dots)$, which gives

$$\Delta S^R_{\text{tot}}[\bar{X}] = k_B \ln \left[\frac{p^R_{\text{start}}(\bar{X}(0))p^R(\bar{X}(\tau)|\bar{X}(0))}{\hat{T}p^R_{\text{end}}(X(0))p^F(X(\tau)|X(0))} \right]. \tag{2.34}$$

If we meet the non-general condition $p_{\text{start}}(X(0)) = \hat{T}p^R_{\text{end}}(X(0))$, then $R[\bar{X}] = \Delta S^R_{\text{tot}}[\bar{X}]$, and our fluctuation theorem becomes

$$\frac{p^F(\Delta S_{\text{tot}}[X] = A)}{p^R(\Delta S^R_{\text{tot}}[\bar{X}] = -A)} = e^{\frac{A}{k_B}}. \tag{2.35}$$

Assuming the arguments of $p^R(\dots)$ implicitly describe the quantity over the reverse process, this becomes

$$\frac{p^F(\Delta S_{\text{tot}})}{p^R(-\Delta S_{\text{tot}})} = e^{\frac{\Delta S_{\text{tot}}}{k_B}} \tag{2.36}$$

which holds when the evolution under the forward process followed by the reverse process brings the system back into the same intitial distribution.

This final result is not the most general fluctuation theorem, but it allows us to gain some physical perspective about them. We can see that the essential meaning is that we are exponentially more likely to observe a forward entropy producing trajectory through phase space than we are to observe the time reversal of that path. If we integrate over all values of A in (2.33), we get the Integral Fluctuation Theorem

$$\left\langle e^{-\frac{\Delta S_{\text{tot}}}{k_B}} \right\rangle = 1. \tag{2.37}$$

Using Jensen's inequality $\langle \exp(z) \rangle \geq \exp \langle z \rangle$, we see

$$\langle \Delta S_{\text{tot}} \rangle \geq 0 \tag{2.38}$$

which when compared to (1.1) we see is the second law in a statistical form. We therefore can see that the fact that $\Delta S_{\text{tot}}[X]$ can both increase and decrease is still compliant with the second law if the second law is considered a statistical law. These properties of the fluctuation theorems reconcile the second law with Loschmidt's paradox, as now we see that reversed processes are indeed possible, but are much less likely. We also note that the fluctuation theorems are powerfully general in that they are true for processes arbitrarily far from equilibrium. We will see that, with the Jarzynski equality, this leads to immense practical use.

Finally we note that another factor in the reconciliation with Loschmidt's paradox is the nature of the derivations of the fluctuation theorems. Here, the use of a master equation approach using stochastic thermodynamics can lead to the interpretation of the second law and the nature of irreversibility as arising from the noisiness of the dynamics of the system. As mentioned above, other derivations have been used, including ones based on deterministic Hamiltonian mechanics [6]. The fluctuation theorems derived this way are powerful in there connections with classical thermodynamics. For instance, [15] uses them to enact a proof of Clausius' theorem, an important result of thermodynamics.

2.2 Derivation of the Jarzynski Equality

The main focus of this report, the Jarzynski equality, is a fluctuation theorem specific for work processes. In deriving it, we again follow the derivation from [9], as this allows us to see certain ideas and results that will be core to the actual research discussed in this report: most pertinently, the Crooks work relation. The standard original derivation of the Jarzynski equality can be found in [16].

For this discussion, and as it will be used greatly later on in the report, we introduce here the overdamped langevin equation. Consider a particle subject to a langevin heat bath specified by (2.9) and under influence from a position dependent force $F(x)$. In the overdamped limit the dissipative

friction term will dominate over the time derivative of the velocity so that the langevin equation takes on a form in terms of the position x

$$\dot{x} = \frac{F(x)}{m\gamma} + \left(\frac{2k_BT}{m\gamma}\right)^{1/2} \xi(t). \tag{2.39}$$

In consideration of work processes, we can examine the force term. Consider $F(x)$ to be dependent on a conservative potential $\phi(x)$ which varies in time under protocol $\lambda_0(t)$ and an external force $f(x)$ which varies in time under protocol $\lambda_1(t)$. Therefore

$$F(x, \lambda_0(t), \lambda_1(t)) = -\frac{\partial\phi(x, \lambda_0(t))}{\partial x} + f(x, \lambda_1(t)). \tag{2.40}$$

Our consideration now falls to identifying the entropy changes in the system and the medium, so as to see what form (2.36) takes in this case. Recall that, to consider (2.36), the process must obey the reversibility condition $p_{\text{start}}(X(0)) = \hat{T}p^R_{\text{end}}(\bar{X}(\tau))$. One type of process to obey this condition is a passage from one equilibrium state to another equilibrium state. The probability distributions at the start and the end of the process are then given by canonical equilibrium distributions, of the form

$$p^{eq}(E) = \frac{1}{Z}e^{-E/k_BT} \tag{2.41}$$

where E is the internal energy of the system and Z is the partition function. By consideration of these distributions, we can identify the changes in entropy in terms of values relevent to the system.

We can identify the energy as being equal to the conservative potential. We can also examine the change in internal energy ΔE of the system over the process, which is related to the work done on the system ΔW and the heat flow into the system ΔQ by the first law of thermodynamics, which holds in stochastic thermodynamics in its standard form

$$\Delta E = \Delta W + \Delta Q. \tag{2.42}$$

Here

$$dE = d\phi(x(t), \lambda_0(t)) \tag{2.43}$$

and therefore

$$\begin{aligned} \Delta E &= \int_0^\tau dE \\ &= \int_0^\tau d\phi(x(t), \lambda_0(t)) \\ &= \phi(x(\tau), \lambda_0(\tau)) - \phi(x(0), \lambda_0(0)) \\ &= \Delta\phi. \end{aligned} \tag{2.44}$$

So that we can define any work processes we consider, we must also examine the form of ΔW. In this discussion, we must consider the differential dx. This can cause difficulties, as x is a stochastic variable which fluctuates over a change in t, which we will make obvious by denoting $x = x(t)$. We can not treat a stochastic differential the same way as a deterministic differential, and must therefore define rules as to which value of t we evaluate $dx(t)$ at. The precise subtleties of this are discussed in [13], or any other good modern book on stochastic processes. The favourite of mathematicians is to use the Ito rules, and therefore evaluate $dx(t)$ for t at the start of the increment. However, to maintain the structure of the chain rule familiar to thermodynamics, we will use Stratanovich rules, whereby $dx(t)$ is evaluated at the mid-point value of t. We will denote the use of these rules in our calculations by $\circ$, as is done in [9]. With this in consideration, it is a standard result of mechanics that the work is the sum of contributions from the change in potential and the application of the external force, so that

$$dW = \frac{\partial\phi(x(t), \lambda_0(t))}{\partial\lambda_0}\frac{d\lambda_0(t)}{dt}\,dt + f(x(t), \lambda_1(t)) \circ dx \tag{2.45}$$

and therefore

$$\begin{aligned} \Delta W &= \int_0^\tau dW \\ &= \int_0^\tau \frac{\partial\phi(x(t), \lambda_0(t))}{\partial\lambda_0}\frac{d\lambda_0(t)}{dt}\,dt + \int_0^\tau f(x(t), \lambda_1(t)) \circ dx. \end{aligned} \tag{2.46}$$

Following these considerations, we see that the equilibrium distributions take the form

$$p^{eq}(x(t), \lambda_0(t)) = \frac{1}{Z(\lambda_0(t))} \exp\left(-\frac{\phi(x(t), \lambda_0(t))}{k_B T}\right). \tag{2.47}$$

As the partition function is related to the Helmholtz free energy via

$$F = -k_B T \ln Z \tag{2.48}$$

we can assert for our initial and final distributions

$$p_{\text{start}}(x(0), \lambda_0(0)) \quad \propto \quad \exp\left[\frac{F(\lambda_0(0)) - \phi(x(0), \lambda_0(0))}{k_B T}\right] \tag{2.49}$$

$$p_{\text{end}}(x(\tau), \lambda_0(\tau)) \quad \propto \quad \exp\left[\frac{F(\lambda_0(\tau)) - \phi(x(\tau), \lambda_0(\tau))}{k_B T}\right]. \tag{2.50}$$

We can then see that our change in system entropy is

$$\begin{aligned}
\Delta S_{\text{sys}} &= k_B \ln\left[\frac{p_{\text{start}}(x(0), \lambda_0(0))}{p_{\text{end}}(x(\tau), \lambda_0(\tau))}\right] \\
&= k_B \ln\left[\frac{\exp\left[\frac{F(\lambda_0(0)) - \phi(x(0), \lambda_0(0))}{k_B T}\right]}{\exp\left[\frac{F(\lambda_0(\tau)) - \phi(x(\tau), \lambda_0(\tau))}{k_B T}\right]}\right] \\
&= \frac{(F(\lambda_0(0)) - F(\lambda_0(\tau)) + \phi(x(\tau), \lambda_0(\tau)) - \phi(x(0), \lambda_0(0)))}{T} \\
&= \frac{\Delta\phi - \Delta F}{T}
\end{aligned} \tag{2.51}$$

and from before we know our change in medium entropy to be

$$\begin{aligned}
\Delta S_{\text{med}} &= -\frac{\Delta Q}{T} \\
&= \frac{\Delta W - \Delta\phi}{T}
\end{aligned} \tag{2.52}$$

from (2.42). Therefore

$$\Delta S_{\text{tot}} = \frac{\Delta W - \Delta F}{T} \tag{2.53}$$

where we can define the work $\Delta W = \Delta W_0 + \Delta W_1$ as the sum of the work due to the conservative potential

$$\Delta W_0 = \int_0^\tau \frac{\partial\phi(x(t), \lambda_0(t))}{\partial\lambda_0} \frac{d\lambda_0(t)}{dt}\, dt \tag{2.54}$$

and the work due to the external force

$$\Delta W_1 = \int_0^\tau f(x(t), \lambda_1(t)) \circ dx. \tag{2.55}$$

If there is no external force, then $\Delta W = \Delta W_0$, and

$$\Delta S_{\text{tot}} = \frac{\Delta W_0 - \Delta F}{T} \tag{2.56}$$

and putting this into (2.36) then gives us

$$\frac{p^F\left((\Delta W_0 - \Delta F)/T\right)}{p^R\left(-(\Delta W_0 - \Delta F)/T\right)} = \exp\left(\frac{\Delta W_0 - \Delta F}{k_B T}\right). \tag{2.57}$$

As ΔF and T are path-independent quantities they can be taken out of the probability terms and cancelled, to give the Crooks work relation [17]

$$\frac{p^F(\Delta W_0)}{p^R(-\Delta W_0)} = \exp\left(\frac{\Delta W_0 - \Delta F}{k_B T}\right). \tag{2.58}$$

Like (2.36), the Crooks work relation states that the likelihood of putting ΔW_0 of work into the system in the forward process is exponentially greater than the likelihood of getting ΔW_0 of work out of the system in the reverse process. Like before, we can integrate over both sides of the relation, which gives us, finally, the Jarzynski equality

$$\left\langle e^{-\Delta W_0/k_BT} \right\rangle = e^{-\Delta F/k_BT}. \tag{2.59}$$

The Jarzynski equality holds for all times for systems starting in equilibrium. Therefore, like the other fluctuation theorems, it holds for times when the system is arbitrarily far from equilibrium. The equality tells us that we can get the value for the change in the free energy simply by taking the average over measurements of the work done over non-equilibrium processes. This is obviously of dramatic practical importance, as it negates the need to perform the process quasistatically to get the value. The equality does have an important limitation, though. Notice that if we allow the work values in the process to fluctuate larger than k_BT, like in the macroscopic limit, then we will be allowing for the introduction of extreme exponential terms which will skew the averaging. Therefore, the equality only holds for small systems, i.e. microscopic or mesoscopic systems. Lastly, again using Jensen's inequality, Jarzynski's equality gives us a statistical statement of the second law for work processes

$$\langle \Delta W_0 \rangle \geq \Delta F \tag{2.60}$$

similar to (2.38). We can compare this to the traditional form $\Delta W_0 \geq \Delta F$, and see again that the second law takes on a statistical form.

Further details on derivations can be found in [18] and [19]. The result has been confirmed both numerically and experimentally [20]. However, to provide a basis for the modelling required within the core research, it is informative to numerically confirm the equality ourselves.

2.3 The System of Interest

Before we can model the equality, we need to define the system to model it on.

We will consider the system of a classical particle in one dimension trapped in a harmonic potential and in thermal contact with an overdamped langevin heat bath. As we have seen before, this is modelled by equation (2.39), where the force is due to the potential $\phi(x, \lambda_0(t)) = \phi(x, \kappa(t)) = \frac{1}{2}\kappa(t)x^2$. Therefore, we wish to model the equation

$$\dot{x} = \frac{\kappa(t)}{m\gamma}x + \left(\frac{2k_BT}{m\gamma}\right)^{1/2}\xi(t). \tag{2.61}$$

To model the Jarzynski equality we then need to consider a protocol to govern the work process this particle undergoes. The protocol in particular that we will consider is, starting in equilibrium at a value κ_0, a step change in $\kappa(t)$ up to the value κ_1, then letting the system continue to evolve at κ_1 for a time Δt arbitrarily short when compared to the relaxation time t_r, followed by a step back down to κ_0, and then finally letting the system rest back to equilibrium [9]. This protocol can be shown in figure 2.1.

2.4 Modelling the Jarzynski Equality

To model (2.61) we first render it in terms of dimensionless variables. We define the dimensionless time, position, and noise as

$$t' = \gamma t \tag{2.62}$$

$$x' = \left(\frac{\kappa_0}{k_BT}\right)^{1/2} x \tag{2.63}$$

$$\xi'(t) = \gamma^{-1/2}\xi(t) \tag{2.64}$$

which we substitute into (2.61) to give

$$\dot{x}' = -\frac{\kappa(t)}{m\gamma^2}x' + \sqrt{2}\left(\frac{\kappa_0}{m\gamma^2}\right)^{1/2}\xi'(t). \tag{2.65}$$

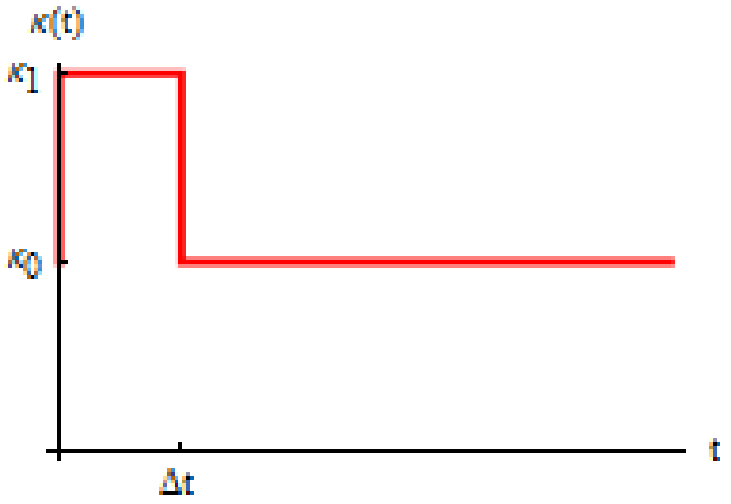

Figure 2.1: Protocol of a step up in $\kappa(t)$ followed by a step down.

Writing the dimensionless spring constant as $\alpha = \kappa/m\gamma^2$ this becomes

$$\dot{x}' = -\alpha(t)x' + \sqrt{2\alpha_0}\,\xi'(t). \tag{2.66}$$

We can express this in finite difference form for a timestep dt' small enough to model the continuous behaviour of the system

$$\frac{x'(t'+dt') - x'(t')}{dt'} = -\alpha(t)x'(t') + \sqrt{2\alpha_0}\,N_{t'}^{t'+dt'}(0,1) \tag{2.67}$$

where we have noted that the noise for finite timestep can be modelled by a unit normal distribution within the timestep. This can then be rearranged, and we express $x'(t'+dt') = x'_{n+1}$ and $x'(t') = x'_n$, to give

$$x'_{n+1} = (1 - \alpha(t)\,dt')\,x'_n + \sqrt{2\alpha_0\,dt'}\,N_{t'}^{t'+dt'}(0,1) \tag{2.68}$$

where we note that $N_{t'}^{t'+dt'}(0,1)$ includes a factor of $\sqrt{dt'}$ implicitly. This then provides a discrete random walk which can be modelled to give numerical solutions for this system.

We can derive a solution for (2.66) via the method discussed in [21]. As the changes in position are given by a series of independent normal distributions, the position itself can be given by a normal distribution. Here

$$\begin{aligned}
\dot{x}' &= -\alpha(t)x' + \sqrt{2\alpha_0}\,N_{t'}^{t'+dt'}(0,1) \\
\Rightarrow \langle \dot{x}' \rangle &= -\alpha(t)\,\langle x' \rangle \\
\Rightarrow \frac{d\,\langle x' \rangle}{dt'} &= -\alpha(t)\,\langle x' \rangle \\
\Rightarrow \langle x' \rangle &= x'_0\,e^{-\alpha(t)t'}
\end{aligned} \tag{2.69}$$

where x'_0 is the initial position at the start of the process, and

$$\begin{aligned}
\frac{dx'^2}{dt'} &= \lim_{dt'\to 0} \frac{[x'(t'+dt')]^2 - [x'(t')]^2}{dt'} \\
&= \lim_{dt'\to 0} \frac{\left[(1-\alpha(t)\,dt')\,x'(t') + \sqrt{2\alpha_0\,dt'}\,N_{t'}^{t'+dt'}(0,1)\right]^2 - x'(t')^2}{dt'} \\
&= \lim_{dt'\to 0} \frac{(1-\alpha(t)\,dt')^2\,x'(t')^2 + 2\,(1-\alpha(t)\,dt')\,x'(t')\sqrt{2\alpha_0\,dt'}\,N_{t'}^{t'+dt'}(0,1)}{dt'} \\
&\quad + \lim_{dt'\to 0} \frac{2\alpha_0\,dt'\left[N_{t'}^{t'+dt'}\right]^2 - x'(t')^2}{dt'} \\
&= \lim_{dt'\to 0} \frac{-2\alpha(t)\,dt'\,x'(t')^2 + 2x'(t')\sqrt{2\alpha_0\,dt'}\,N_{t'}^{t'+dt'}(0,1) + 2\alpha_0\,dt'\left[N_{t'}^{t'+dt'}(0,1)\right]^2}{dt'}
\end{aligned} \tag{2.70}$$

dropping the terms of order higher than dt'

$$\begin{aligned}
\Rightarrow \frac{d\left\langle x'^2\right\rangle}{dt'} &= -2\alpha(t)\left\langle x'^2\right\rangle + 2\sqrt{2\alpha_0}\left\langle x'\right\rangle\left\langle N_{t'}^{t'+dt'}(0,1)\right\rangle + 2\alpha_0\left\langle N_{t'}^{t'+dt'}(0,1)^2\right\rangle \\
&= -2\alpha(t)\left\langle x'^2\right\rangle + 2\sqrt{2\alpha_0}\left\langle x'\right\rangle\left\langle N_{t'}^{t'+dt'}\right\rangle + 2\alpha_0 \\
&= 2\alpha_0 - 2\alpha(t)\left\langle x'^2\right\rangle \\
\Rightarrow \left\langle x'^2\right\rangle &= x_0'^2 e^{-2\alpha(t)t'} + \frac{\alpha_0}{\alpha(t)}\left(1 - e^{-2\alpha(t)t'}\right)
\end{aligned} \tag{2.71}$$

then the variance $\mathrm{Var}(x')$ is

$$\begin{aligned}
\mathrm{Var}(x') &= \left\langle x'^2\right\rangle - \left\langle x'\right\rangle^2 \\
&= x_0'^2 e^{-2\alpha(t)t'} + \frac{\alpha_0}{\alpha(t)}\left(1 - e^{-2\alpha(t)t'}\right) - x_0'^2 e^{-2\alpha(t)t'} \\
&= \frac{\alpha_0}{\alpha(t)}\left(1 - e^{-2\alpha(t)t'}\right).
\end{aligned} \tag{2.72}$$

Therefore, the position is given by

$$x'(t') = N_0^{t'}\left[x_0' e^{-\alpha(t)t'}, \frac{\alpha_0}{\alpha(t)}\left(1 - e^{-2\alpha(t)t'}\right)\right]. \tag{2.73}$$

This gives the expected result for Ornstein-Uhlenbeck processes of a travelling mean and decreasing variance over time.

We can therefore compare numerical results from (2.68) with the theoretical prediction given in (2.73). This can be done by comparing a histogram of the numerical results to a histogram generated from the distribution in (2.73). For the modelling, we choose $dt' = 10^{-5}$, $x_0 = 0$, and $\alpha(t) = \alpha_0 = 1$. Therefore, the theoretical prediction is $x'(t') = N\left(0, \left(1 - e^{-2t'}\right)\right)$ and the numerical update follows

$$x'_{n+1} = 0.99999\, x'_n + N\left(0, 0.00002\right). \tag{2.74}$$

Results for 10000, 50000, and 100000 time steps with samples of 1000 positions for each are given in figures 2.2, 2.3, and 2.4 respectively. As can be seen, the numerical results do indeed compare favourably to the theoretical distribution.

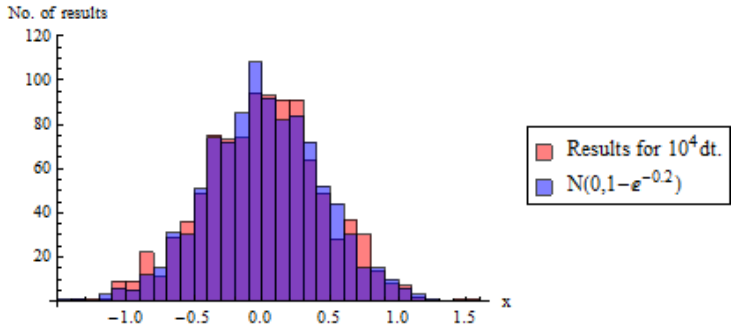

Figure 2.2: Results from sample of 1000 positions from an update of 10000 time steps compared to a histogram generated from the theoretical distribution.

Finally, the Jarzynski equality can now be modelled by applying the protocol from figure 2.1 to a particle undergoing the random walk in (2.68) and repeating for N cycles, where N is large enough to gain an effective average of the exponentiated quantities over all the cycles. From each cycle we measure a dimensionless work value $\Delta W'_0 = \Delta W'_{0\to1} + \Delta W'_{1\to0}$ where

$$\Delta W'_{0\to1} = \frac{\alpha_1 - \alpha_0}{2\alpha_0} x_u'^2 = \frac{\Delta W_{0\to1}}{k_B T} = \frac{1}{2}\left(\kappa_1 - \kappa_0\right) x_u^2 / k_B T \tag{2.75}$$

$$\Delta W'_{1\to0} = \frac{\alpha_0 - \alpha_1}{2\alpha_0} x_d'^2 = \frac{\Delta W_{1\to0}}{k_B T} = \frac{1}{2}\left(\kappa_0 - \kappa_1\right) x_d^2 / k_B T \tag{2.76}$$

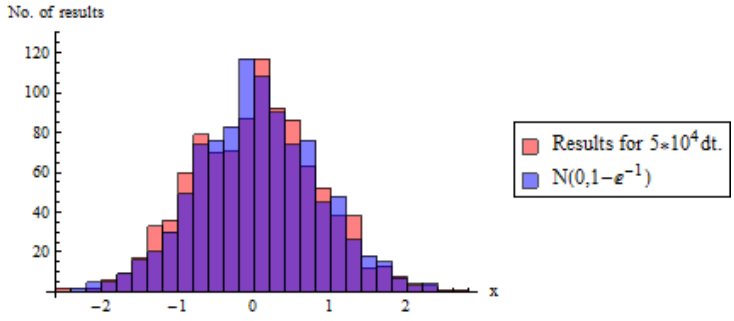

Figure 2.3: Results from sample of 1000 positions from an update of 50000 time steps compared to a histogram generated from the theoretical distribution.

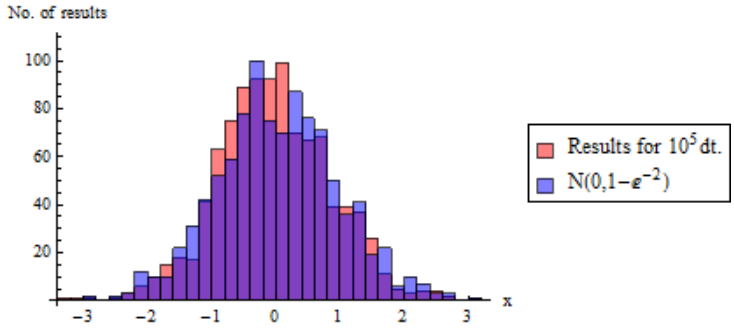

Figure 2.4: Results from sample of 1000 positions from an update of 100000 time steps compared to a histogram generated from the theoretical distribution.

where x_u is the position at the step up and x_d is the position at the step down, then average the exponentials of these values over all the cycles

$$\left\langle e^{-\Delta W_0'} \right\rangle = \frac{1}{N} \sum_{i=1}^{N} e^{-\Delta W_{0,i}'} \tag{2.77}$$

and compare this value to the theoretical Jarzynski equality, which in this case is

$$\left\langle e^{-\Delta W_0'} \right\rangle = 1 \tag{2.78}$$

as $\Delta F = 0$ due to the cyclic nature of the process. Recall that the time after the step back down must be long compared to the relaxation time, which is given by $t_r = 1/\gamma$ [22]. Here we will therefore take $t_r = 1$.

Figure 2.5 shows the results for processes with various increases in spring constant. Each result is taken from a statistical average of 20 repeats of a process of 1000 cycles of 800000 time steps. Each time step is $dt' = 10^{-5}$, and within each cycle the step up step down protocol takes place over half the timesteps, so the system is allowed to rest for the other half before the next cycle, and therefore $\Delta t' = 4$. Each process starts at an initial position $x_0' = 0$ and is allowed to reach equilibrium before the cycles begin. For all the processes, $\alpha_0 = 1$. A different α_1 value is used for each different process. The results show that the numerical modelling successfully reproduces the Jarzynski equality. Also of note is the increase in statistical error, given in the figure by one standard deviation either side of the data point, as the increase in α gets larger. This agrees with what was discussed earlier, in that an allowance for larger fluctuations in the work leads to a skewing of the average of the exponentiated values. This would then lead to an increase in unpredictability in the actual measured value of the average, as shown here.

Lastly for this section, we can examine the variance of $e^{-\Delta W_0'}$ to see how the values of the exponentiated work fluctuates about the mean value of 1. Numerically, this can be done in a similar fashion to

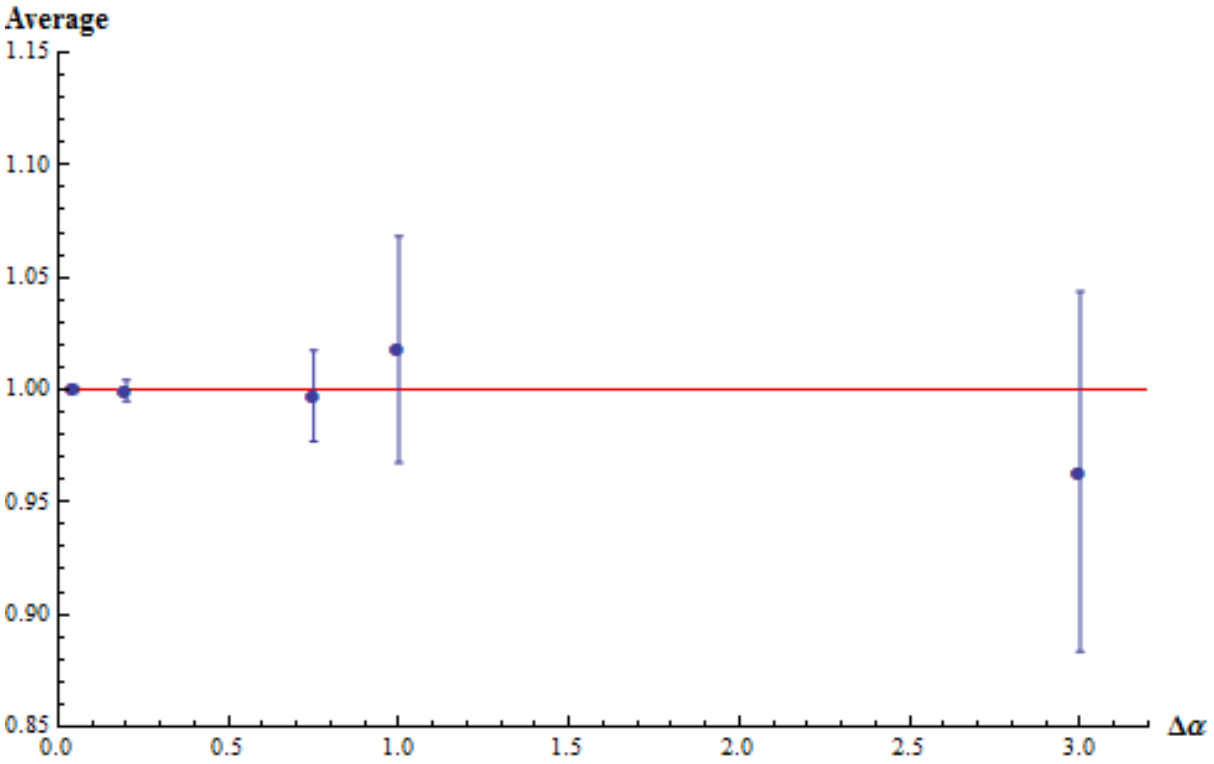

Figure 2.5: Numerical results for averages of exponentiated work values, given by blue data points, plotted against the theoretical prediction, given by a red line, for increasing changes in α, $\Delta\alpha = \alpha_1 - \alpha_0$, from an initial value $\alpha_0 = 1$.

how the mean was modelled

$$\begin{aligned} \mathrm{Var}\left(e^{-\Delta W_0'}\right) &= \left\langle e^{-2\,\Delta W_0'}\right\rangle - \left\langle e^{-\Delta W_0'}\right\rangle^2 \\ &= \frac{1}{N}\sum_{i=1}^{N} e^{-2\,\Delta W_{0,i}'} - \left(\frac{1}{N}\sum_{i=1}^{N} e^{-\Delta W_{0,i}'}\right)^2 . \end{aligned} \tag{2.79}$$

The theoretical value can be found for the process of a step up and step down in spring constant by averaging over the equilibrium distribution of being at the start of the process and the transition distribution of the process given by (2.14)

$$\begin{aligned} \left\langle e^{-2\,\Delta W_0'}\right\rangle &= \int dx_u\, dx_d\, p_{eq}(x_u)\, p_{OU}^{T}(x_d)\, e^{-2\,\Delta W_0/k_BT} \\ &= \int dx_u\, dx_d \left(\frac{\kappa_0}{2\pi k_BT}\right)^{1/2} e^{-\kappa_0 x_u^2/2k_BT} \\ &\quad \times \left(\frac{\kappa_1}{2\pi k_BT\left(1-e^{-2\kappa_1 t/m\gamma}\right)}\right)^{1/2} e^{-\kappa_1\left(x_d - x_u e^{-\kappa_1 t/m\gamma}\right)/2k_BT\left(1-e^{-2\kappa_1 t/m\gamma}\right)} \\ &\quad \times e^{-(\kappa_1-\kappa_0)x_u^2/k_BT} e^{-(\kappa_0-\kappa_1)x_d^2/k_BT} \\ &= \left[\frac{1-e^{2\kappa_1 t/m\gamma}}{1-e^{-2\kappa_1 t/m\gamma}} \frac{\kappa_0\kappa_1}{2\left(e^{2\kappa_1 t/m\gamma}-1\right)\left(\kappa_0^2+\kappa_1^2\right)+\left(4-5e^{2\kappa_1 t/m\gamma}\right)\kappa_0\kappa_1}\right]^{1/2} \\ &= \left[\frac{1-e^{2\alpha_1 t'}}{1-e^{-2\alpha_1 t'}} \frac{\alpha_0\alpha_1}{2\left(e^{2\alpha_1 t'}-1\right)\left(\alpha_0^2+\alpha_1^2\right)+\left(4-5e^{2\alpha_1 t'}\right)\alpha_0\alpha_1}\right]^{1/2} \end{aligned} \tag{2.80}$$

rendered in terms of dimensionless variables as before. Therefore, the variance is

$$\mathrm{Var}\left(e^{-\Delta W_0'}\right) = \left[\frac{1-e^{2\alpha_1 t'}}{1-e^{-2\alpha_1 t'}}\,\frac{\alpha_0\alpha_1}{2\left(e^{2\alpha_1 t'}-1\right)\left(\alpha_0^2+\alpha_1^2\right)+\left(4-5e^{2\alpha_1 t'}\right)\alpha_0\alpha_1}\right]^{1/2} - 1 \tag{2.81}$$

where the time t' in the expression is the time from the step up in spring constant to the step back down.

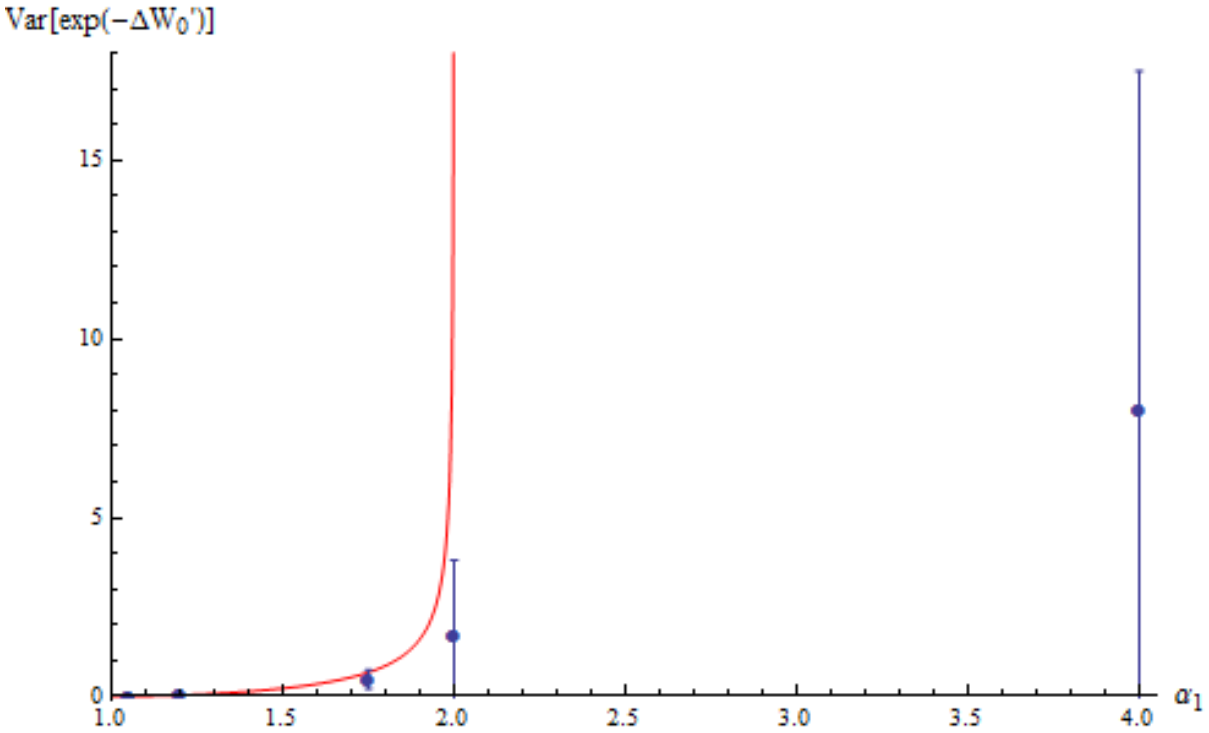

Figure 2.6: Numerical results for variances of exponentiated work values, given by blue data points, plotted against the theoretical prediction, given by a red curve, for different values of α_1 from an initial value $\alpha_0 = 1$.

The numerical results in figure 2.6 were modelled for a system with the same conditions as that modelled in figure 2.5 where t' in (2.81) is given by $\Delta t' = 4$. As can be seen, the numerical results fit the theoretical prediction well for small changes in α. However, for larger changes (2.81) appears to be asymptotic to $\alpha_1 = 2$, and can therefore not be used to calculate the variance for much larger changes in spring constant. The numerical results do show a continued steady increase in the variance as the change in spring constant gets larger than the boundary set by the theoretical prediction, but also the statistical error becomes so large that the result is unreliable.

Chapter 3

The Jarzynski-Sagawa-Ueda Equality

3.1 Measurement and Feedback

In chapter 2 we laid down the foundations for the investigation by deriving the Jarzynski equality and examining how it can be modelled numerically. Now we go on to the main purpose: exploring generalisations of the Jarzynski equality in the aim of extending the current understanding of the equality and to provide numerical confirmation in order to strengthen the theoretical foundation for future experimental work in this area.

The first generalisation is a very intriguing one, combining the non-equilibrium fluctuation theorems with information thermodynamics: systems with measurement and feedback. This chapter presents and builds upon the work found in [23], which the reader should refer to for further information on the theoretical grounding of the investigation here.

The classical example of a system with measurement and feedback is Maxwell's demon [7], a pictoral representation of which is shown on the title page. A classical gas of particles is held within an impermiable adiabatic container with a wall in the middle separating the gas in to two halves. In the wall is a door, which when open is the only part of the wall the particles can pass through. An intelligence (which does not need to be a biological intelligence [24]), the "demon", observes the particles as they move about the container. It opens the door only if it allows, for instance, the cold particles on the left to pass to the right, and the hot particles on the right to pass to the left. By doing so it brings the system to a more ordered state and thereby reduces the entropy.

The simplest way to see how this applies to work processes, such as the process we considered in chapter 2, is via Szilard's engine [25], as depicted in figure 3.1.

The Szilard engine consists of a single particle within a container in thermal contact only with a heat bath of constant temperature. In figure 3.1 step 1, the particle is in thermal equilibrium with the heat bath and moves about the container at random. In step 2, an impermiable wall is inserted into the centre of the container, and a measurement device (the "demon" from Maxwell's demon) attached to the system measures whether the particle is on the left or right hand side in step 3. By doing this, the measurement device gains information from the system. The measurement has an associated error, and as this error gets larger the amount of information gained via the measurement gets smaller. In step 4, the device applies feedback to the system based on the measurement. If the measurement states that the particle is on the left hand side, the central wall is allowed to expand all the way to the right, and vice versa. By doing so, work is gained from the system. The smaller the error in measurement, the more effective the feedback applied, and the greater the work gained out of the system. The feedback uses information to convert one type of energy in the system into another.

Essentially, instead of allowing the process to continue from beginning to end, the measurement device observes the system part way through the process and changes something in the system so as to reduce the entropy of the system. Note, though, that this does not result in breaking the second law of thermodynamics. The measurement device has to be considered part of the total system, and so any entropy change in the device must also be considered. According to Landauer's principle, for the process to truly be cyclic the measurement device must erase the information it has gained. Erasure of information is an irreversible process and therefore has an associated increase in entropy which counterracts the

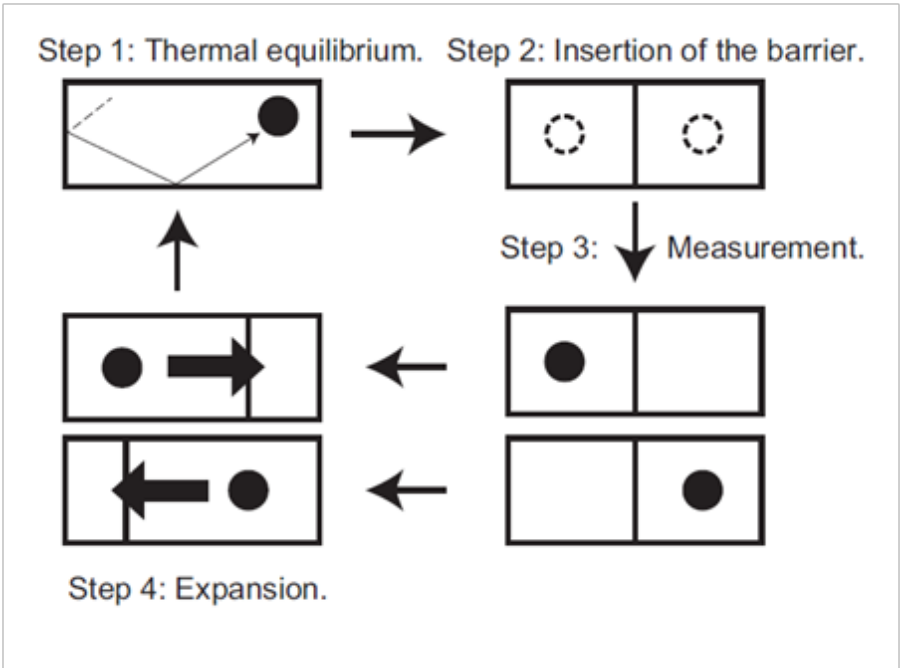

Figure 3.1: The Szilard engine, from chapter 2 of [23].

decrease in the system. Therefore the overall change in entropy still obeys the second law [26].

Systems with measurement and feedback are of great importance in recent and current research, especially in modelling nanosystems. The application of measurement and feedback is useful for stabilising unstable dynamics or increasing performance [27].

Further information on Maxwell's demon and its applications can be found in [8].

3.2 Alteration of the Jarzynski Equality

From (2.59), taking the free energy term on to the left hand side gives

$$\langle \exp\left(-\left(\Delta W_0 - \Delta F\right)/k_B T\right)\rangle = 1. \tag{3.1}$$

Therefore, we want to examine how the use of measurement and feedback affects the average of the quantity $\exp\left(-\left(\Delta W_0 - \Delta F\right)/k_B T\right)$. We denote the measurement outcome as y with an associated error σ. We must then average over both x and y. Therefore

$$\langle \exp\left(-\left(\Delta W_0 - \Delta F\right)/k_B T\right)\rangle = \int dy\, dx\, p(x,y) \left\langle \exp\left(-\left(\Delta W_0 - \Delta F\right)/k_B T\right)\right\rangle_x \tag{3.2}$$

where $\left\langle \exp\left(-\left(\Delta W_0 - \Delta F\right)/k_B T\right)\right\rangle_x$ is the average over all trajectories starting in equilibrium at a specified position $x = x_0 = x(0)$, and $p(x,y)$ is the joint distribution of x and y. Here

$$\left\langle \exp\left(-\left(\Delta W_0 - \Delta F\right)/k_B T\right)\right\rangle_x = \int dx_\tau\, T_{\lambda_y}\left(x_\tau | x_0\right) \exp\left(-\left(\Delta W_0 - \Delta F\right)/k_B T\right) \tag{3.3}$$

where we are still only considering the quantity for initial position x, and averaging over final positions $x_\tau = x(\tau)$ where $T_{\lambda_y}\left(x_\tau | x_0\right)$ is the transition probability over the process of going to x_τ given the initial position x_0 under a time dependent protocol $\lambda_y(t)$ dependent on the measurement y.

From the Crooks work relation, the quantity $\exp\left(-\left(\Delta W_0 - \Delta F\right)/k_B T\right)$ can be related to the ratio of the distribution of the forward trajectory of the process to the distribution of the reverse trajectory via (2.58). The distribution of the process is given by the product of the starting distribution and the transition distribution. For the forward process the starting distribution is the equilibrium distribution $p_{\mathrm{eq},\lambda_0}(x)$ where $\lambda_0 = \lambda_y(0)$ is the initial value of the protocol. For the reverse process it is the reverse equilibrium distribution $p^R_{\mathrm{eq},\lambda_y(\tau)}(\bar{x}_0)$, where the time reversed position is $\bar{x}_t = \bar{x}(t) = x(\tau - t)$ and the

time reversed protocol is $\bar{\lambda}_y(t) = \lambda_y(\tau - t)$. The transition probabilities are $T_{\lambda_y}(x_\tau|x_0)$ and $T_{\bar{\lambda}_y}(\bar{x}_\tau|\bar{x}_0)$ for the forward and reverse process respectively. Therefore

$$\exp\left(\left(\Delta W_0 - \Delta F\right)/k_B T\right) = \frac{p_{\mathrm{eq},\lambda_0}(x)\, T_{\lambda_y}(x_\tau|x_0)}{p^R_{\mathrm{eq},\lambda_y(\tau)}(\bar{x}_0)\, T_{\bar{\lambda}_y}(\bar{x}_\tau|\bar{x}_0)}. \tag{3.4}$$

From these considerations and as $p(x,y) = p(y|x)p(x)$

$$\begin{aligned}
\langle \exp\left(-\left(\Delta W_0 - \Delta F\right)/k_B T\right)\rangle &= \int dy\, dx\, p(y|x)p(x)\, dx_\tau\, T_{\lambda_y}(x_\tau|x_0) \\
&\quad \times \frac{p^R_{\mathrm{eq},\lambda_y(\tau)}(\bar{x}_0)\, T_{\bar{\lambda}_y}(\bar{x}_\tau|\bar{x}_0)}{p_{\mathrm{eq},\lambda_0}(x)\, T_{\lambda_y}(x_\tau|x_0)} \\
&= \int dy\, dx\, p(y|x)\frac{p(x)}{p_{\mathrm{eq},\lambda_0}(x)} \\
&\quad \times dx_\tau\, p^R_{\mathrm{eq},\lambda_y(\tau)}(\bar{x}_0) T_{\bar{\lambda}_y}(\bar{x}_\tau|\bar{x}_0) \\
&= \int dy\, d\bar{x}_\tau\, p\left(y|\bar{x}_\tau\right)\frac{p(\bar{x}_\tau)}{p_{\mathrm{eq},\lambda_0}(\bar{x}_\tau)} \\
&\quad \times d\bar{x}_0\, p^R_{\mathrm{eq},\lambda_y(\tau)}(\bar{x}_0) T_{\bar{\lambda}_y}(\bar{x}_\tau|\bar{x}_0) \\
&= \int dy\, d\bar{x}_\tau\, p\left(y|\bar{x}_\tau\right)\frac{p(\bar{x}_\tau)}{p_{\mathrm{eq},\lambda_0}(\bar{x}_\tau)} p^R_{\bar{\lambda}_y}(\bar{x}_\tau) \\
&= \int dy\, d\bar{x}_\tau\, p^R_{\bar{\lambda}_y}(y,\bar{x}_\tau)\frac{p(\bar{x}_\tau)}{p_{\mathrm{eq},\lambda_0}(\bar{x}_\tau)}
\end{aligned} \tag{3.5}$$

where $p^R_{\bar{\lambda}_y}(\bar{x}_\tau)$ is the distribution of the position at the end of the reverse protocol, and $p^R_{\bar{\lambda}_y}(y,\bar{x}_\tau)$ is the joint distribution of this position and its measurement.

If we write

$$\gamma_E = \int dy\, d\bar{x}_\tau\, p^R_{\bar{\lambda}_y}(y,\bar{x}_\tau)\frac{p(\bar{x}_\tau)}{p_{\mathrm{eq},\lambda_0}(\bar{x}_\tau)} \tag{3.6}$$

then we get the Jarzynski-Sagawa-Ueda equality [28]

$$\left\langle e^{-(\Delta W_0 - \Delta F)/k_B T}\right\rangle = \gamma_E. \tag{3.7}$$

γ_E is known as the efficacy parameter and is a constant that can differ from unity depending on the distributions of the trajectory under measurement and feedback. It measures the effectiveness of the feedback in using the information gained via measurement to get work out of the system. The greater the effectiveness, the greater the value of γ_E. The Jarzynski-Sagawa-Ueda equality is the subject of continued experimental verification and interest [29].

Note that there are more subtleties to the derivation of this result than are presented here. For instance, measurement has no time-reversal, so reverse processes need to be defined in this case [30]. Also, the Jarzynski-Sagawa-Ueda equality can be presented in an alternate form which gives deeper insight into its meaning. For further information on all this and for different derivations, the reader is directed to [23], [31], and [32].

3.3 Modelling the Jarzynski-Sagawa-Ueda Equality

It is simple to apply measurement and feedback to the process considered in chapter 2. Again, we consider a classical particle in one dimension obeying the overdamped langevin equation (2.39), undergoing N cycles of the work process of a step up and step down in spring constant. A measurement is taken of the position x_u at the start of each cycle, returning a result y with error σ. Dependent on the result y, the spring constant κ is changed as shown in figure 3.2. If y is within a range $-y_a \leq y \leq +y_a$ centred around the centre of the potential, then the spring constant is allowed to change to κ_1 for that cycle. However, if it is outside the chosen range, then the spring constant is kept at the initial value κ_0 for the cycle. Essentially, we choose to change the spring constant only for cycles where the initial position is close enough to the centre of the potential such that the change in spring constant only involves putting

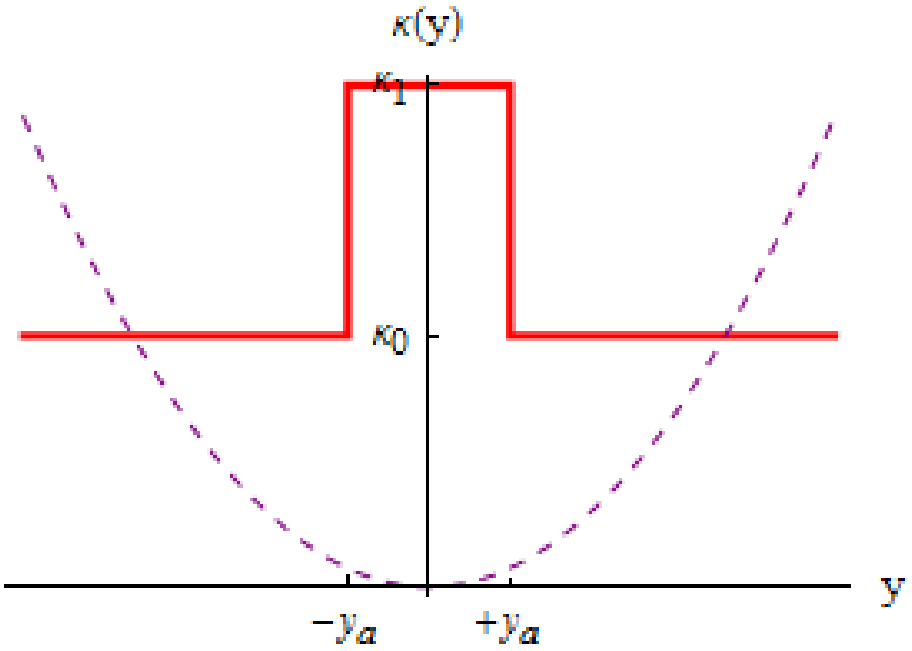

Figure 3.2: The application of measurement and feedback to the system. The purple dashed line denotes the potential. The solid red line denotes the change made in spring constant at the start of the cycle dependent on the measurement outcome y.

a small amount of work into the system. Averaging over all N cycles, we then get more work out of the system on average than we put in.

At the start of the cycle we assume the position x_u to obey the equilibrium distribution $p(x_u) = p_{\mathrm{eq},\kappa_0}(x_u) = (\kappa_0/2\pi k_B T)^{1/2} \exp\left(-\kappa_0 x_u^2/2k_B T\right)$. We also assume that the position x_d at time Δt has settled to an equilibrium distribution under κ_1, $p(x_d) = p_{\mathrm{eq},\kappa_1}(x_d) = (\kappa_1/2\pi k_B T)^{1/2} \exp\left(-\kappa_1 x_d^2/2k_B T\right)$. From this, we see that in (3.6) $p(\bar{x}_\tau) = p_{\mathrm{eq},\lambda_0}(\bar{x}_\tau)$. For the reverse process, $p^R_{\lambda_y}(\bar{x}_\tau) = (\kappa_0/2\pi k_B T)^{1/2} \times \exp\left(-\kappa_0 \bar{x}_\tau^2/2k_B T\right)$ for the case of no change in spring constant and $p^R_{\lambda_y}(\bar{x}_\tau) = (\kappa_1/2\pi k_B T)^{1/2} \exp\left(-\kappa_1 \bar{x}_\tau^2/2k_B T\right)$ for the case of a change in spring constant. Lastly, we take the distribution of the measurement conditional on an initial position for the reverse process to be $p(y|\bar{x}_\tau) = \left(2\pi\sigma^2\right)^{-1/2} \exp\left(-\left(y-\bar{x}_\tau\right)^2/2\sigma^2\right)$. Therefore, (3.6) becomes

$$\gamma_E = \int dy\, d\bar{x}_\tau \, \frac{1}{\sqrt{2\pi}\sigma} e^{-(y-\bar{x}_\tau)^2/2\sigma^2} \left(\frac{\kappa(y)}{2\pi k_B T}\right)^{1/2} e^{-\kappa(y)\bar{x}_\tau^2/2k_B T}. \tag{3.8}$$

As the system evolves at κ_1 when y is within $\pm y_a$, and evolves at κ_0 when y is outside of $\pm y_a$, this can be broken up into multiple terms

$$\begin{aligned}
\gamma_E &= 2\int_0^{y_a} dy \int_{-\infty}^{+\infty} d\bar{x}_\tau \, \frac{1}{\sqrt{2\pi}\sigma} e^{-(y-\bar{x}_\tau)^{1/2}/2\sigma^2} \left(\frac{\kappa_1}{2\pi k_B T}\right)^{1/2} e^{-\kappa_1 \bar{x}_\tau^2/2k_B T} \\
&\quad + 2\int_{y_a}^{+\infty} dy \int_{-\infty}^{+\infty} d\bar{x}_\tau \, \frac{1}{\sqrt{2\pi}\sigma} e^{-(y-\bar{x}_\tau)^{1/2}/2\sigma^2} \left(\frac{\kappa_0}{2\pi k_B T}\right)^{1/2} e^{-\kappa_0 \bar{x}_\tau^2/2k_B T} \\
&= 2\int_0^{y_a} dy\, G_1(y) + 2\int_{y_a}^{\infty} dy\, G_0(y)
\end{aligned} \tag{3.9}$$

where the gaussian functions are

$$G_i(y) = \left(\frac{\kappa_i}{2\pi k_B T\left(\left(\kappa_i\sigma^2/k_B T\right)+1\right)}\right)^{1/2} \exp\left(-\frac{\kappa_i y^2}{2k_B T\left(\left(\kappa_i\sigma^2/k_B T\right)+1\right)}\right). \tag{3.10}$$

This can then be rearranged as

$$\begin{aligned}\gamma_E &= 2\int_0^{y_a} dy\, G_1(y) + 2\int_{y_a}^{\infty} dy\, G_0(y) \\ &= \int_{-y_a}^{+y_a} dy\, G_1(y) + \int_{-\infty}^{+\infty} dy\, G_0(y) - \int_{-y_a}^{+y_a} dy\, G_1(y) \\ &= \int_{-y_a}^{+y_a} \left(G_1(y) - G_0(y)\right)\, dy + 1 \end{aligned} \tag{3.11}$$

which can also be written in terms of error functions

$$\gamma_E = \mathrm{erf}\left(\frac{y_a}{\sqrt{2\left(\sigma^2 + k_BT/\kappa_1\right)}}\right) - \mathrm{erf}\left(\frac{y_a}{\sqrt{2\left(\sigma^2 + k_BT/\kappa_0\right)}}\right) + 1. \tag{3.12}$$

For now we will consider the case with no error in measurement, such that $\sigma = 0$, $y = x_u$, and $y_a = x_a$ is a range in the actual position x_u. Here

$$\begin{aligned}\gamma_E &= \mathrm{erf}\left(\sqrt{\frac{\kappa_1}{2k_BT}}x_a\right) - \mathrm{erf}\left(\sqrt{\frac{\kappa_0}{2k_BT}}x_a\right) + 1 \\ &= \mathrm{erf}\left(\sqrt{\frac{\alpha_1}{2\alpha_0}}x'_a\right) - \mathrm{erf}\left(\frac{1}{\sqrt{2}}x'_a\right) + 1 \end{aligned} \tag{3.13}$$

rendered dimensionless using the substitution $x'_a = \left(\kappa_0/k_BT\right)^{1/2} x_a$ like before.

This situation can be modelled numerically using the same method used in chapter 2. However, as mentioned before, for each cycle the spring constant is increased if the starting position is within the range $\pm x'_a$ and is kept the same if it is outside the range $\pm x'_a$. Figure 3.3 shows the results for numerical modelling of the efficacy parameter for changes to various α_1 values with 20 repeats each of 1000 cycle processes, each cycle containing 800000 time steps of value $dt' = 10^{-5}$. Each process starts at $x'_0 = 0$ and then rests to equilibrium before the cycles begin. $\alpha_0 = 1$ and $x'_a = 0.5$ for all processes, and for cycles where the step up step down action is applied, they are kept at α_1 for $\Delta t' = 4$. The theoretical result shows a gradually decreasing increase in the efficacy parameter for an increase in the jump in the spring constant. The numerical results follow this prediction well, and can be taken as indicative that the result is correct. The numerical results deviate more from the prediction as the jump in spring constant increases, and the error in the results also increases along the same lines.

Figure 3.4 shows the same results but focusses on the smaller changes in spring constant, showing how closely the numerical results do indeed follow (3.13).

Results can also be gained for the variance of the quantity $e^{-\Delta W'}$, as was done in chapter 2. For the same processes as figures 3.3 and 3.4, the results for the variance are given in figure 3.5. As before, for higher changes in spring constant the errors in the results become so large as to make them unreliable.

Figure 3.6 focusses on the results for the smaller changes in spring constant. The variance is observed to start very low, and to show an increase with an increasingly positive gradient over increasing changes in spring constant.

To maximise the value of γ_E in this case, an optimal value of y_a can be chosen. From expression (3.11), we can see that γ_E is given by the integral of the difference between the gaussians $G_1(y)$ and $G_0(y)$. γ_E can therefore be maximised by maximising the area under these gaussians that is included in the integral. This can be done by choosing y_a (dimensionless x'_a in the case of zero error) where $G_1(y)$ and $G_0(y)$ intersect

$$\begin{aligned} G_0(y_a) &= G_1(y_a) \\ \Rightarrow \left(\frac{\kappa_0}{2\pi k_BT\left(\left(\kappa_0\sigma^2/k_BT\right)+1\right)}\right)^{1/2} &\times \exp\left(-\frac{\kappa_0 y_a^2}{2k_BT\left(\left(\kappa_0\sigma^2/k_BT\right)+1\right)}\right) = \\ \left(\frac{\kappa_1}{2\pi k_BT\left(\left(\kappa_1\sigma^2/k_BT\right)+1\right)}\right)^{1/2} &\times \exp\left(-\frac{\kappa_1 y_a^2}{2k_BT\left(\left(\kappa_1\sigma^2/k_BT\right)+1\right)}\right) \\ \Rightarrow \frac{1}{2}\ln\left(\frac{1}{2\pi\left(\sigma^2 + k_BT/\kappa_0\right)}\right) &- \frac{y_a^2}{2\left(\sigma^2 + k_BT/\kappa_0\right)} = \\ \frac{1}{2}\ln\left(\frac{1}{2\pi\left(\sigma^2 + k_BT/\kappa_1\right)}\right) &- \frac{y_a^2}{2\left(\sigma^2 + k_BT/\kappa_1\right)} \end{aligned} \tag{3.14}$$

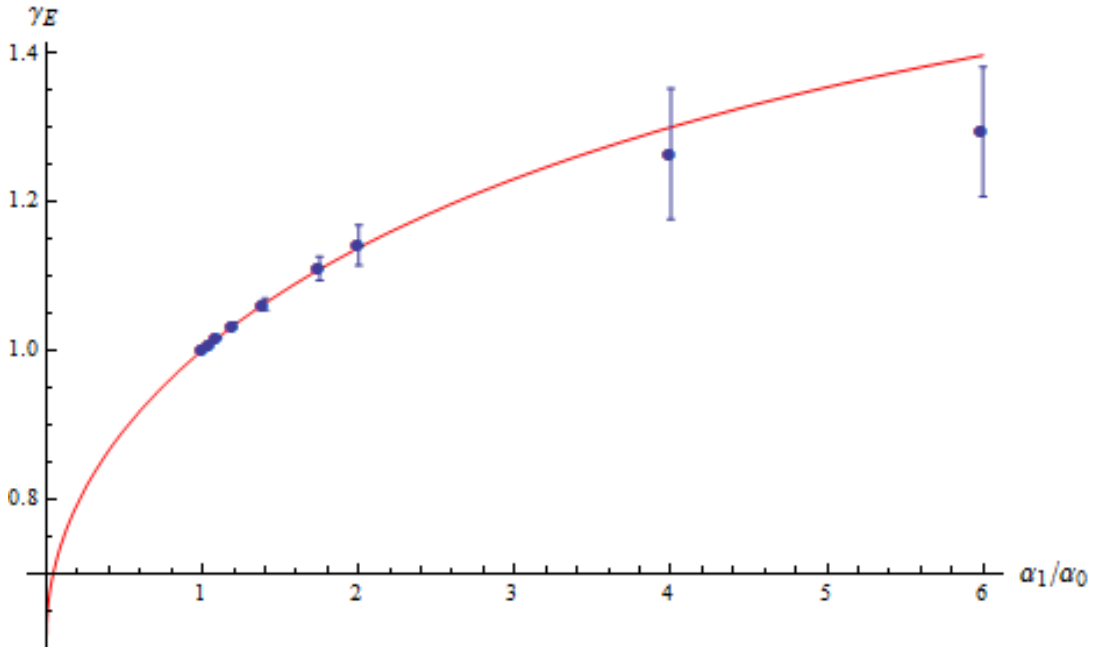

Figure 3.3: Results for numerically modelling the efficacy parameter, given by the blue data points, shown against the theoretical prediction, given by the red curve, for changes to various α_1 values from $\alpha_0 = 1$ for arbitrarily chosen range $x'_a = 0.5$.

which gives

$$y_a^2 = \frac{\left(\sigma^2 + k_B T/\kappa_1\right)\left(\sigma^2 + k_B T/\kappa_0\right)}{k_B T\left(\kappa_0^{-1} - \kappa_1^{-1}\right)} \ln\left(\frac{\sigma^2 + k_B T/\kappa_0}{\sigma^2 + k_B T/\kappa_1}\right). \tag{3.15}$$

In the limit of zero error this gives

$$x_a^2 = \frac{k_B T}{\kappa_1 - \kappa_0} \ln\frac{\kappa_1}{\kappa_0} \tag{3.16}$$

which can be rendered dimensionless as

$$x_a'^2 = \frac{1}{\alpha_1 - \alpha_0} \ln\left(\frac{\alpha_1}{\alpha_0}\right). \tag{3.17}$$

Numerical results for processes with the same value parameters as in figure 3.3 except using the optimal value for x'_a, and with $\Delta t' = 1$ and only 10 repeats per result, are given in figure 3.7. The results show a definite increase in γ_E above the case for arbitrarily chosen range, as expected, and the numerical results follow the theoretical prediction very closely, with increasing error as the change in spring constant increases, as before.

As before, figure 3.8 shows the same results focussing on the smaller changes in spring constant. It shows even clearer the increase in γ_E for the use of the optimal range, and how closely the numerical results follow the theoretical prediction.

Like before, variances can be found from the numerical data and are given in figure 3.9. The figure focusses on the smaller changes in spring constant, as it was shown before that the errors for the higher changes are so large as to render them unreliable.

3.4 Time Dependent Efficacy Parameter, Measurements with Error

It is worthwhile to explore further features of the efficacy parameter. First, we can consider cases where $\Delta t'$ is so short that the system does not have enough time to equilibrate and settle to κ_1. Here, we can model the system for different values of $\Delta t'$, and with the same values for all other parameters as we have used before. Then we can compare the numerical results to expression (3.13) with κ_1 replaced by

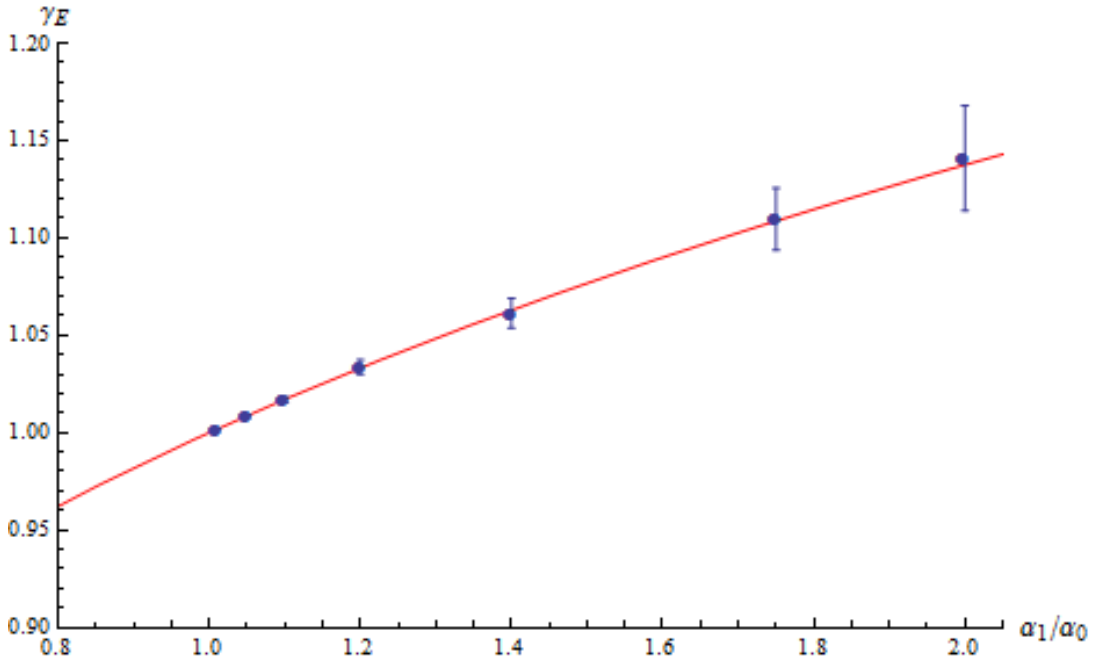

Figure 3.4: Results for numerically modelling the efficacy parameter, given by the blue data points, shown against the theoretical prediction, given by the red curve, for changes to various α_1 values from $\alpha_0 = 1$ for arbitrarily chosen range $x'_a = 0.5$, focussing on the lower changes in spring constant.

a time dependent value between κ_1 and κ_0, $\tilde{\kappa}(\Delta t)$, given by

$$\tilde{\kappa}(\Delta t) = \frac{\kappa_0 \kappa_1}{\kappa_0 + e^{-2\kappa_1 \Delta t/m\gamma}\left(\kappa_1 - \kappa_0\right)} \tag{3.18}$$

which is rendered dimensionless as

$$\tilde{\alpha}(\Delta t') = \frac{\alpha_0 \alpha_1}{\alpha_0 + e^{-2\alpha_1 \Delta t'}\left(\alpha_1 - \alpha_0\right)}. \tag{3.19}$$

With these considerations and using the optimal range given in (3.17), the efficacy parameter in (3.13) becomes

$$\begin{aligned}\gamma_E(\Delta t') \quad = \quad & \operatorname{erf}\left[\sqrt{\frac{\alpha_1}{2\alpha_0\alpha_1 - 2\alpha_0^2 - 2e^{-2\alpha_1\Delta t'}\left(\alpha_1 - \alpha_0\right)}\ln\left(\frac{\alpha_1}{\alpha_0 + e^{-2\alpha_1\Delta t'}\left(\alpha_1 - \alpha_0\right)}\right)}\right] \\ & -\operatorname{erf}\left[\sqrt{\frac{\alpha_0 + e^{-2\alpha_1\Delta t'}\left(\alpha_1 - \alpha_0\right)}{2\alpha_0\alpha_1 - 2\alpha_0^2 - 2e^{-2\alpha_1\Delta t'}\left(\alpha_1 - \alpha_0\right)}\ln\left(\frac{\alpha_1}{\alpha_0 + e^{-2\alpha_1\Delta t'}\left(\alpha_1 - \alpha_0\right)}\right)}\right] \\ & +1. \end{aligned} \tag{3.20}$$

Figure 3.10 shows the results for modelling this for $\alpha_0 = 1$ and $\alpha_1 = 1.2$. The efficacy parameter increases over time, but at a decreasing rate, which implies that it will tend to a maximum value. The numerical results are very close to the theoretical prediction, indicating the result to be correct. Figure 3.11 shows the results for modelling the variance over time, and it too increases but at a very slow rate.

Another area to explore is the affect of errors in measurement on the efficacy parameter. As γ_E increases as the feedback becomes more effective, it would be expected to decrease as errors in measurement decrease. The efficacy parameter is given by (3.12), and can be rendered dimensionless by making the usual replacements $\sigma' = \left(\kappa_0/k_BT\right)^{1/2}\sigma$ and $y'_a = \left(\kappa_0/k_BT\right)^{1/2} y_a$, giving

$$\gamma_E = \operatorname{erf}\left[\frac{y'_a}{\sqrt{2\left(\sigma'^2 + \alpha_0/\alpha_1\right)}}\right] - \operatorname{erf}\left[\frac{y'_a}{\sqrt{2\left(\sigma'^2 + 1\right)}}\right] + 1. \tag{3.21}$$

The optimal range y_a here is given by

$$y_a = \frac{\left(\sigma^2 + k_BT/\kappa_1\right)\left(\sigma^2 + k_BT/\kappa_0\right)}{k_BT\left(\kappa_0^{-1} - \kappa_1^{-1}\right)}\ln\left(\frac{\sigma^2 + k_BT/\kappa_0}{\sigma^2 + k_BT/\kappa_1}\right) \tag{3.22}$$

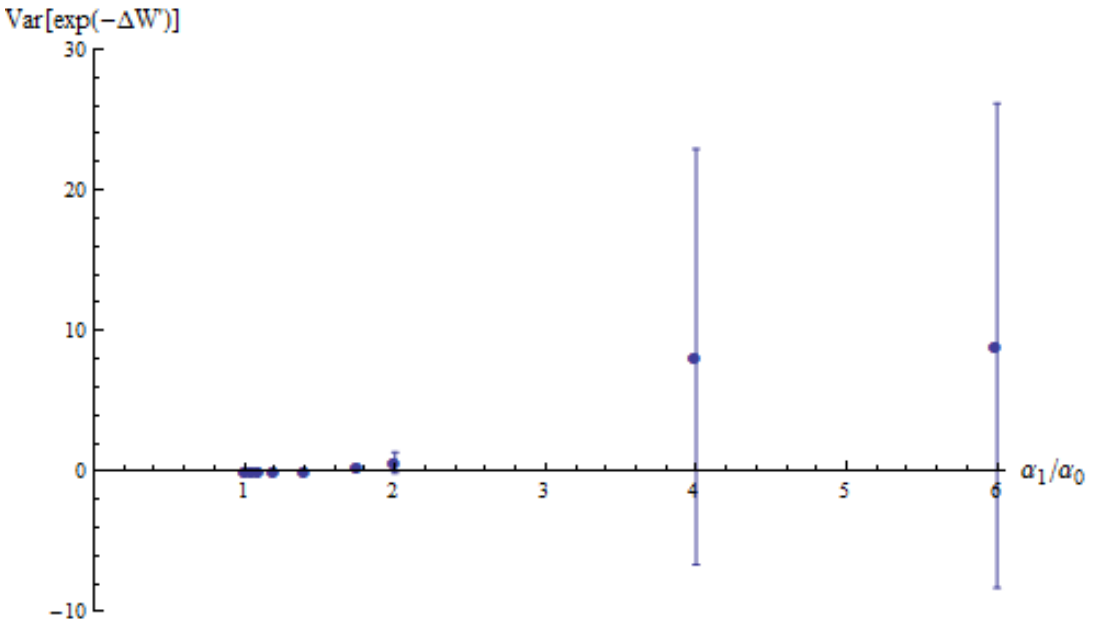

Figure 3.5: Results for numerically modelling the variance of $\exp(-\Delta W')$ for changes to various α_1 values from $\alpha_0 = 1$ for arbitrarily chosen range $x'_a = 0.5$.

which is rendered dimensionless as

$$y'^2_a = \frac{\left(\sigma'^2 + \alpha_0/\alpha_1\right)\left(\sigma'^2 + 1\right)}{\left(1 - \alpha_0/\alpha_1\right)} \ln\left(\frac{\sigma'^2 + 1}{\sigma'^2 + \alpha_0/\alpha_1}\right). \tag{3.23}$$

The results for numerical modelling of the process for the usual parameters (for each different result we have $x'_0 = 0$, $\Delta t' = 1$, and $dt' = 10^{-5}$ for 10 repeats of processes of 1000 cycles of 800000 time steps) with changes from $\alpha_0 = 1$ to $\alpha_1 = 1.2$ at various error values are given in figure 3.12. The results show a gradual decrease from a maximum value at $\sigma' = 0$ to a minimum value of 1 beyond the range of the figure. The numerical results follow the same curve, with results for smaller error deviating away from the theoretical prediction a little more than results for larger error.

Numerical results for the intrinsic variance are given in figure 3.13. They appear to follow a gradual increase with increase in σ', though the change is incredibly slow and fluctuative. It does imply a slight increase in the spread of work fluctuations as the error in measurement is increased. The feedback loses its effectiveness, and the work values start to fluctuate more as the mean tends back to 1.

Lastly, we can compare the evolution of the efficacy parameter with respect to the change in spring constant for measurement with error to that which is for measurement with no error. Figure 3.14 gives the results for numerically modelling this with the same parameters as before but with fixed error $\sigma' = 0.5$ and changes to various α_1 values. The expected decrease compared to a process with no error is evident, and the numerical data too shows this decrease, but with some deviation from the theoretical prediction for larger changes in spring constant. Figure 3.15 focusses on the smaller changes in spring constant, and shows the definite difference between the two different cases, as well as the numerical data following the prediction well.

As before, the variance can also be examined. Figure 3.16 shows the expected steady increase in variance from extremely small values for small changes in spring constant up to higher values for bigger changes, as seen in the other cases examined.

3.5 Optimal Change in Spring Constant

It is evidently desirous to maximise the value of the efficacy parameter so as to ensure that the feedback is as effective as possible in using information to gain work from the system. It has already been shown by others that the optimal protocol to achieve this is an instantaneous change in the Hamiltonian of the system after measurement [33]. For the system we have considered so far, we already feature an

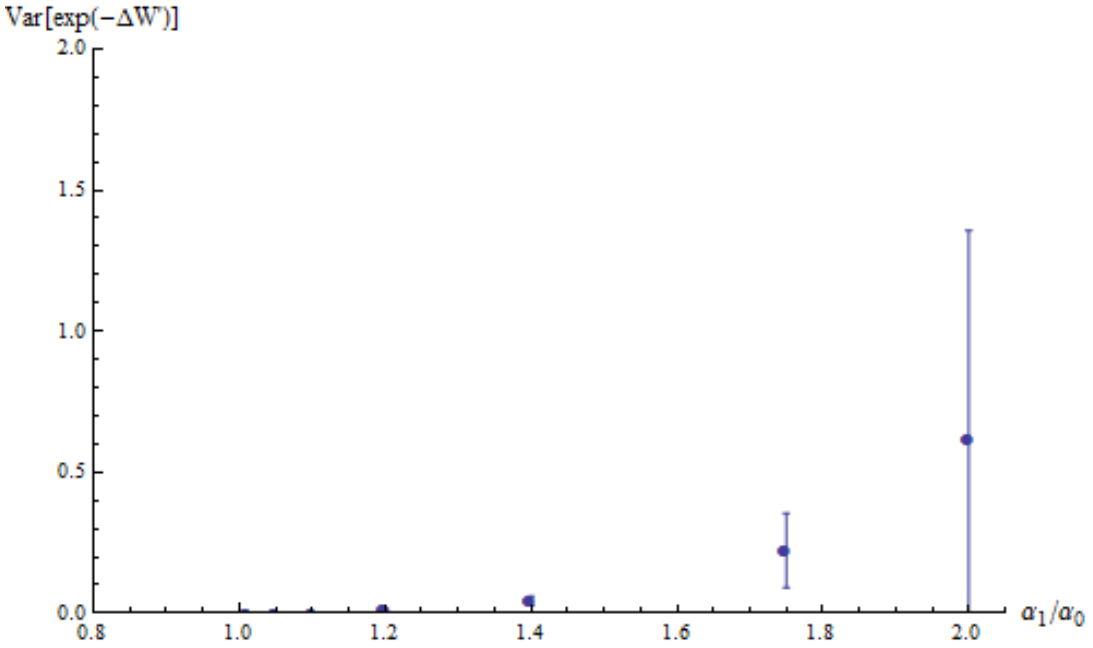

Figure 3.6: Results for numerically modelling the variance of $\exp(-\Delta W')$ for changes to various α_1 values from $\alpha_0 = 1$ for arbitrarily chosen range $x'_a = 0.5$, focussing on the lower changes in spring constant.

immediate change in the value of the spring constant. However, it is beneficial to consider what value of the spring constant it is optimal to change to in order to maximise the efficacy parameter.

It can be shown (but will not be here, it has been shown in currently unpublished work by the supervisor Ian J. Ford) that the optimal value of κ to change to is

$$\kappa(y) \propto \frac{1}{y^2}. \tag{3.24}$$

However, there is an obvious problem with this value. It is divergent if the measurement result y returns the value at the centre of the potential. This effectively renders a situation where the measurement device is omniscient. Therefore, we will consider modelling the characteristics of this value. Figure 3.17 shows the form of the optimal spring constant. As before, when y is close to the centre of the potential the spring constant value is increased. However, when y is much further out, we see that the spring constant value tends to zero. This indicates that we should take a step down in this case instead of just remaining at the same value.

Therefore, we shall model the case shown in figure 3.18 whereby at the start of the cycle we increase the spring constant from κ_0 to κ_u if $-y_a \leq y \leq +y_a$, decrease it to κ_l if $y \leq -y_b$ or $y \geq +y_b$, or keep it at κ_0 otherwise.

In this case (3.6) can be broken up like before

$$\begin{aligned}
\gamma_E &= 2\int_0^{y_a} dy\, G_u(y) + 2\int_{y_a}^{y_b} dy\, G_0(y) + 2\int_{y_b}^{\infty} dy\, G_l(y) \\
&= \int_{-y_a}^{+y_a} dy\, G_u(y) + \int_{-y_b}^{+y_b} dy\, G_0(y) - \int_{-y_a}^{+y_a} dy\, G_0(y) + \int_{-\infty}^{+\infty} dy\, G_l(y) \\
&\quad - \int_{-y_b}^{+y_b} dy\, G_l(y) \\
&= \int_{-y_a}^{+y_a} (G_u(y) - G_0(y))\, dy + \int_{-y_b}^{+y_b} (G_0(y) - G_l(y))\, dy + 1
\end{aligned} \tag{3.25}$$

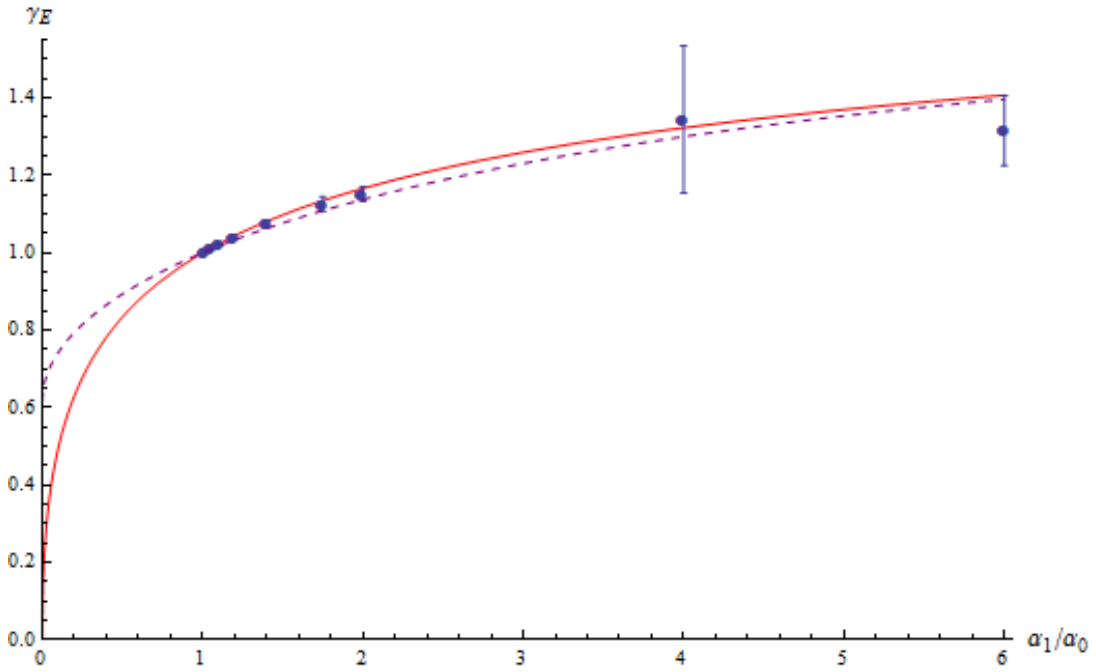

Figure 3.7: Results for numerically modelling the efficacy parameter, given by the blue data points, shown against the theoretical prediction for the optimal range, given by the red curve, also shown against the theoretical prediction for arbitrarily chosen range $x'_a = 0.5$, given by the purple dashed curve, for changes to various α_1 values from $\alpha_0 = 1$.

which can be written in terms of error functions

$$\begin{aligned}\gamma_E &= \operatorname{erf}\left[\frac{y_a}{\left(2\left(\sigma^2+(k_BT/\kappa_u)\right)\right)^{1/2}}\right] - \operatorname{erf}\left[\frac{y_a}{\left(2\left(\sigma^2+(k_BT/\kappa_0)\right)\right)^{1/2}}\right] \\ &\quad + \operatorname{erf}\left[\frac{y_b}{\left(2\left(\sigma^2+(k_BT/\kappa_0)\right)\right)^{1/2}}\right] - \operatorname{erf}\left[\frac{y_b}{\left(2\left(\sigma^2+(k_BT/\kappa_l)\right)\right)^{1/2}}\right] + 1 \end{aligned} \tag{3.26}$$

which for $\sigma = 0$, so $y_a = x_a$ and $y_b = x_b$, with dimensionless variables is

$$\gamma_E = \operatorname{erf}\left(\sqrt{\frac{\alpha_u}{2\alpha_0}}x'_a\right) - \operatorname{erf}\left(\frac{1}{\sqrt{2}}x'_a\right) + \operatorname{erf}\left(\frac{1}{\sqrt{2}}x'_b\right) - \operatorname{erf}\left(\sqrt{\frac{\alpha_l}{2\alpha_0}}x'_b\right) + 1. \tag{3.27}$$

We can also fnd the optimal ranges, given by the points where the gaussians in the integrals intersect

$$y_a^2 = \frac{\left(\sigma^2+(k_BT/\kappa_u)\right)\left(\sigma^2+(k_BT/\kappa_0)\right)}{k_BT\left(\kappa_0^{-1}-\kappa_u^{-1}\right)}\ln\left[\frac{\sigma^2+(k_BT/\kappa_0)}{\sigma^2+(k_BT/\kappa_u)}\right] \tag{3.28}$$

$$y_b^2 = \frac{\left(\sigma^2+(k_BT/\kappa_0)\right)\left(\sigma^2+(k_BT/\kappa_l)\right)}{k_BT\left(\kappa_l^{-1}-\kappa_0^{-1}\right)}\ln\left[\frac{\sigma^2+(k_BT/\kappa_l)}{\sigma^2+(k_BT/\kappa_0)}\right] \tag{3.29}$$

which for zero error and in dimensionless variables reduce to

$$x'^2_a = \frac{1}{\alpha_u-\alpha_0}\ln\left(\frac{\alpha_u}{\alpha_0}\right) \tag{3.30}$$

$$x'^2_b = \frac{1}{\alpha_0-\alpha_l}\ln\left(\frac{\alpha_0}{\alpha_l}\right). \tag{3.31}$$

This can be modelled by simply using the same methods as described in the preceding sections, but with the use of this new measurement-conditional protocol. Numerical results for processes with the same parameters as before (i.e. changes from $\alpha_0 = 1$ to various α_u values and with $\alpha_l = 0.8$ for all processes, where for each different α_u process results are found for 10 repeats of processes that start at

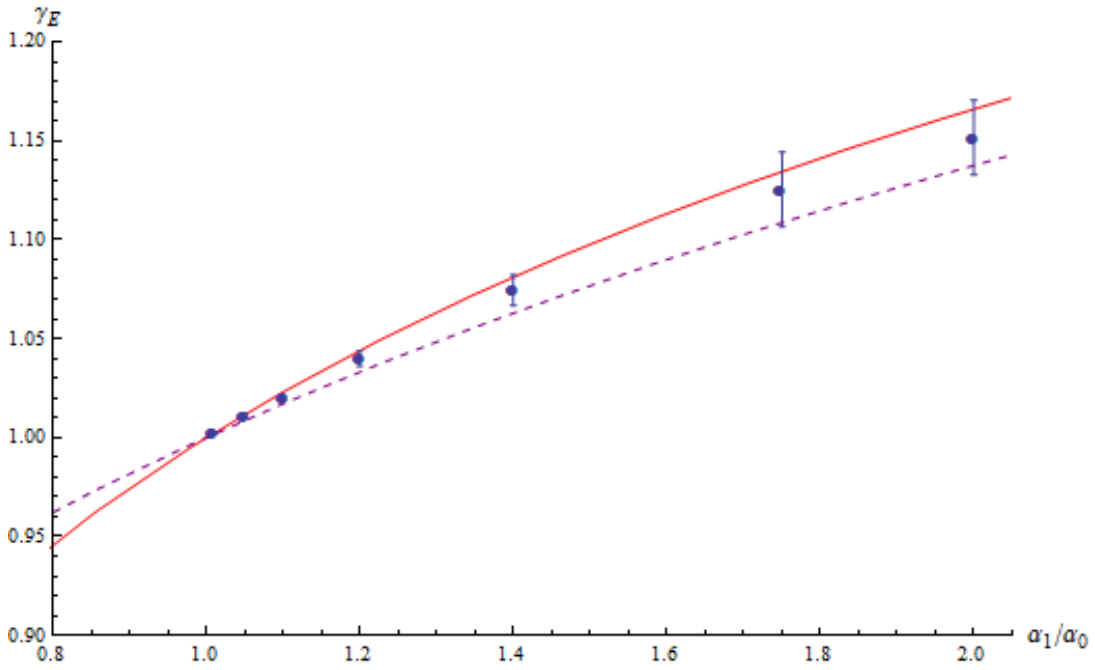

Figure 3.8: Results for numerically modelling the efficacy parameter, given by the blue data points, shown against the theoretical prediction for the optimal range, given by the red curve, also shown against the theoretical prediction for arbitrarily chosen range $x'_a = 0.5$, given by the purple dashed curve, for changes to various α_1 values from $\alpha_0 = 1$, focussing on lower changes in spring constant.

$x_0 = 0$ and are allowed to settle to equilibrium before starting on 1000 cycles of 800000 timesteps of size $dt' = 10^{-5}$, where the system is kept at α_u for $\Delta t' = 1$ for each cycle) are found in figure 3.19. The theoretical prediction shows a definite increase over the non-optimal protocol. Focussing in on the lower changes in spring constant in figure 3.20 shows a definite increase where the numerical results are close to the theoretical optimal γ_E value. However, 3.19 shows that the errors get large enough for the larger changes to not necessarily show the increase from the non-optimal value for those results.

Finally, we can examine numerical results for the variance in this case as well. Figure 3.21 shows the expected results now of a very small variance value for small changes in spring constant, gradually increasing with the increase in change in spring constant, but with larger errors settling in at much lower changes in spring constant than seen previously.

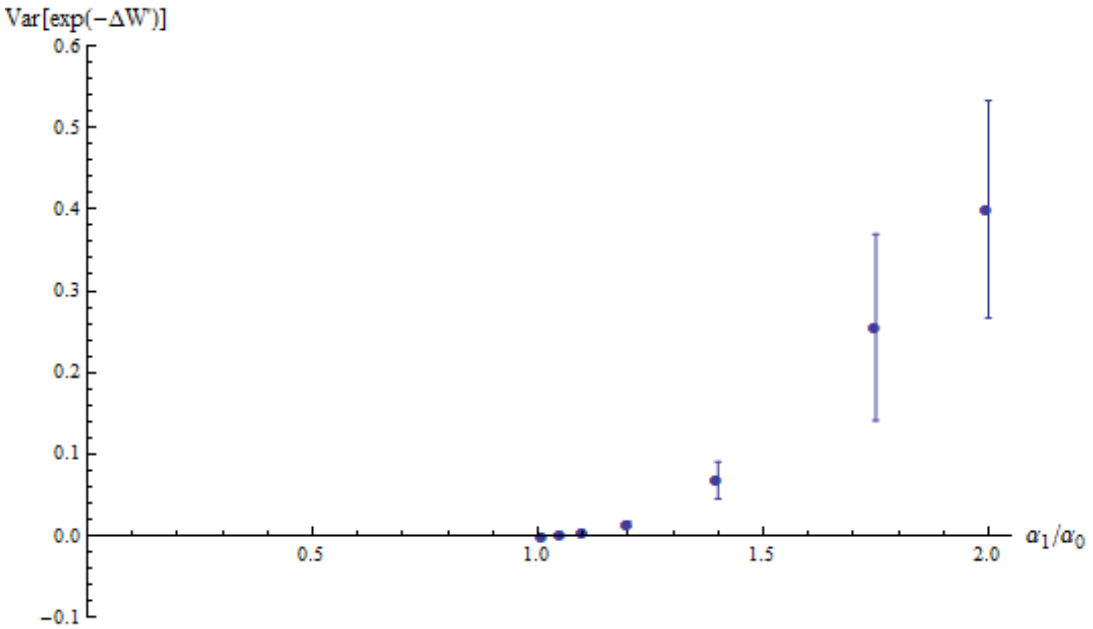

Figure 3.9: Results for numerically modelling the variance of $\exp(-\Delta W')$ for changes to various α_1 values from $\alpha_0 = 1$ for optimal range.

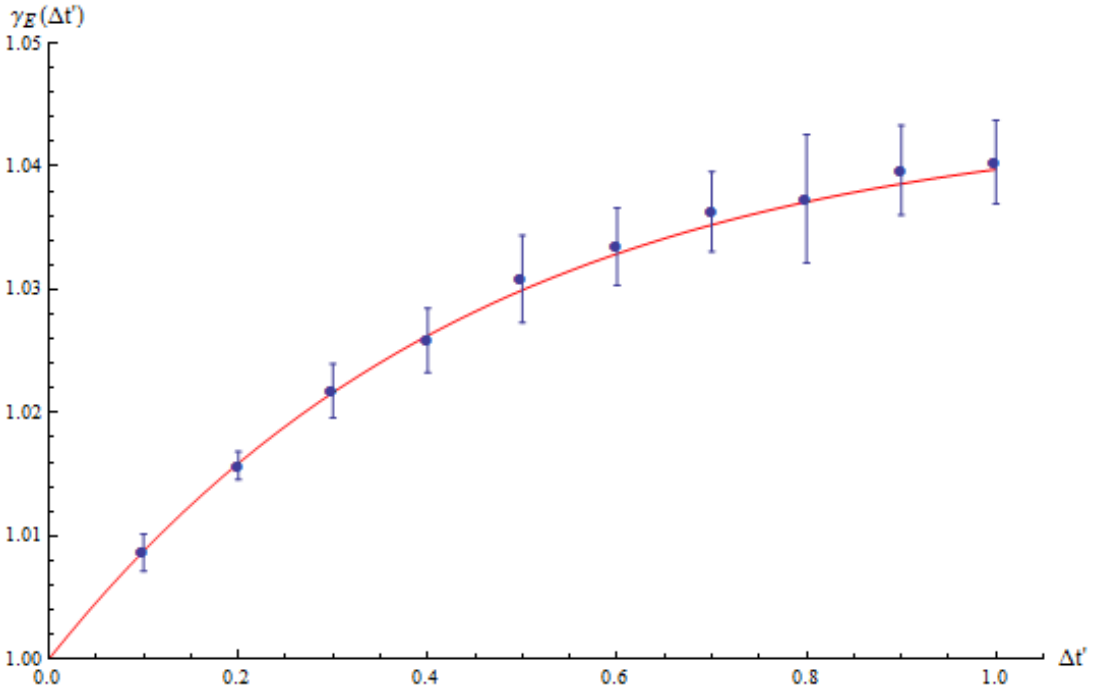

Figure 3.10: Results for numerically modelling γ_E dependent on the time the system spends at α_1, given by the blue data points, shown against the theoretical prediction, given by the red curve, for $\alpha_0 = 1$ and $\alpha_1 = 1.2$.

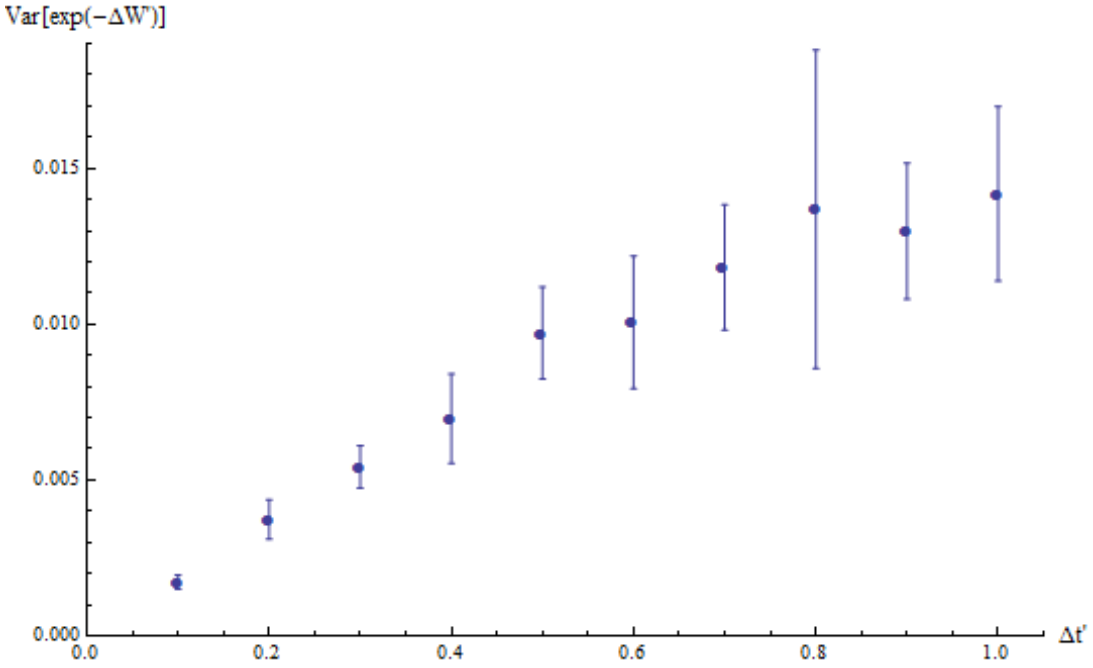

Figure 3.11: Results for numerically modelling the variance dependent on the time the system spends at α_1, given by the blue data points, for $\alpha_0 = 1$ and $\alpha_1 = 1.2$.

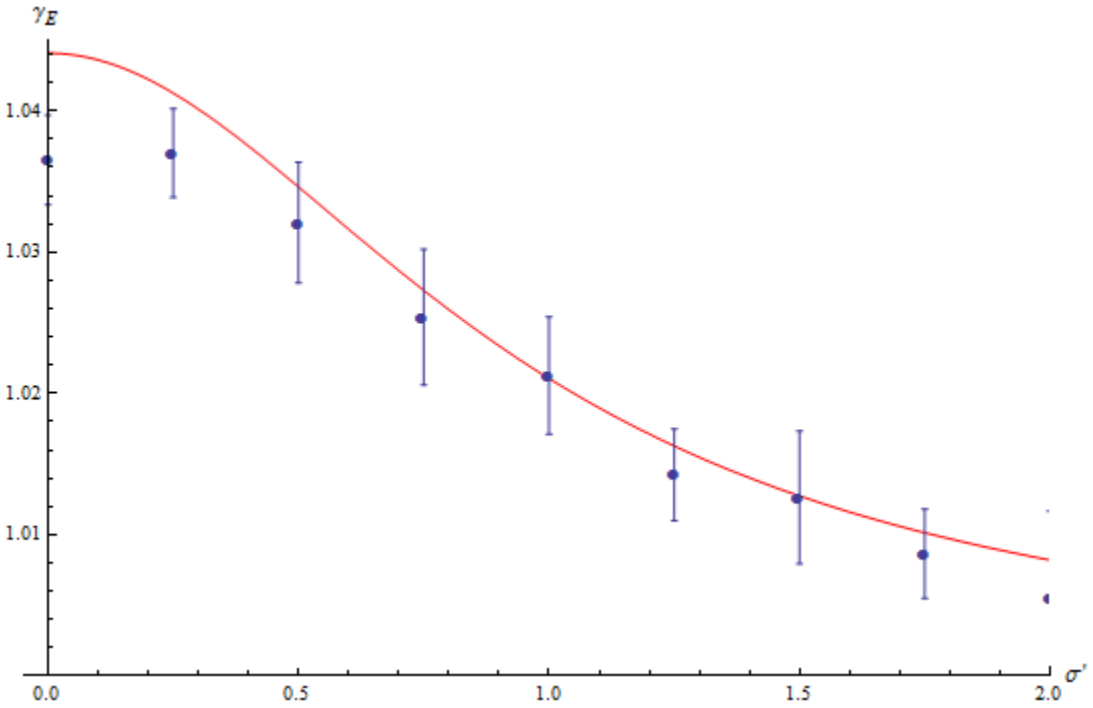

Figure 3.12: Results for numerically modelling the efficacy parameter dependent on the error in measurement, given by the blue data points, shown against the theoretical prediction, given by the red curve, for $\alpha_0 = 1$ and $\alpha_1 = 1.2$.

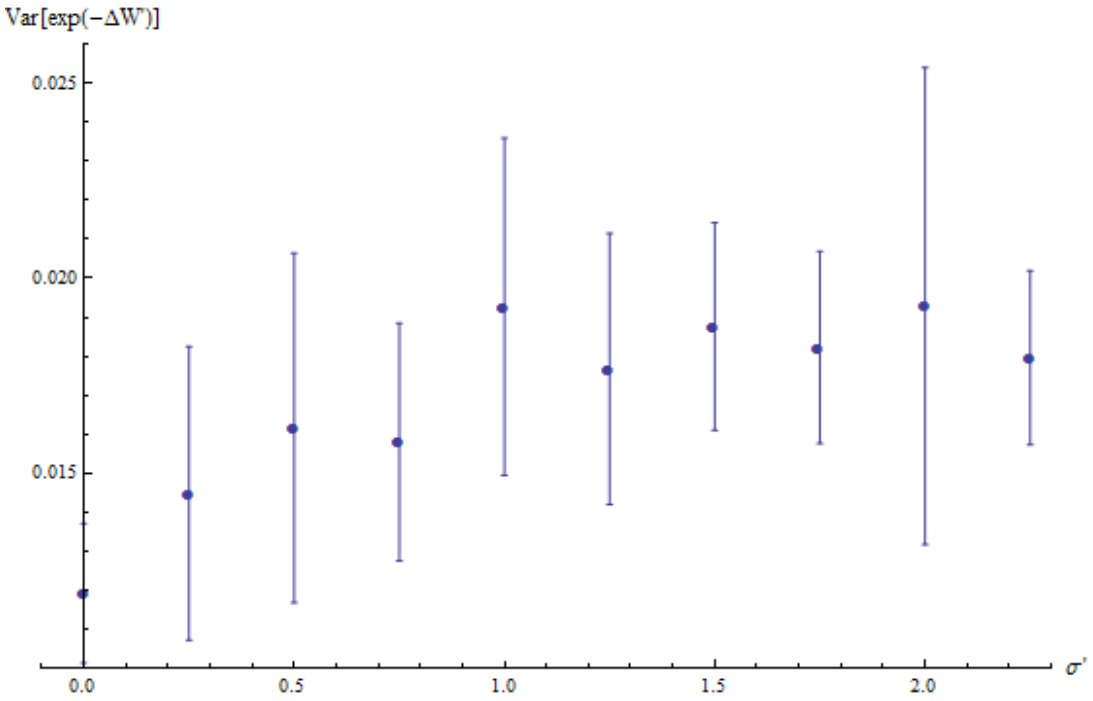

Figure 3.13: Results for numerically modelling the variance dependent on the error in measurement, given by the blue data points, for $\alpha_0 = 1$ and $\alpha_1 = 1.2$.

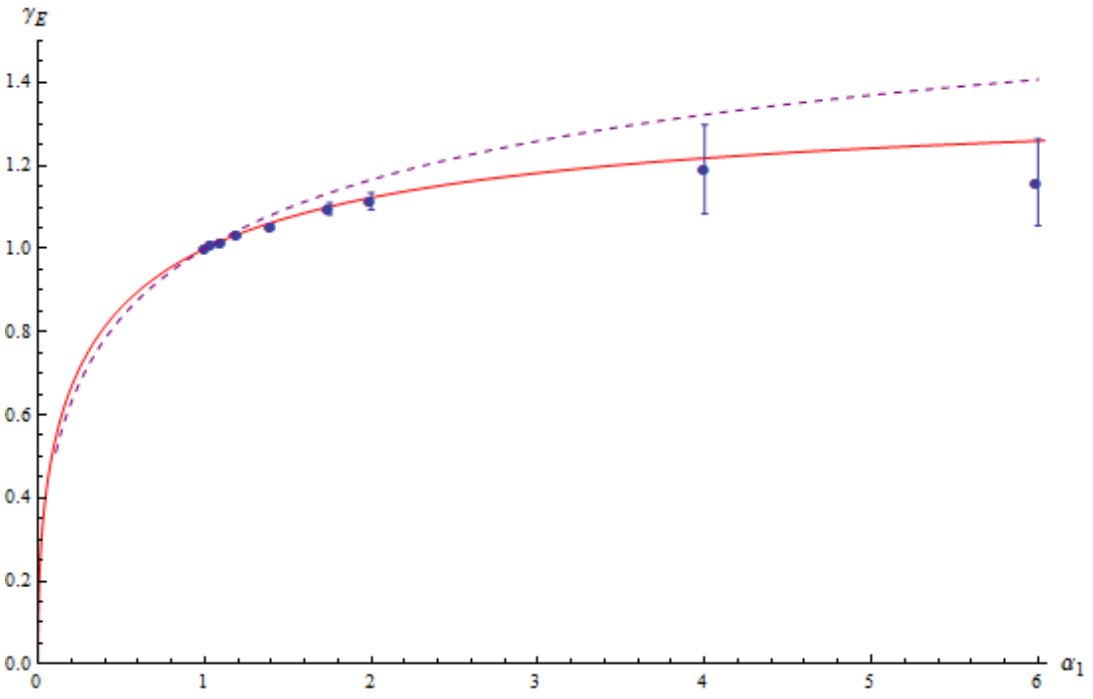

Figure 3.14: Results for numerically modelling the efficacy parameter for processes with error in measurement $\sigma' = 0.5$, given by the blue data points, compared to the theoretical prediction, given by the red curve, and also compared to the theoretical prediction for no error in measurement, given by the purple dashed curve, for changes from $\alpha_0 = 1$ to various α_1 values.

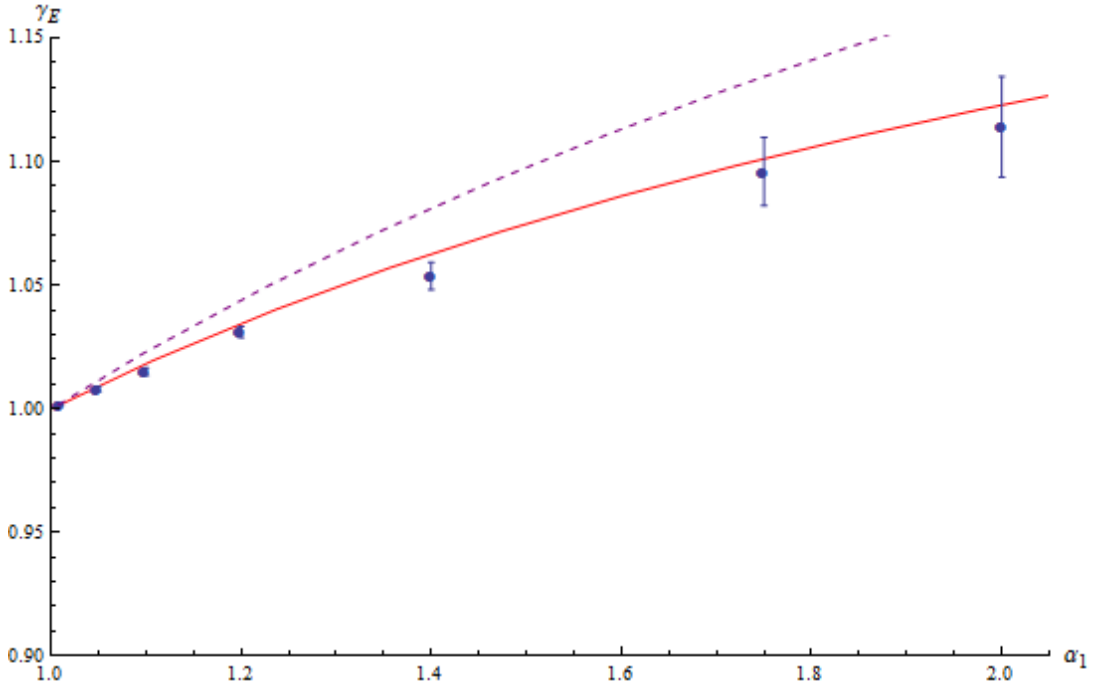

Figure 3.15: Results for numerically modelling the efficacy parameter for processes with error in measurement $\sigma' = 0.5$, given by the blue data points, compared to the theoretical prediction, given by the red curve, and also compared to the theoretical prediction for no error in measurement, given by the purple dashed curve, for changes from $\alpha_0 = 1$ to various α_1 values, focussing on the lower changes in spring constant.

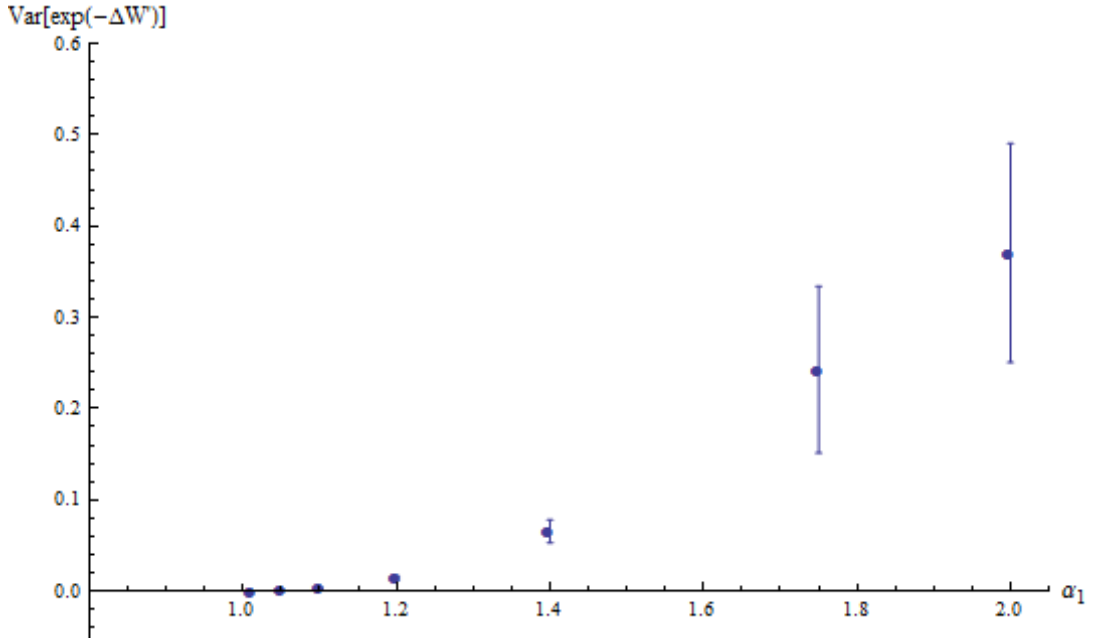

Figure 3.16: Results for numerically modelling the efficacy parameter for processes with error in measurement $\sigma' = 0.5$, given by the blue data points, for changes from $\alpha_0 = 1$ to various α_1 values.

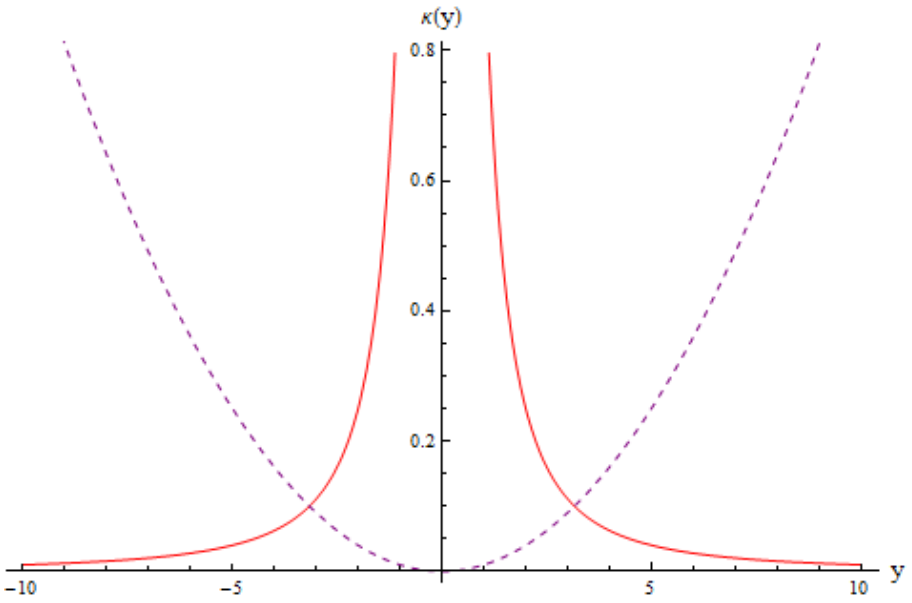

Figure 3.17: Optimal change in spring constant, given by the red curve, shown against the potential, given by the purple dashed line.

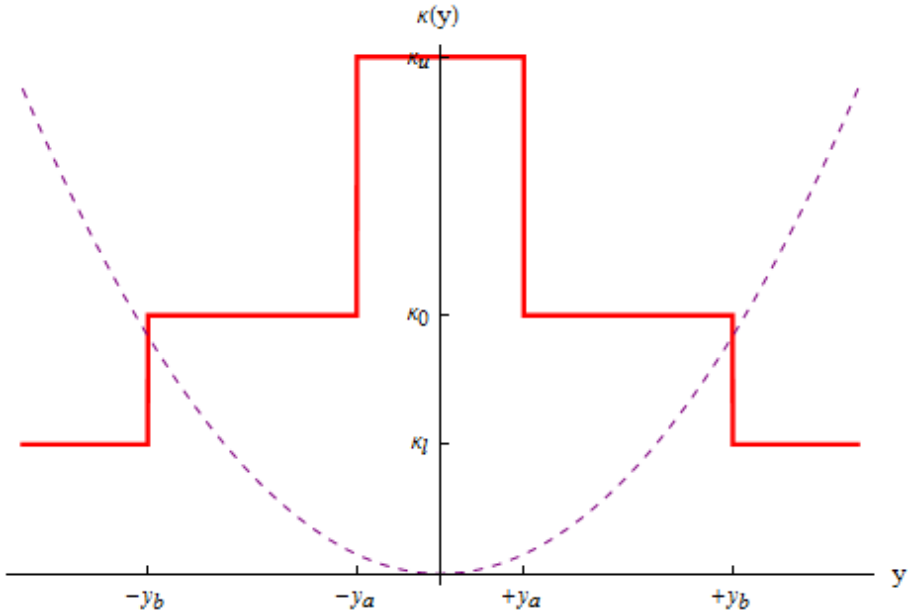

Figure 3.18: Change in spring constant to be modelled, given by the red curve, shown against the potential, given by the purple dashed line.

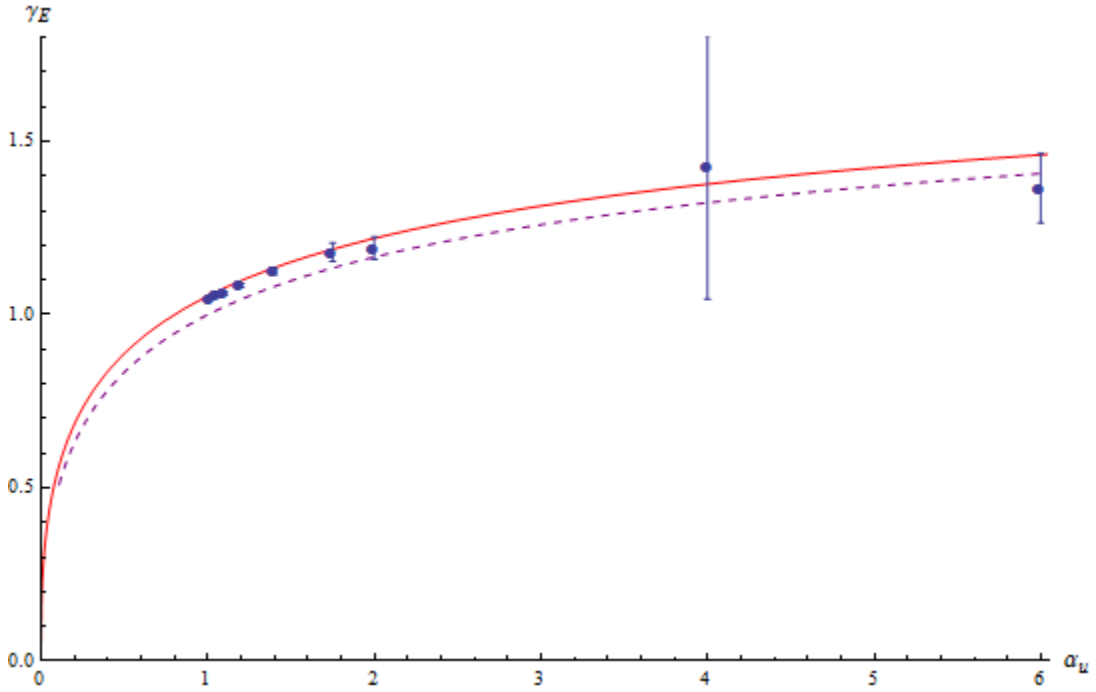

Figure 3.19: Results for numerically modelling the efficacy parameter under the optimal protocol, given by the blue data points, shown against the theoretical prediction for the optimal protocol, given by the red curve, also shown against the theoretical prediction for the usual protocol, given by the purple dashed curve, for changes to various α_u values from $\alpha_0 = 1$ and with $\alpha_l = 0.8$.

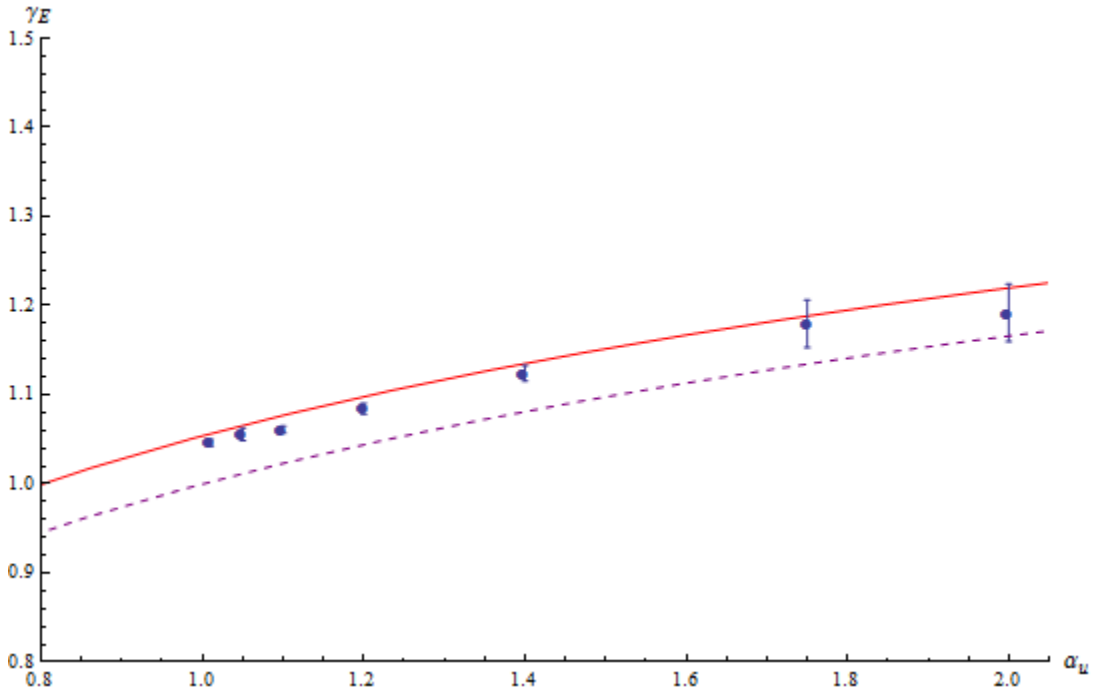

Figure 3.20: Results for numerically modelling the efficacy parameter under the optimal protocol, given by the blue data points, shown against the theoretical prediction for the optimal protocol, given by the red curve, also shown against the theoretical prediction for the usual protocol, given by the purple dashed curve, for changes to various α_u values from $\alpha_0 = 1$ and with $\alpha_l = 0.8$, focussing on lower changes in spring constant.

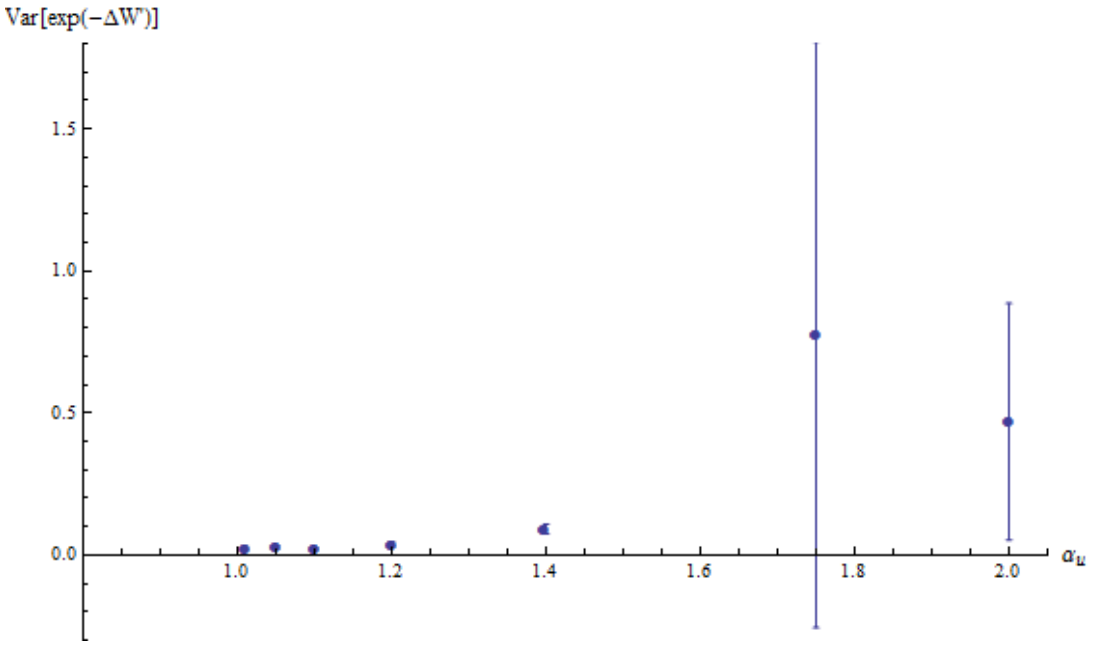

Figure 3.21: Results for numerically modelling the variance under the optimal protocol, given by the blue data points, for changes to various α_u values from $\alpha_0 = 1$ and with $\alpha_l = 0.8$.

Chapter 4

The Jarzynski-Tsallis Equality

4.1 Non-Isothermal Systems

A new generalisation of the Jarzynski equality can be found for non-isothermal systems, which have not been considered so far to the extent that feedback control systems have. Note that for this chapter we revert back to the process we considered in chapter 2, with the same protocol always being supplied for every cycle and no measurement taking place.

Instead of having a constant environment temperature, we consider a system with a position dependent temperature $T(x)$ such that the overdamped langevin equation (2.39) takes on the form

$$\dot{x} = -\frac{1}{m\gamma}\frac{\partial\phi(x,t)}{\partial x} + \left(\frac{2k_BT(x)}{m\gamma}\right)^{1/2}\xi(t) \tag{4.1}$$

which can be written in terms of differentials as

$$dx = -\frac{1}{m\gamma}\frac{\partial\phi(x,t)}{\partial x}\,dt + \left(\frac{2k_BT(x)}{m\gamma}\right)^{1/2}dW(t) \tag{4.2}$$

where $dW(t) = \xi(t)\,dt$ is the differential Wiener process.

We define a new stochastic function dependent on x, $\Theta = \Theta(x)$, which obeys the isothermal equation of motion

$$\dot{\Theta} = -\frac{1}{m\gamma}\frac{\partial\Phi(\Theta,t)}{\partial\Theta} + \left(\frac{2k_BT_0}{m\gamma}\right)^{1/2}\xi(t) \tag{4.3}$$

where $\Phi(\Theta,t)$ is the effective potential of Θ, and T_0 is a constant temperature parameter. This too can be expressed in terms of differentials as

$$d\Theta = -\frac{1}{m\gamma}\frac{\partial\Phi(\Theta,t)}{\partial\Theta}\,dt + \left(\frac{2k_BT_0}{m\gamma}\right)^{1/2}dW(t). \tag{4.4}$$

According to Ito's lemma [13] [14] the chain rule for a stochastic function $\Theta(x)$ is

$$d\Theta = \left(a(x,t)\frac{\partial\Theta}{\partial x} + \frac{1}{2}b(x,t)^2\frac{\partial^2\Theta}{\partial x^2}\right)dt + b(x,t)\frac{\partial\Theta}{\partial x}\,dW(t) \tag{4.5}$$

where $a(x,t)$ and $b(x,t)$ are given by (4.2) as

$$a(x,t) = -\frac{1}{m\gamma}\frac{\partial\phi(x,t)}{\partial x} \tag{4.6}$$

$$b(x,t) = \left(\frac{2k_BT(x)}{m\gamma}\right)^{1/2} \tag{4.7}$$

giving

$$d\Theta = \left(-\frac{1}{m\gamma}\frac{\partial\phi(x,t)}{\partial x}\frac{\partial\Theta}{\partial x} + \frac{k_BT(x)}{m\gamma}\frac{\partial^2\Theta}{\partial x^2}\right)dt + \left(\frac{2k_BT(x)}{m\gamma}\right)^{1/2}\frac{\partial\Theta}{\partial x}\,dW(t). \tag{4.8}$$

Comparing the coefficient of the $dW(t)$ term in (4.8) to that in (4.4) gives

$$\begin{aligned}\left(\frac{2k_BT(x)}{m\gamma}\right)^{1/2}\frac{\partial\Theta}{\partial x} &= \left(\frac{2k_BT_0}{m\gamma}\right)^{1/2}\\ \Rightarrow \frac{\partial\Theta}{\partial x} &= \frac{T_0^{1/2}}{T(x)^{1/2}}.\end{aligned} \tag{4.9}$$

We consider a system where the temperature has a quadratic dependence on the position, similar to that of the potential

$$\phi(x,t) = \frac{1}{2}\kappa(t)x^2 \tag{4.10}$$

such that

$$T(x) = T_0\left(1+\frac{\kappa_T x^2}{2k_BT_0}\right) \tag{4.11}$$

where $\kappa_T \geq 0$ is a parameter determining how far the system is from being isothermal. Inserting this into our expression and integrating

$$\begin{aligned}\Theta &= \int \frac{1}{\left(1+\frac{\kappa_T x^2}{2k_BT_0}\right)^{1/2}}\,dx\\ &= \sqrt{\frac{2k_BT_0}{\kappa_T}}\int\frac{1}{(1+u^2)^{1/2}}\,du\end{aligned} \tag{4.12}$$

making the substitution $u = \sqrt{\kappa_T/2k_BT_0}x$. Making the further substitution $\sinh\theta = u$

$$\begin{aligned}\Theta &= \sqrt{\frac{2k_BT_0}{\kappa_T}}\int\frac{\cosh\theta}{\left(1+\sinh^2\theta\right)^{1/2}}\,d\theta\\ &= \sqrt{\frac{2k_BT_0}{\kappa_T}}\int\frac{\cosh\theta}{\left(\cosh^2\theta\right)^{1/2}}\,d\theta\\ &= \sqrt{\frac{2k_BT_0}{\kappa_T}}\int d\theta\\ &= \sqrt{\frac{2k_BT_0}{\kappa_T}}\theta + \text{constant}\\ &= \sqrt{\frac{2k_BT_0}{\kappa_T}}\text{arcsinh}u + \text{constant}\\ \Rightarrow \Theta(x) &= \sqrt{\frac{2k_BT_0}{\kappa_T}}\text{arcsinh}\left(\sqrt{\frac{\kappa_T}{2k_BT_0}}x\right) + \text{constant}.\end{aligned} \tag{4.13}$$

From this

$$\frac{\partial\Theta}{\partial x} = \frac{1}{\left(1+\frac{\kappa_T x^2}{2k_BT_0}\right)^{1/2}} \tag{4.14}$$

$$\frac{\partial^2\Theta}{\partial x^2} = -\frac{\kappa_T x}{2k_BT_0}\frac{1}{\left(1+\frac{\kappa_T x^2}{2k_BT_0}\right)^{3/2}}. \tag{4.15}$$

Comparing the dt terms in (4.4) and (4.8) gives

$$\begin{aligned}
-\frac{1}{m\gamma}\frac{\partial\Phi(\Theta,t)}{\partial\Theta} &= -\frac{1}{m\gamma}\frac{\partial\phi}{\partial x}\frac{\partial\Theta}{\partial x}+\frac{k_BT(x)}{m\gamma}\frac{\partial^2\Theta}{\partial x^2}\\
\Rightarrow \frac{\partial\Phi(\Theta,t)}{\partial\Theta} &= \kappa(t)x\frac{\partial\Theta}{\partial x}-k_BT_0\left(1+\frac{\kappa_Tx^2}{2k_BT_0}\right)\frac{\partial^2\Theta}{\partial x^2}\\
&= \frac{\kappa(t)x}{\left(1+\frac{\kappa_Tx^2}{2k_BT_0}\right)^{1/2}}+\frac{k_BT_0\kappa_Tx}{2k_BT_0}\frac{\left(1+\frac{\kappa_Tx^2}{2k_BT_0}\right)}{\left(1+\frac{\kappa_Tx^2}{2k_BT_0}\right)^{3/2}}\\
&= \frac{\left(\kappa(t)+\frac{1}{2}\kappa_T\right)x}{\left(1+\frac{\kappa_Tx^2}{2k_BT_0}\right)^{1/2}}\\
&= \left(\kappa(t)+\frac{1}{2}\kappa_T\right)\sqrt{\frac{2k_BT_0}{\kappa_T}}\frac{\sinh\left(\sqrt{\frac{\kappa_t}{2k_BT_0}}\Theta\right)}{\left(1+\sinh^2\left(\sqrt{\frac{\kappa_T}{2k_BT_0}}\Theta\right)\right)^{1/2}}\\
&= \left(\kappa(t)+\frac{1}{2}\kappa_T\right)\sqrt{\frac{2k_BT_0}{\kappa_T}}\frac{\sinh\left(\sqrt{\frac{\kappa_T}{2k_BT_0}}\Theta\right)}{\cosh\left(\sqrt{\frac{\kappa_T}{2k_BT_0}}\Theta\right)}\\
\Rightarrow \Phi(\Theta,t) &= \left(\kappa(t)+\frac{1}{2}\kappa_T\right)\sqrt{\frac{2k_BT_0}{\kappa_T}}\int\frac{\sinh\left(\sqrt{\frac{\kappa_T}{2k_BT_0}}\Theta\right)}{\cosh\left(\sqrt{\frac{\kappa_T}{2k_BT_0}}\Theta\right)}\,d\Theta\\
&= \left(\kappa(t)+\frac{1}{2}\kappa_T\right)\left(\frac{2k_BT_0}{\kappa_T}\right)\int\frac{\sinh\nu}{\cosh\nu}\,d\nu
\end{aligned}\tag{4.16}$$

where we have made the substitution $\nu=\sqrt{\kappa_T/2k_BT_0}\Theta$, which gives

$$\begin{aligned}
\Phi(\Theta,t) &= \left(\kappa(t)+\frac{1}{2}\kappa_T\right)\left(\frac{2k_BT_0}{\kappa_T}\right)\int\frac{e^{\nu}-e^{-\nu}}{e^{\nu}+e^{-\nu}}\,d\nu\\
&= \left(\kappa(t)+\frac{1}{2}\kappa_T\right)\left(\frac{2k_BT_0}{\kappa_T}\right)\int\frac{1}{\omega}\,d\omega
\end{aligned}\tag{4.17}$$

making the substitution $\omega=\frac{1}{2}\left(e^{\nu}+e^{-\nu}\right)$, so

$$\begin{aligned}
\Phi(\Theta,t) &= \left(\kappa(t)+\frac{1}{2}\kappa_T\right)\left(\frac{2k_BT_0}{\kappa_T}\right)\ln\omega\\
&= \left(\kappa(t)+\frac{1}{2}\kappa_T\right)\left(\frac{2k_BT_0}{\kappa_T}\right)\ln\left(\frac{1}{2}e^{\nu}+\frac{1}{2}e^{-\nu}\right)\\
&= \left(\kappa(t)+\frac{1}{2}\kappa_T\right)\left(\frac{2k_BT_0}{\kappa_T}\right)\ln\left(\cosh u\right)\\
&= \left(\kappa(t)+\frac{1}{2}\kappa_T\right)\left(\frac{2k_BT_0}{\kappa_T}\right)\ln\left[\cosh\left(\sqrt{\frac{\kappa_T}{2k_BT_0}}\Theta\right)\right]\\
&= \left(\kappa(t)+\frac{1}{2}\kappa_T\right)\left(\frac{2k_BT_0}{\kappa_T}\right)\frac{1}{2}\ln\left[\cosh^2\left(\sqrt{\frac{\kappa_T}{2k_BT_0}}\Theta\right)\right]\\
&= \left(\kappa(t)+\frac{1}{2}\kappa_T\right)\left(\frac{2k_BT_0}{\kappa_T}\right)\frac{1}{2}\ln\left[1+\sinh^2\left(\sqrt{\frac{\kappa_T}{2k_BT_0}}\Theta\right)\right]\\
&= \left(\kappa(t)+\frac{1}{2}\kappa_T\right)\left(\frac{2k_BT_0}{\kappa_T}\right)\frac{1}{2}\ln\left[1+\frac{\kappa_tx^2}{2k_BT_0}\right].
\end{aligned}\tag{4.18}$$

For the step up step down process we considered in chapter one, the effective work $\Delta\Omega_0$ for Θ is given by

$$\begin{aligned}
\Delta\Omega_0 &= \Phi(\Theta_u,\kappa_1)-\Phi(\Theta_u,\kappa_0)+\Phi(\Theta_d,\kappa_0)-\Phi(\Theta_d,\kappa_1)\\
&= \Phi(x_u,\kappa_1)-\Phi(x_u,\kappa_0)+\Phi(x_d,\kappa_0)-\Phi(x_d,\kappa_1)
\end{aligned}\tag{4.19}$$

where Θ_u and x_u are the values of Θ and x at the step up, Θ_d and x_d are the values at the step down, κ_0 is the spring constant at the start of the process, and κ_1 is the spring constant that we step up to. We see here that

$$\begin{aligned}
-\frac{\Phi(x_u,\kappa_1)-\Phi(x_u,\kappa_0)}{k_BT_0} &= -\frac{\kappa_1+\frac{1}{2}\kappa_T}{k_BT_0}\frac{2k_BT_0}{\kappa_T}\frac{1}{2}\ln\left[1+\frac{\kappa_T x_u^2}{2k_BT_0}\right]+\frac{\kappa_0+\frac{1}{2}\kappa_T}{k_BT_0}\frac{2k_BT_0}{\kappa_T}\frac{1}{2}\ln\left[1+\frac{\kappa_T x_u^2}{2k_BT_0}\right] \\
&= \ln\left[1+\frac{\kappa_T x_u^2}{2k_BT_0}\right]\left(\frac{\kappa_0+\frac{1}{2}\kappa_T-\kappa_1-\frac{1}{2}\kappa_T}{\kappa_T}\right) \\
&= \ln\left[\left(1+\frac{\kappa_T x_u^2}{2k_BT_0}\right)^{\frac{\kappa_0-\kappa_1}{\kappa_T}}\right] \qquad (4.20)
\end{aligned}$$

and similarly

$$-\frac{\Phi(x_d,\kappa_0)-\Phi(x_d,\kappa_1)}{k_BT_0} = \ln\left[\left(1+\frac{\kappa_T x_d^2}{2k_BT_0}\right)^{\frac{\kappa_1-\kappa_0}{\kappa_T}}\right]. \qquad (4.21)$$

Therefore

$$\begin{aligned}
e^{-\Delta\Omega_0/k_BT_0} &= \left(1+\frac{\kappa_T x_u^2}{2k_BT_0}\right)^{\frac{\kappa_0-\kappa_1}{\kappa_T}}\times\left(1+\frac{\kappa_T x_d^2}{2k_BT_0}\right)^{\frac{\kappa_1-\kappa_0}{\kappa_T}} \\
&= \left(1+\left(1-\left(1+\frac{\kappa_T}{\kappa_1-\kappa_0}\right)\right)\frac{\left(-\frac{1}{2}\left(\kappa_1-\kappa_0\right)x_u^2\right)}{2k_BT_0}\right)^{\frac{1}{1-\left(1+\frac{\kappa_T}{\kappa_1-\kappa_0}\right)}} \\
&\quad\times\left(1+\left(1-\left(1-\frac{\kappa_T}{\kappa_1-\kappa_0}\right)\right)\frac{\left(-\frac{1}{2}\left(\kappa_0-\kappa_1\right)x_d^2\right)}{2k_BT_0}\right)^{\frac{1}{1-\left(1-\frac{\kappa_T}{\kappa_1-\kappa_0}\right)}}. \qquad (4.22)
\end{aligned}$$

Recall that $\Delta W_{0\to1}=\frac{1}{2}\left(\kappa_1-\kappa_0\right)x_u^2$ and $\Delta W_{1\to0}=\frac{1}{2}\left(\kappa_0-\kappa_1\right)x_d^2$, and define

$$q_\pm = 1\pm\frac{\kappa_T}{\kappa_1-\kappa_0} \qquad (4.23)$$

so this gives us

$$e^{-\Delta\Omega_0/k_BT_0} = \left(1+\left(1-q_+\right)\left(-\Delta W_{0\to1}/k_BT\right)\right)^{\frac{1}{1-q_+}}\times\left(1+\left(1-q_-\right)\left(-\Delta W_{1\to0}/k_BT\right)\right)^{\frac{1}{1-q_-}}. \qquad (4.24)$$

Here we introduce the Tsallis q-exponential [34], which is defined as

$$\exp_q(z) = \left(1+\left(1-q\right)z\right)^{\frac{1}{1-q}} \qquad (4.25)$$

where q is a constant parameter characteristic of the system, and $\exp_1(z)=\exp(z)$. The inverse of this is the Tsallis q-logarithm

$$\ln_q(z) = \frac{z^{1-q}-1}{1-q} \qquad (4.26)$$

where $\ln_1(z)=\ln(z)$.

Therefore, we see that

$$e^{-\Delta\Omega_0/k_BT_0} = \exp_{q_+}\left(-\Delta W_{0\to1}/k_BT_0\right)\exp_{q_-}\left(-\Delta W_{1\to0}/k_BT_0\right). \qquad (4.27)$$

As Θ obeys the isothermal Langevin equation, as in chapter 2 it must obey the Jarzynski equality, which for the cyclic process is

$$\left\langle e^{-\Delta\Omega_0/k_BT_0}\right\rangle = 1. \qquad (4.28)$$

For the averaging $\langle\ldots\rangle$ we note that $d\Theta_u\,d\Theta_d\,p(\Theta_u,\Theta_d)=dx_u\,dx_d\,p(x_u,x_d)$, so we can therefore write out the Jarzynski equality of Θ in terms of x. The Jarzynski equality for non-isothermal systems for the step process we are considering can then be written as

$$\left\langle\exp_{q_+}\left(-\Delta W_{0\to1}/k_BT_0\right)\exp_{q_-}\left(-\Delta w_{1\to0}/k_BT_0\right)\right\rangle = 1 \qquad (4.29)$$

which is a new equality we shall call here the Jarzynski-Tsallis equality for the simple step up step down process.

Note that, due to the nature of the derivation in considering an effective work split into steps, it is possible to then generalise this equality to processes formed from many steps.

4.2 Modelling the Jarzynski-Tsallis Equality

To model the Jarzynski-Tsallis equality we must first re-write (4.1) as a finite difference update equation. Firstly, the equation is

$$\dot{x} = -\frac{\kappa(t)}{m\gamma}x + \left[\frac{2k_BT_0}{m\gamma}\left(1 + \frac{\kappa_T}{2k_BT_0}x^2\right)\right]^{1/2}\xi(t). \tag{4.30}$$

Using (2.62), (2.63), and (2.64), this equation can then be rendered in terms of dimensionless variables

$$\dot{x}' = -\alpha(t)x' + \left(2\alpha_0 + \alpha_T x'^2\right)^{1/2}\xi'(t) \tag{4.31}$$

which can be expressed in finite difference form as

$$\frac{x'(t'+dt') - x'(t')}{dt'} = -\alpha(t)x'(t') + \left(2\alpha_0 + \alpha_T x'^2(t')\right)^{1/2} N_{t'}^{t'+dt'}(0,1) \tag{4.32}$$

where $\alpha_i = \kappa_i/m\gamma^2$ as before, and writing $x'_{n+1} = x'(t'+dt')$ and $x'_n = x'(t')$ this can be rearranged into an update equation for the position

$$x'_{n+1} = (1 - \alpha(t)\,dt')\,x'_n + \left[\left(2\alpha_0 + \alpha_T x'^2_n\right)dt'\right]^{1/2} N_{t'}^{t'+dt'}(0,1). \tag{4.33}$$

Like in chapter 2, this update can then be run for N cycles of the step up step down process. The dimensionless work values $\Delta W'_{0\to1} = \Delta W_{0\to1}/k_BT_0$ and $\Delta W'_{1\to0} = \Delta W_{1\to0}/k_BT_0$ are measured for each cycle, and the numerical average of the Tsallis q-exponentials can be calculated using

$$\left\langle \exp_{q_+}\left(-\Delta W'_{0\to1}\right)\exp_{q_-}\left(-\Delta W'_{1\to0}\right)\right\rangle = \frac{1}{N}\sum_{i=1}^{N}\exp_{q_+}\left(-\Delta W'_{0\to1,i}\right)\exp_{q_-}\left(-\Delta W'_{1\to0,i}\right) \tag{4.34}$$

where the q values can be given in terms of dimensionless spring constants $q_\pm = 1 \pm \alpha_t/(\alpha_1 - \alpha_0)$. This can then be compared against the prediction

$$\left\langle \exp_{q_+}\left(-\Delta W'_{0\to1}\right)\exp_{q_-}\left(-\Delta W'_{1\to0}\right)\right\rangle = 1. \tag{4.35}$$

The variance can also be modelled using the same method in chapter 2

$$\begin{aligned}\mathrm{Var}\left(\exp_{q_+}\left(-\Delta W'_{0\to1}\right)\exp_{q_-}\left(-\Delta W'_{1\to0}\right)\right) =& \frac{1}{N}\sum_{i=1}^{N}\left(\exp_{q_+}\left(-\Delta W'_{0\to1,i}\right)\exp_{q_-}\left(-\Delta W'_{1\to0,i}\right)\right)^2 \\ &+ \left(\frac{1}{N}\sum_{i=1}^{N}\exp_{q_+}\left(-\Delta W'_{0\to1,i}\right)\exp_{q_-}\left(-\Delta W'_{1\to0,i}\right)\right)^2.\end{aligned} \tag{4.36}$$

Numerical results are shown in figure 4.1. For each result for changes from $\alpha_0 = 1$ to each various α_1 value, results are found as before from 20 repeats of a process starting at $x_0 = 0$ and resting to equilibrium before embarking on 1000 cycles of the protocol. Each cycle is 800000 timesteps long, each timestep has size $dt' = 10^{-5}$, and within each cycle the system spends $\Delta t' = 4$ at α_1. The results show a very close fit to the theoretical prediction, and are indicative of the new relation being correct. As for each process a different α_T value was used, the results are also displayed in table 4.1. Again, this shows the close correlation of the results. As throughout the report, all error values are given by one statistical standard deviation of the repeated results.

Figure 4.2 shows the results for the variance. These results are also stored in table 4.1. As is predictable from previous results and the knowledge that this equality too is only meant for small systems, these results show an increase in the variance for larger changes in spring constant value. The higher results are not shown in the figure, as, like before, the statistical errors are so large for them as to render them unreliable.

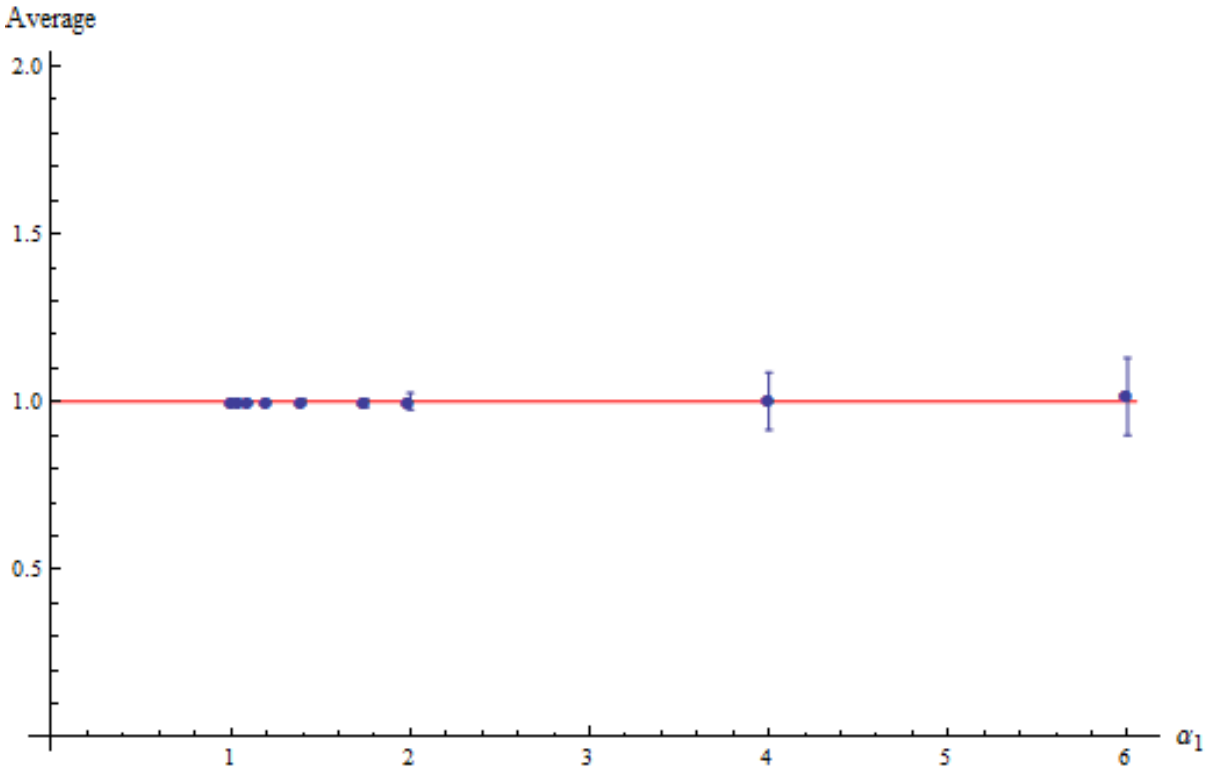

Figure 4.1: Numerical results for averages of Tsallis q-exponentiated work values, given by blue data points, plotted against the theoretical prediction, given by a red line, for increasing changes in α from an initial value $\alpha_0 = 1$ for a non-isothermal system, with various chosen α_T values.

4.3 The Crooks-Tsallis Work Relation

One last final point of interest is in examining the statistics of the non-isothermal system, and in examining the generalisation of the Crooks work relation (2.58) as well.

Firstly, we examine the initial distribution of the position. We assume that the effective function Θ starts in equilibrium, such that

$$p_{\text{eq}}(\Theta) \propto \exp\left(-\Phi(\Theta)/k_B T_0\right) \tag{4.37}$$

α_1	α_T	Average	Variance
1.01	1.005	1.0000 ± 0.0001	0.000056 ± 0.00000257
1.05	1.025	1.000 ± 0.0011	0.0014 ± 0.000124
1.10	1.050	1.000 ± 0.0017	0.0053 ± 0.000519
1.20	1.100	0.9996 ± 0.0021	0.0195 ± 0.0021
1.40	1.200	1.0008 ± 0.0072	0.0699 ± 0.0121
1.75	1.375	0.9963 ± 0.0122	0.2353 ± 0.1066
2.00	1.000	1.0016 ± 0.0245	0.6745 ± 0.6714
4.00	2.500	1.0019 ± 0.0852	5.7448 ± 15.1328
6.00	3.500	1.0157 ± 0.1150	14.8405 ± 29.9929

Table 4.1: Results for numerical test of the Jarzynski-Tsallis equality, with $\alpha_0 = 1.0$, $\Delta t = 10^{-5}$, and $N = 10^3$.

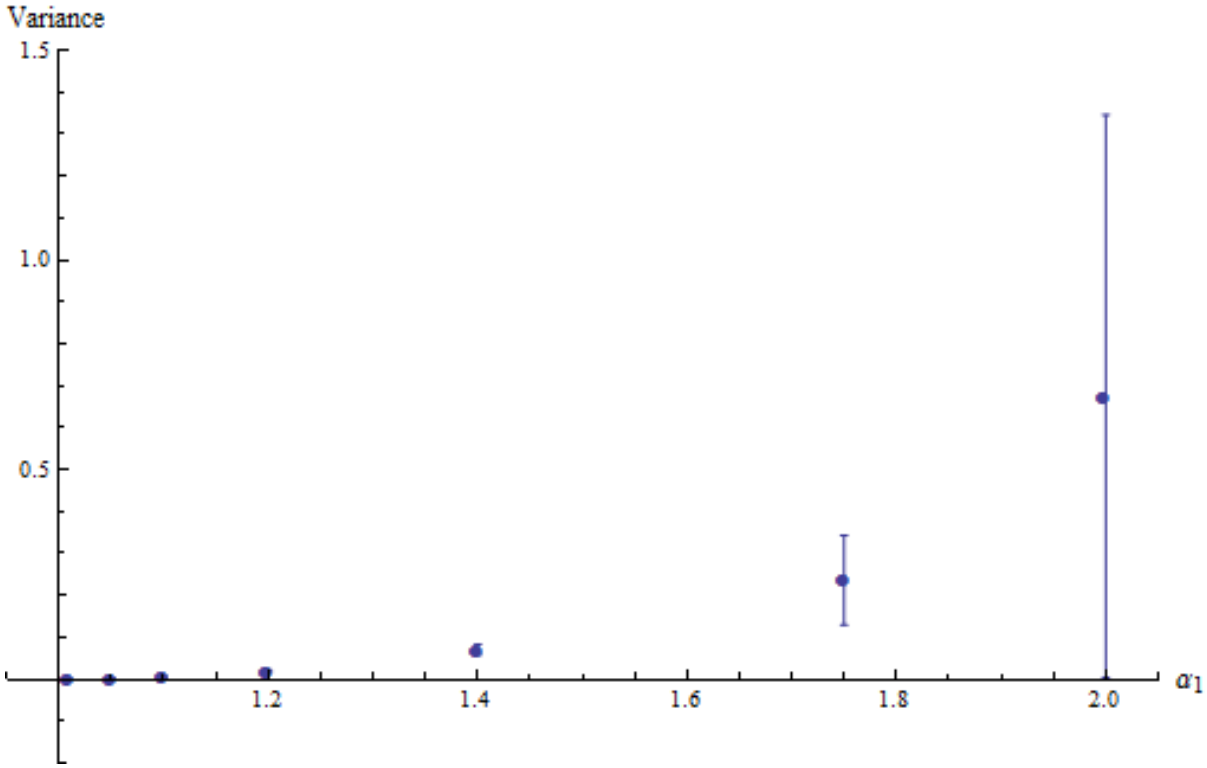

Figure 4.2: Numerical results for variances of the q-exponentiated work values, given by blue data points, for increasing changes in α from an initial value $\alpha_0 = 1$ for a non-isothermal system, with various chosen α_T values.

so that the initial distribution of the position $p_0(x)$ is

$$\begin{aligned} p_0(x) &\propto \frac{d\Theta}{dx}\exp\left(-\Phi(\Theta)/k_BT_0\right) \\ &= \frac{1}{\left(1+\frac{\kappa_T x^2}{2k_BT_0}\right)^{1/2}}\exp\left[-\left(\kappa_0+\frac{1}{2}\kappa_T\right)\left(\frac{2k_BT_0}{\kappa_T}\right)\frac{1}{2}\ln\left(1+\frac{\kappa_T x^2}{2k_BT_0}\right)/k_BT_0\right] \\ &= \frac{1}{\left(1+\frac{\kappa_T x^2}{2k_BT_0}\right)^{1/2}}\left[\left(1+\frac{\kappa_T x^2}{2k_BT_0}\right)^{1/2}\right]^{-\frac{2\left(\kappa_0+\frac{1}{2}\kappa_T\right)}{\kappa_T}} \\ &= \left[\left(1+\frac{\kappa_T x^2}{2k_BT_0}\right)^{1/2}\right]^{-2\kappa_0/\kappa_T-1-1} \\ &= \left(1+\frac{\kappa_T x^2}{2k_BT_0}\right)^{-\kappa_0/\kappa_T-1} \end{aligned} \tag{4.38}$$

which normalises to

$$p_0(x) = \sqrt{\frac{\kappa_T}{2\pi k_BT_0}}\frac{\Gamma\left(\frac{\kappa_0+\kappa_T}{\kappa_T}\right)}{\Gamma\left(\frac{1}{2}+\frac{\kappa_0}{\kappa_T}\right)}\left(1+\frac{\kappa_T x^2}{2k_BT_0}\right)^{-\kappa_0/\kappa_T-1} \tag{4.39}$$

where $\Gamma(\ldots)$ is the Euler gamma function. This can also be written as

$$p_0(x) = \sqrt{\frac{\kappa_T}{2\pi k_BT_0}}\frac{\Gamma\left(\frac{\kappa_0+\kappa_T}{\kappa_T}\right)}{\Gamma\left(\frac{1}{2}+\frac{\kappa_0}{\kappa_T}\right)}\exp_{q_0}\left(\frac{(\kappa_0+\kappa_T)\,x^2}{2k_BT_0}\right) \tag{4.40}$$

where $q_0 = (\kappa_0+2\kappa_T)\,/\,(\kappa_0+\kappa_T)$.

The distribution in (4.39) can be written in terms of dimensionless position

$$p_0(x') = \sqrt{\frac{\alpha_T}{2\pi\alpha_0}} \frac{\Gamma\left(\frac{\alpha_0+\alpha_T}{\alpha_T}\right)}{\Gamma\left(\frac{1}{2}+\frac{\alpha_0}{\alpha_T}\right)} \left(1+\frac{\alpha_T x'^2}{2\alpha_0}\right)^{-\alpha_0/\alpha_T-1}. \tag{4.41}$$

The update in (4.33) can be repeated from the same initial value a number of times to get a sample of positions for the same α_0 and α_T values. Numerical results for precisely this, with 1000 repeats of the non-isothermal process evolving at $\alpha_0 = 1$ and $\alpha_T = 1.1$ for 800000 time steps of $dt' = 10^{-5}$ starting at position $x_0 = 0$, are given in figure 4.3. The results fit very closely to the predicted distribution.

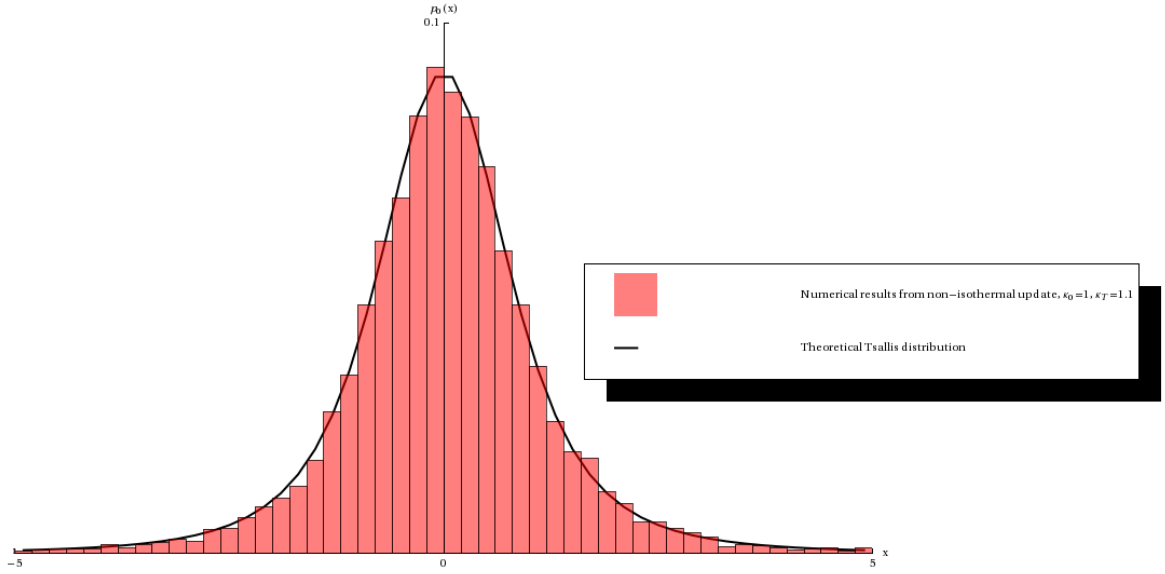

Figure 4.3: Numerical results for positions evolving at $\alpha_0 = 1$ and $\alpha_T = 1.1$ shown as a histogram against the theoretical Tsallis distribution.

We now wish to examine the distributions of the work values. Let us consider a simpler process of a single step at equilibrium from an initial spring constant value κ_0 to a higher value κ_1 at a time Δt in a process of total time τ, as shown in figure 4.4. The reverse process is then a step down from κ_1 to κ_0 at time $\tau - \Delta t$, as shown in figure 4.5.

For the forward process, the position at the step up x_u is in distribution

$$p_0(x_u) = \sqrt{\frac{\kappa_T}{2\pi k_B T_0}} \frac{\Gamma\left(\frac{\kappa_0+\kappa_T}{\kappa_T}\right)}{\Gamma\left(\frac{1}{2}+\frac{\kappa_0}{\kappa_T}\right)} \left(1+\frac{\kappa_T x_u^2}{2k_B T_0}\right)^{-\kappa_0/\kappa_T-1} \tag{4.42}$$

and the work done ΔW has value

$$\Delta W = \frac{1}{2}(\kappa_1 - \kappa_0)\, x_u^2 \tag{4.43}$$

so that the forward distribution of the work done is

$$\begin{aligned} p^F(\Delta W) &\propto p_0(x_u)\frac{dx_u}{d\Delta W} \\ &= \sqrt{\frac{1}{4\pi k_B T_0}} \sqrt{\frac{\kappa_T}{\kappa_1-\kappa_0}} \frac{\Gamma\left(\frac{\kappa_0+\kappa_T}{\kappa_T}\right)}{\Gamma\left(\frac{1}{2}+\frac{\kappa_0}{\kappa_T}\right)} \Delta W^{-1/2} \left[1+\left(\frac{\kappa_T}{\kappa_1-\kappa_0}\right)\frac{\Delta W}{k_B T_0}\right]^{-\frac{\kappa_0}{\kappa_T}-1} H(\Delta W) \end{aligned} \tag{4.44}$$

where $H(\Delta W)$ is the Heaviside step function. Normalising this gives

$$p^F(\Delta W) = \sqrt{\frac{1}{\pi k_B T_0}} \sqrt{\frac{\kappa_T}{\kappa_1-\kappa_0}} \frac{\Gamma\left(\frac{\kappa_0+\kappa_T}{\kappa_T}\right)}{\Gamma\left(\frac{1}{2}+\frac{\kappa_0}{\kappa_T}\right)} \Delta W^{-1/2} \left[1+\left(\frac{\kappa_T}{\kappa_1-\kappa_0}\right)\frac{\Delta W}{k_B T_0}\right]^{-\frac{\kappa_0}{\kappa_T}-1} H(\Delta W) \tag{4.45}$$

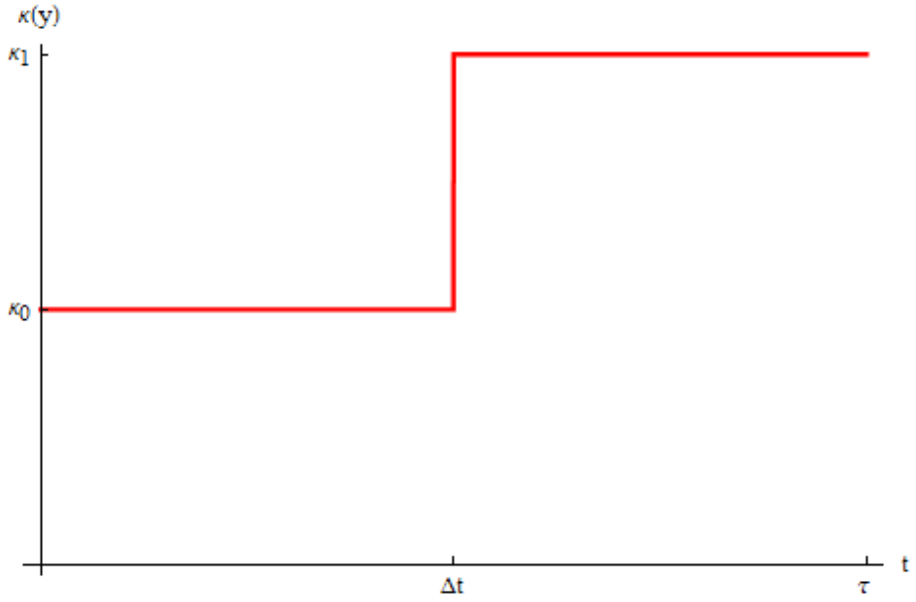

Figure 4.4: Forward step work process.

and this can be written as

$$p^F(\Delta W) = \sqrt{\frac{1}{\pi k_B T_0}}\sqrt{\frac{\kappa_T}{\kappa_1-\kappa_0}}\frac{\Gamma\left(\frac{\kappa_0+\kappa_T}{\kappa_T}\right)}{\Gamma\left(\frac{1}{2}+\frac{\kappa_0}{\kappa_T}\right)}\Delta W^{-1/2}\exp_{q_0}\left[-\left(\frac{\kappa_0+\kappa_T}{\kappa_1-\kappa_0}\right)\frac{\Delta W}{k_B T_0}\right]H(\Delta W) \tag{4.46}$$

where $q_0 = (\kappa_0 + 2\kappa_T)/(\kappa_0 + \kappa_T)$. This can then be written in terms of dimensionless work $\Delta W' = \Delta W/k_B T_0$ using the same methods used in chapter 2

$$p^F(\Delta W') = \sqrt{\frac{1}{\pi}}\sqrt{\frac{\alpha_T}{\alpha_1-\alpha_0}}\frac{\Gamma\left(\frac{\alpha_0+\alpha_T}{\alpha_T}\right)}{\Gamma\left(\frac{1}{2}+\frac{\alpha_0}{\alpha_T}\right)}\Delta W'^{-1/2}\left[1+\left(\frac{\alpha_T}{\alpha_1-\alpha_0}\right)\Delta W'\right]^{-\frac{\alpha_0}{\alpha_T}-1}H(\Delta W'). \tag{4.47}$$

For the reverse process, the position at the step up x_d is in distribution

$$p_1(x_d) = \sqrt{\frac{\kappa_T}{2\pi k_B T_0}}\frac{\Gamma\left(\frac{\kappa_1+\kappa_T}{\kappa_T}\right)}{\Gamma\left(\frac{1}{2}+\frac{\kappa_1}{\kappa_T}\right)}\left(1+\frac{\kappa_T x_d^2}{2k_B T_0}\right)^{-\kappa_1/\kappa_T-1} \tag{4.48}$$

and the work done ΔW has value

$$\Delta W = \frac{1}{2}(\kappa_0-\kappa_1)x_d^2 \tag{4.49}$$

so that the reverse distribution of the work done is

$$\begin{aligned} p^R(\Delta W) &\propto p_1(x_d)\frac{dx_d}{d\Delta W} \\ &= \sqrt{\frac{1}{4\pi k_B T_0}}\sqrt{\frac{\kappa_T}{\kappa_0-\kappa_1}}\frac{\Gamma\left(\frac{\kappa_1+\kappa_T}{\kappa_T}\right)}{\Gamma\left(\frac{1}{2}+\frac{\kappa_1}{\kappa_T}\right)}\Delta W^{-1/2}\left[1+\left(\frac{\kappa_T}{\kappa_0-\kappa_1}\right)\frac{\Delta W}{k_B T_0}\right]^{-\frac{\kappa_1}{\kappa_T}-1}H(-\Delta W) \end{aligned} \tag{4.50}$$

where $H(\Delta W)$ is the Heaviside step function. Normalising this gives

$$p^R(\Delta W) = \sqrt{\frac{1}{\pi k_B T_0}}\sqrt{\frac{\kappa_T}{\kappa_0-\kappa_1}}\frac{\Gamma\left(\frac{\kappa_1+\kappa_T}{\kappa_T}\right)}{\Gamma\left(\frac{1}{2}+\frac{\kappa_1}{\kappa_T}\right)}\Delta W^{-1/2}\left[1+\left(\frac{\kappa_T}{\kappa_0-\kappa_1}\right)\frac{\Delta W}{k_B T_0}\right]^{-\frac{\kappa_1}{\kappa_T}-1}H(-\Delta W). \tag{4.51}$$

This then gives us

$$p^R(-\Delta W) = \sqrt{\frac{1}{\pi k_B T_0}}\sqrt{\frac{\kappa_T}{\kappa_1-\kappa_0}}\frac{\Gamma\left(\frac{\kappa_1+\kappa_T}{\kappa_T}\right)}{\Gamma\left(\frac{1}{2}+\frac{\kappa_1}{\kappa_T}\right)}\Delta W^{-1/2}\left[1+\left(\frac{\kappa_T}{\kappa_1-\kappa_0}\right)\frac{\Delta W}{k_B T_0}\right]^{-\frac{\kappa_1}{\kappa_T}-1}H(\Delta W) \tag{4.52}$$

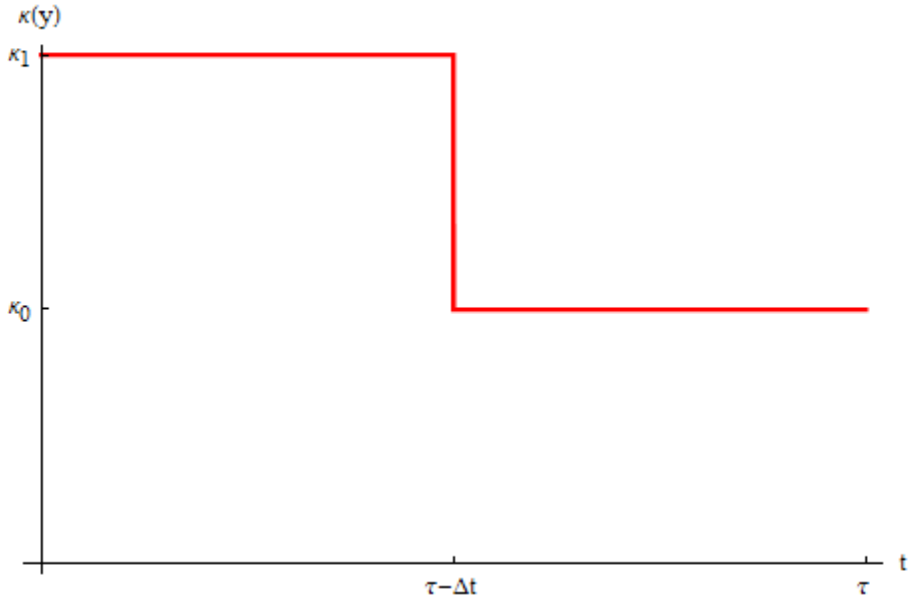

Figure 4.5: Reverse step work process.

which can be written as

$$p^R(-\Delta W) = \sqrt{\frac{1}{\pi k_B T_0}}\sqrt{\frac{\kappa_T}{\kappa_1-\kappa_0}}\frac{\Gamma\left(\frac{\kappa_1+\kappa_T}{\kappa_T}\right)}{\Gamma\left(\frac{1}{2}+\frac{\kappa_1}{\kappa_T}\right)}\Delta W^{-1/2}\exp_{q_1}\left[-\left(\frac{\kappa_1+\kappa_T}{\kappa_1-\kappa_0}\right)\frac{\Delta W'}{k_B T_0}\right]H(\Delta W) \tag{4.53}$$

where $q_1 = (\kappa_1 + 2\kappa_T)/(\kappa_1 + \kappa_T)$. In terms of dimensionless work we then have

$$p^R(-\Delta W') = \sqrt{\frac{1}{\pi}}\sqrt{\frac{\alpha_T}{\alpha_1-\alpha_0}}\frac{\Gamma\left(\frac{\alpha_1+\alpha_T}{\alpha_T}\right)}{\Gamma\left(\frac{1}{2}+\frac{\alpha_1}{\alpha_T}\right)}\Delta W'^{-1/2}\left[1+\left(\frac{\alpha_T}{\alpha_1-\alpha_0}\right)\Delta W'\right]^{-\frac{\alpha_1}{\alpha_T}-1}H(\Delta W'). \tag{4.54}$$

Figures 4.6 and 4.7 show numerical results for the forward and reverse work distributions respectively compared to both the Tsallis distributions just derived and the gaussian distributions of the isothermal process. 10000 numerical results were used, for the non-isothermal step process with $\alpha_0 = 1$, $\alpha_1 = 1.2$, and $\alpha_T = 5$. The Tsallis distributions show a clear fit to the numerical results, whilst the gaussian distribution diverges away from the results at the tail of the distribution as expected.

Finally, we can take the ratio of (4.45) and (4.52) to give the Crooks-Tsallis work relation for the simple step process

$$\frac{p^F(\Delta W)}{p^R(-\Delta W)} = \frac{\Gamma\left(\frac{\kappa_0+\kappa_T}{\kappa_T}\right)\Gamma\left(\frac{1}{2}+\frac{\kappa_1}{\kappa_T}\right)}{\Gamma\left(\frac{\kappa_1+\kappa_T}{\kappa_T}\right)\Gamma\left(\frac{1}{2}+\frac{\kappa_0}{\kappa_T}\right)}\left[1+\left(\frac{\kappa_T}{\kappa_1-\kappa_0}\right)\frac{\Delta W}{k_B T_0}\right]^{(\kappa_1-\kappa_0)/\kappa_T} \tag{4.55}$$

which as before can be written as

$$\frac{p^F(\Delta W)}{p^R(-\Delta W)} = \frac{\Gamma\left(\frac{\kappa_0+\kappa_T}{\kappa_T}\right)\Gamma\left(\frac{1}{2}+\frac{\kappa_1}{\kappa_T}\right)}{\Gamma\left(\frac{\kappa_1+\kappa_T}{\kappa_T}\right)\Gamma\left(\frac{1}{2}+\frac{\kappa_0}{\kappa_T}\right)}\exp_{q_-}\left(\frac{\Delta W}{k_B T_0}\right) \tag{4.56}$$

where $q_- = 1 - \kappa_T/(\kappa_1 - \kappa_0)$. Writing this new relation in terms of dimensionless work

$$\frac{p^F(\Delta W')}{p^R(-\Delta W')} = \frac{\Gamma\left(\frac{\alpha_0+\alpha_T}{\alpha_T}\right)\Gamma\left(\frac{1}{2}+\frac{\alpha_1}{\alpha_T}\right)}{\Gamma\left(\frac{\alpha_1+\alpha_T}{\alpha_T}\right)\Gamma\left(\frac{1}{2}+\frac{\alpha_0}{\alpha_T}\right)}\left[1+\left(\frac{\alpha_T}{\alpha_1-\alpha_0}\right)\Delta W'\right]^{(\alpha_1-\alpha_0)/\alpha_T}. \tag{4.57}$$

Taking the gamma factors over to the left hand side and then taking the q-logarithm of each side then gives

$$\ln_{q_-}\left[\frac{\Gamma\left(\frac{\alpha_1+\alpha_T}{\alpha_T}\right)\Gamma\left(\frac{1}{2}+\frac{\alpha_0}{\alpha_T}\right)}{\Gamma\left(\frac{\alpha_0+\alpha_T}{\alpha_T}\right)\Gamma\left(\frac{1}{2}+\frac{\alpha_1}{\alpha_T}\right)}\frac{p^F(\Delta W')}{p^R(-\Delta W')}\right] = \Delta W'. \tag{4.58}$$

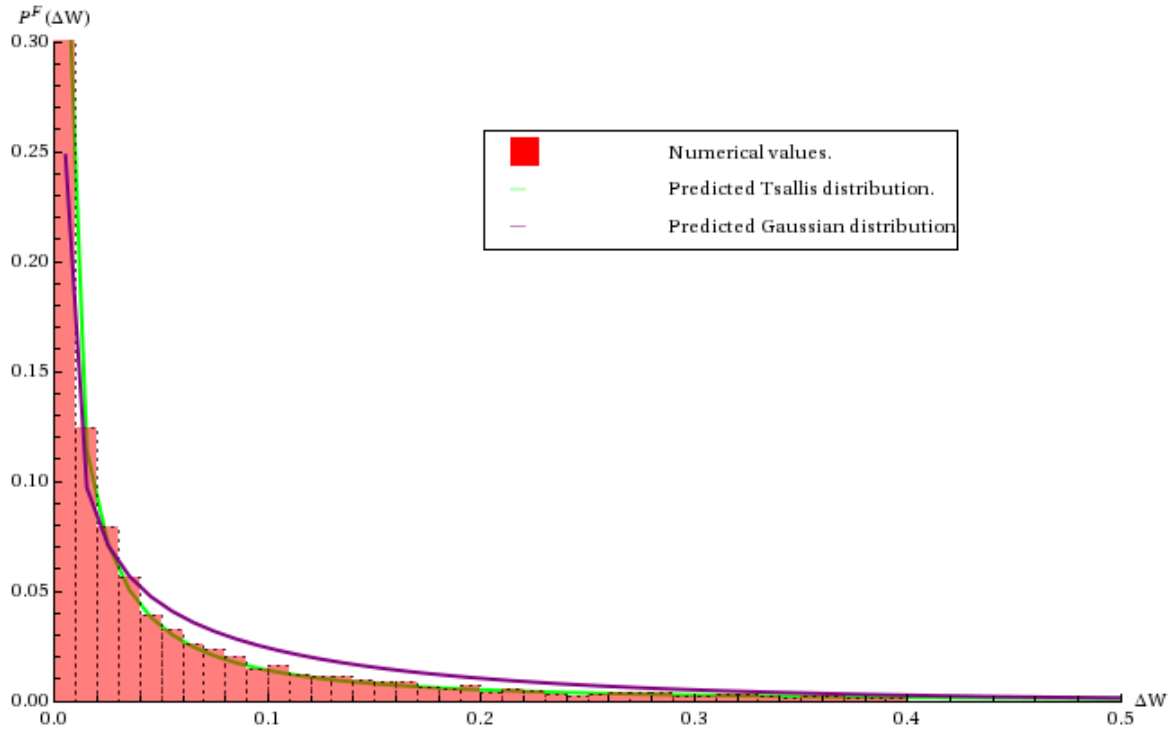

Figure 4.6: Numerical results of work values from the forward step process shown as a histogram against both the predicted Tsallis distribution, the green curve, and the traditional gaussian distribution, the purple curve. Results were found for $\alpha_0 = 1$, $\alpha_1 = 1.2$, and $\alpha_T = 5$.

By modelling the forward and reverse processes, numerical distributions of the work for both can be found. Taking the ratio of these distributions, multiplying them by the gamma factors, and then taking the q-logarithm gives a numerical result that can then be compared to the theoretical prediction.

Figure 4.8 gives the results of this modelling for 3 repeats of 20000 work results for processes starting at $x'_0 = 0$ and evolving to equilibrium for 800000 time steps of size $dt' = 10^{-5}$ before applying the protocol. These values were found for values $\alpha_0 = 1$, $\alpha_1 = 1.2$, and $\alpha_T = 1.1$. The results do seem to show correlation to the theoretical prediction for the very low work values, as shown by figure 4.9 focussing in on those results. However, for larger work values large noise fuctuations set in, often pushing the data points and errors beyond the scope of the figure. Further work is definitely warranted in exploring this result.

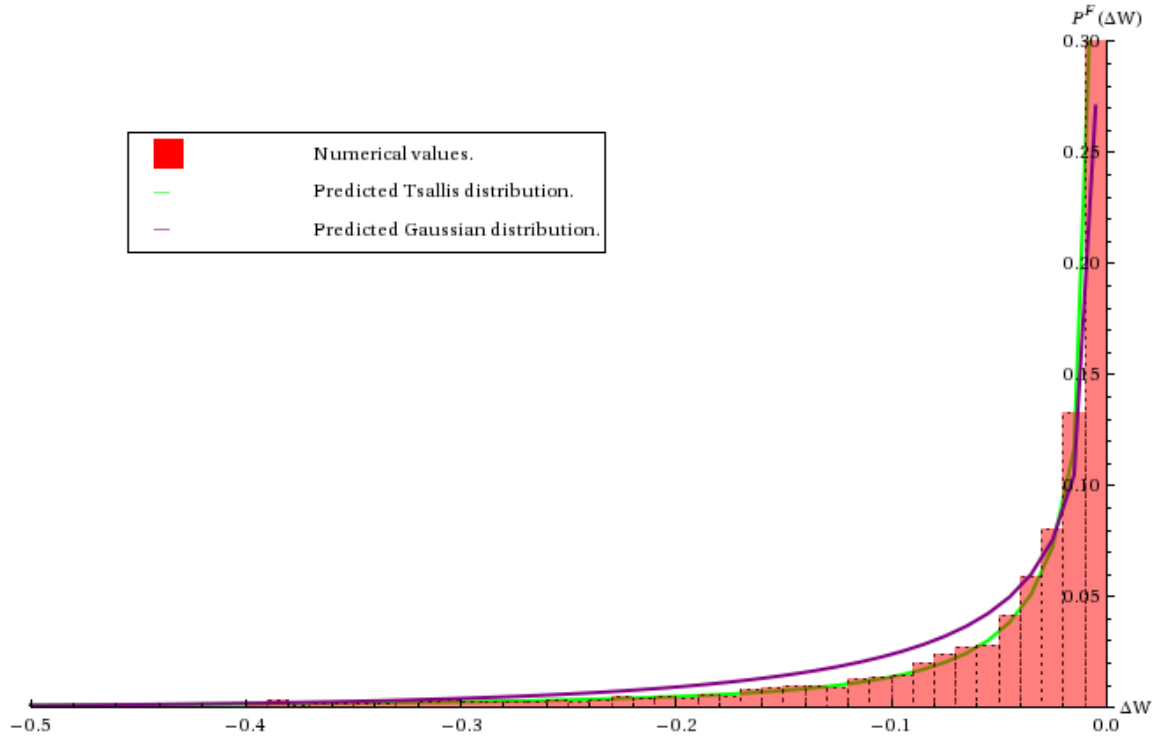

Figure 4.7: Numerical results of work values from the reverse step process shown as a histogram against both the predicted Tsallis distribution, the green curve, and the traditional gaussian distribution, the purple curve. Results were found for $\alpha_0 = 1$, $\alpha_1 = 1.2$, and $\alpha_T = 5$.

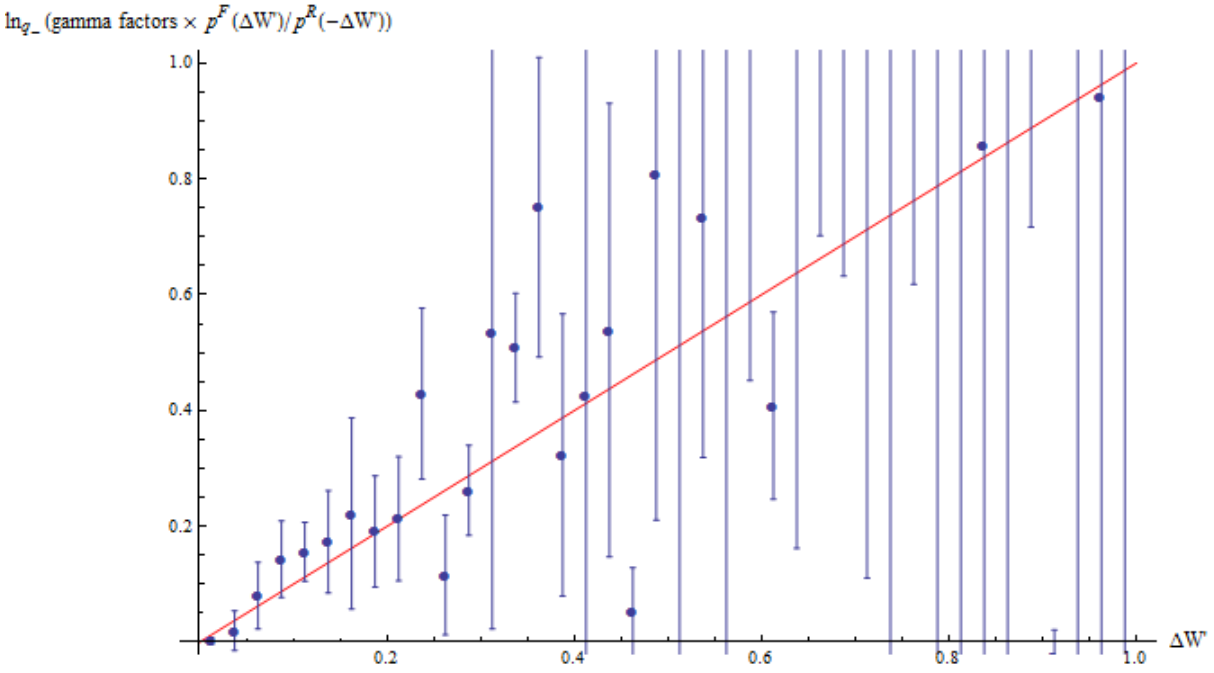

Figure 4.8: Numerical results for the Crooks Tsallis work relation for the simple step process, given by the blue data points, shown against the theoretical prediction, given by the red line, for $\alpha_0 = 1$, $\alpha_1 = 1.2$, and $\alpha_T = 1.1$.

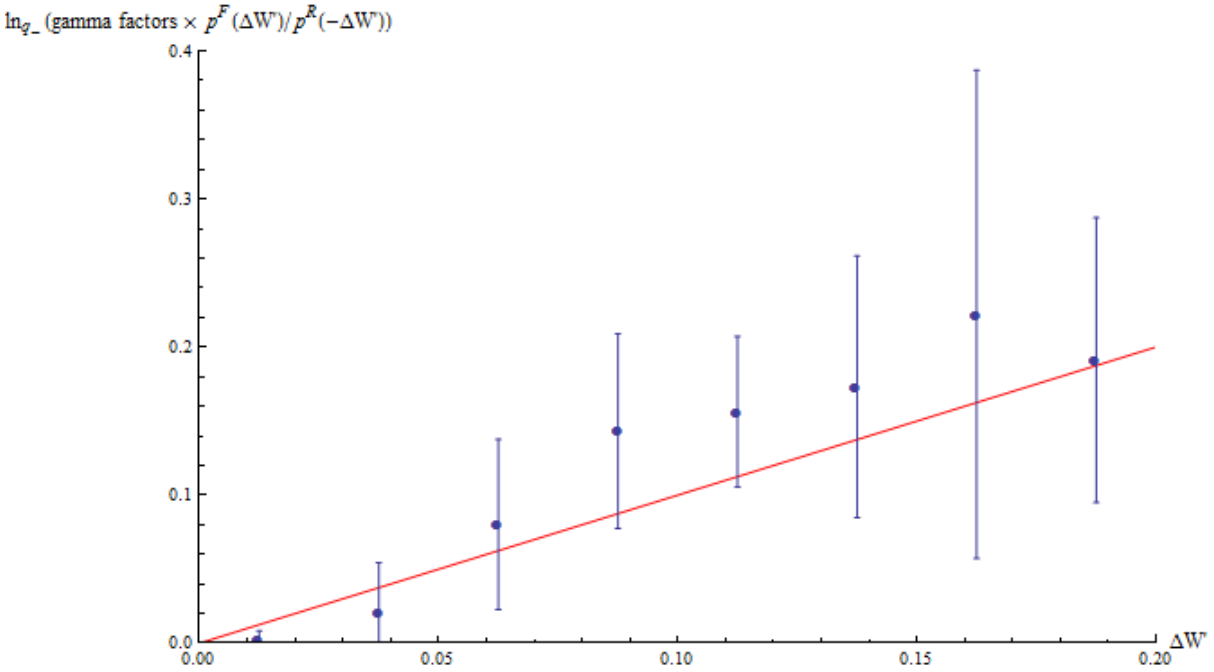

Figure 4.9: Numerical results for the Crooks Tsallis work relation for the simple step process, given by the blue data points, shown against the theoretical prediction, given by the red line, for $\alpha_0 = 1$, $\alpha_1 = 1.2$, and $\alpha_T = 1.1$, focussing on the lower work values.

Chapter 5

Literature Review

Before bringing this report to a conclusion, it is informative to very briefly review the work completed in this area by others. This will allow us to see the context of this report, how it fits in with work already done, and what advancements it brings.

Chapter 2 was meant as primarily a theoretical basis for the rest of the report. The Jarzynski equality, as well as the other fluctuation theorems, are well established and the numerical modelling done in that chapter served more to confirm that the method for the modelling works rather than to actually confirm the equality itself. As mentioned before, further information on the Jarzynski equality, in the context of the fluctuation theorems, as well as the many other fluctuation theorems that have been derived for various systems, can be found in [9] and [6]. The fluctuation theorems are immensely useful relations, hence the importance of any work involving them such as the work done within this investigation. An excellent example of this, mentioned in chapter 2, is given in [15], whereby they prove the Clausius inequality not by assuming the second law, but rather by assuming the laws of mechanics, a T-mixing property, an ergodic consistency condition, and the axiom of causality, and by using the relaxation and dissipation theorems and, of course, the fluctuation theorems: specifically, the Evans-Searles and the Crooks fluctuation theorems.

Though the Jarzynski equality is the main focus of this report, the Crooks work relation is also of great interest. Work focussing on this relation is cited in chapter 2. Another example can be found in [35], which considers the form of the relation for a special case of symmetry of the work distribution for non-cyclic work processes on an isolated harmonic oscillator.

Throughout the report we have focussed on the use of stochastic thermodynamics. Further information on this area and how it can apply to the first law of thermodynamics, as well as the second, is given in [12]. Further work on how the consideration of a Brownian particle can be used to derive fluctuation theorems can also be found in [11].

We also noted in chapter 2 that, though the original derivation is given in [16], and we too gave a derivation taken from [9], they are by no means the only derivations. For instance, [18] derives the equality via a master equation approach, and [19] uses a Hamiltonian model more general than that used in the original derivation. Also, we noted that the Jarzynski equality has been experimentally verified, as in [20] where the equality was used to calculate accurately the free energy changes for non-quasistatic stretching of a single RNA molecule. With all this in consideration, we can see that the new work committed by this investigation begins in chapter 3.

We can first note that the Jarzynski-Sagawa-Ueda equality in chapter 3 is not constricted to the kind of system we considered. First off, we only considered a classical particle. It is perfectly achievable to find a form for this equality and other related equalities for feedback control systems in terms of a quantum particle. Considerations on quantum feedback control and its application to the second law and to the Jarzynski equality are given in [36], [37], and [38]. Also, whilst we considered position-dependent feedback control via our use of the overdamped langevin equation, it is entirely possible to consider the modification of the Jarzynski equality under velocity-dependent feedback control without going to the overdamped limit, as shown in [39].

Like with the Jarzynski equality, there are different ways to derive the Jarzynski-Sagawa-Ueda equality. Examples are given by the citations in chapter 3, as well as by [31] which uses a Hamiltonian approach. Also, the Jarzynski equality is not the only fluctuation theorem which alters for feedback control systems, as discussed in [40]. For example, alteration of the detailed fluctuation theorem is given in both [41] and [42].

As with the Jarzynski equality itself, the Jarzynski-Sagawa-Ueda equality has been experimentally verified, such as in [29] where a particle is forced up a "spiral staircase-like" potential via the use of measurement and feedback, and the free energy change is shown to have been increased over the work by the use of the information gained via measurement.

The main focus of chapter 3 then is in the maximisation of the efficacy parameter. Maximising the work gotten out of the system is a subject of great interest, such as in [43]. We considered maximising the efficacy parameter by the effect of the length of time the system has been left at κ_1, the amount of error allowed in the measurement, and the choice of an optimal value of κ_1. Though work has not been done in these considerations so precisely, work has been done in the general areas. Error in measurement has been considered for various different purposes, such as in [44]. The optimal protocol was also considered in [33], which showed it to be a step change, the type of protocol which we have considered throughout this investigation. We can see here, then, that the importance of the work within this report is in the consideration of how these changes to our system maximise the efficacy parameter. These considerations will be valuable to experimental work.

Lastly, the work in chapter 4 done on non-isothermal systems has very little literature to draw on in comparison to feedback control systems. Therefore, this can be considered fresher ground with a more theoretical interest. We do note, however, the existence of [45], which derives its own Jarzynski-Tsallis equality via the consideration of a system obeying Tsallis statistics. It may be of interest to compare our two equalities to see if they may be related in any way.

Chapter 6

Summary and Conclusions

This report has been concerned with examining the Jarzynski equality and its generalisations to systems with feedback control and to non-isothermal systems. The Jarzynski equality is a statistical statement of the second law for small systems undergoing work processes due to conservative potentials which holds arbitrarily far from equilibrium. It proves valuable as a theoretical relation in its use in examining the nature of entropy production in these systems, and as a practical tool in its ability to relate the value of the change in free energy over a process to the average of measurements of the work done over that process.

In chapter 2 we showed how the Jarzynski equality can be modelled numerically by consideration of a Brownian particle trapped in a harmonic potential and in thermal contact with an overdamped langevin heat bath. The results of this modelling agreed with the equality, as expected. As the equality is already a well-verified relation, it is wiser to take these results as verification of the method. We also calculated the variance associated with the equality, and found it to have an asymptotic limit in terms of what size change in spring constant it applies to. Throughout the investigation, modelling of the variance for all results proved ineffective for the higher changes in spring constant as massively large statistical errors set in. We do see from numerical results, though, that the variance of the Jarzynski equality increases over increase in the change in spring constant. This is to be expected, as greater fluctuations in work are allowed leading to a greater spread in the values.

Systems with feedback control are systems that come coupled with some form of measurement device. The device takes measurements of the system, and based on the results of these measurements applies feedback in order to reduce the entropy within the system. By doing this, it is essentially using information to change one type of energy within the system to another. In this case, the Jarzynski equality takes on a generalised form known as the Jarzynski-Sagawa-Ueda equality involving a constant called the efficacy parameter which measures the effectiveness of the application of the feedback. This equality can be modelled numerically using the same methods as in chapter 2. The variance of this equality was also modelled, with the familiar result of a greater spread in work values for a greater change in the spring constant.

This equality is currently of great experimental interest. Indeed, work is currently being performed within the Physics and Astronomy department at University College London in trapping a particle with the aim of applying measurement and feedback to it. In chapter 3, we considered the maximisation of the efficacy parameter in the hope of providing a strong theoretical and numerical basis for this experimental work. Firstly, as in chapter 2, numerical results verified the equality itself for the most standard considerations we can have for our system. The more interesting work is in the considerations given in sections 3.4 and 3.5.

We considered how the time spent at κ_1 can affect the efficacy parameter. It was found, and numerical results agree with this, that the efficacy parameter is found to increase as the system is allowed to spend longer at κ_1. Therefore, the longer the system is given to settle, the more effective the feedback is. This implies a trade off between effectiveness of the feedback and efficiency in how much time the feedback takes. The variance in exponentiated work is also shown to increase as this time parameter is increased. As the system is allowed to evolve at κ_1 for longer, a greater spread of work values is achieved.

We also considered how errors in measurement effect the value of the efficacy parameter. Firstly, in comparing the value of the efficacy parameter for one select change in spring constant over various values for the error in measurement. It was shown that as the error increases, the efficacy parameter decreases from a maximum zero error value to a minimum value of 1, as expected. As the error increases, the

feedback gets less effective. The variance of the exponentiated work is actually shown to decrease slowly over an increase in error. Secondly, we considered the form of the efficacy parameter over an increasing change in spring constant for a set error value. It is shown to follow the same form as in an errorless feedback process, but with a decrease in the value for all changes in spring constant. The variance shows the same increase as before.

Finally for the efficacy parameter, and most interestingly, we considered an optimal value of the spring constant to change to. It can be shown that we should increase the spring constant when we are close to the centre of the potential, decrease it when we are very far out from the centre, and keep it the same otherwise. This then follows the characteristics of the optimal value, but ignores the issues it entails. Results from modelling this case did show an increase over the efficacy parameter of the standard protocol case. As before, the variance showed the same style of increase.

It is hoped that these results and conclusions prove useful for the experimental work. Here, we can conclude that the optimal protocol of allowing both steps up and steps down in spring constant dependent on position will result in much more effective feedback. This will prove useful in the experimental work, which at the same time can act as experimental verification of these findings. We have also seen that, within the experimental work, both error and cycle time need to be considered. Obviously, a smaller cycle time makes the whole process more efficient, but it also makes the feedback less effective. As said before, a trade off must be made. Also, as is obvious from any considerations, we have shown that the error in measurement must be minimised in order to make the feedback as effective as possible.

In chapter 4, we showed that for our step process in a non-isothermal system the Jarzynski equality can be generalised to the new Jarzynski-Tsallis equality. Modelling of this system provided results that agreed with the new equality. However, obviously further numerical and experimental confirmation of the equality is needed. We also examined and modelled the statistics of the system, showing confirmation that the system follows Tsallis distributions instead of the standard gaussian distributions. We also derived a generalisation of the Crooks work relation for a simple non-cyclic single step process. Numerical modelling of this relation did seem to show a correlation, but further modelling is certainly needed.

This work opens the possibility of further generalisations of the Jarzynski equality for various non-isothermal processes. It also considers the interest in examining the unusual statistics that arise in this case. It is hoped that much further work in this area can be done, leading to applications of the Jarzynski equality in experimentation on non-isothermal systems.

Bibliography

[1] D'Abramo, G. The peculiar status of the second law of thermodynamics and the quest for its violation. *Studies in History and Philosophy of Science Part B: Studies in History and Philosophy of Modern Physics* **43**, 226–235 (2012).

[2] Callen, H. B. *Thermodynamics and an Introduction to Thermostatistics, 2nd Edition* (Wiley-VCH, 1985).

[3] Eddington, A. *The Nature of the Physical World* (New York: Macmillan, 1948).

[4] Loschmidt, J. Uber den zustand des warmegleichgewichetes eines systems von korpern mit rucksicht auf die schwerkraft, I. *Sitzungsber. Kais. Akad. Wiss. Wien, Math. Naturwiss. Classe* **II Abteilung 73**, 128 (1876).

[5] Cucic, D. A. Paradoxes of thermodynamics and statistical physics. *arXiv preprint arXiv:0912.1756* (2009).

[6] Evans, D. J. & Searles, D. J. The fluctuation theorem. *Advances in Physics* **51**, 1529–1585 (2002).

[7] Maxwell, J. C. *Theory of heat* (Dover Publications, 2001).

[8] Leff, H. & Rex, A. F. *Maxwell's Demon 2 Entropy, Classical and Quantum Information, Computing*, vol. 2 (Taylor & Francis, 2002).

[9] Spinney, R. E. & Ford, I. J. Fluctuation relations: a pedagogical overview. *arXiv preprint arXiv:1201.6381* (2012).

[10] Seifert, U. Entropy production along a stochastic trajectory and an integral fluctuation theorem. *Physical review letters* **95**, 40602 (2005).

[11] Imparato, A. & Peliti, L. Fluctuation relations for a driven brownian particle. *Physical Review E* **74**, 026106 (2006).

[12] Seifert, U. Stochastic thermodynamics: principles and perspectives. *The European Physical Journal B-Condensed Matter and Complex Systems* **64**, 423–431 (2008).

[13] Gardiner, C. W. *Stochastic methods: a handbook for the natural and social sciences*, vol. 4 (Springer, 2009).

[14] Ford, I. J. PHAS3423 Stochastic processes course notes. *UCL Physics and Astronomy Department* .

[15] Evans, D. J., Williams, S. R. & Searles, D. J. A proof of clausius' theorem for time reversible deterministic microscopic dynamics. *The Journal of chemical physics* **134**, 204113–204113 (2011).

[16] Jarzynski, C. Nonequilibrium equality for free energy differences. *Physical Review Letters* **78**, 2690 (1997).

[17] Crooks, G. E. Entropy production fluctuation theorem and the nonequilibrium work relation for free energy differences. *Physical Review E* **60**, 2721 (1999).

[18] Jarzynski, C. Equilibrium free energy differences from nonequilibrium measurements: a master equation approach. *arXiv preprint cond-mat/9707325* (1997).

[19] Jarzynski, C. Nonequilibrium work theorem for a system strongly coupled to a thermal environment. *Journal of Statistical Mechanics: Theory and Experiment* **2004**, P09005 (2004).

[20] Liphardt, J., Dumont, S., Smith, S. B., Tinoco Jr, I. & Bustamante, C. Equilibrium information from nonequilibrium measurements in an experimental test of jarzynski's equality. *Science* **296**, 1832–1835 (2002).

[21] Lemons, D. S. *An introduction to stochastic processes in physics* (Johns Hopkins University Press, 2002).

[22] Ullersma, P. An exactly solvable model for brownian motion: I. derivation of the langevin equation. *Physica* **32**, 27–55 (1966).

[23] Sagawa, T. & Ueda, M. Information thermodynamics: Maxwell's demon in nonequilibrium dynamics. *arXiv preprint arXiv:1111.5769* (2011).

[24] Van Ness, H. C. *Understanding thermodynamics* (Dover Publications, 1983).

[25] Szilard, L. On the decrease of entropy in a thermodynamic system by the intervention of intelligent beings (1923).

[26] Landauer, R. Irreversibility and heat generation in the computing process. *IBM journal of research and development* **5**, 183–191 (1961).

[27] Cao, F. J. & Feito, M. Thermodynamics of feedback controlled systems. *Physical Review E* **79**, 041118 (2009).

[28] Sagawa, T. & Ueda, M. Generalized jarzynski equality under nonequilibrium feedback control. *Physical review letters* **104**, 90602 (2010).

[29] Toyabe, S., Sagawa, T., Ueda, M., Muneyuki, E. & Sano, M. Experimental demonstration of information-to-energy conversion and validation of the generalized jarzynski equality. *Nature Physics* **6**, 988–992 (2010).

[30] Horowitz, J. M. & Parrondo, J. M. Thermodynamic reversibility in feedback processes. *EPL (Europhysics Letters)* **95**, 10005 (2011).

[31] Sagawa, T. Hamiltonian derivations of the generalized jarzynski equalities under feedback control. In *Journal of Physics: Conference Series*, vol. 297, 012015 (IOP Publishing, 2011).

[32] Sagawa, T. & Ueda, M. Nonequilibrium thermodynamics of feedback control. *Physical Review E* **85**, 021104 (2012).

[33] Horowitz, J. M. & Parrondo, J. M. Designing optimal discrete-feedback thermodynamic engines. *New Journal of Physics* **13**, 123019 (2011).

[34] Tsallis, C. *Introduction to nonextensive statistical mechanics: approaching a complex world* (Springer, 2009).

[35] Ford, I. J., Minor, D. S. & Binnie, S. J. Symmetries of cyclic work distributions for an isolated harmonic oscillator. *European Journal of Physics* **33**, 1789 (2012).

[36] Sagawa, T. & Ueda, M. Second law of thermodynamics with discrete quantum feedback control. *Physical review letters* **100**, 80403 (2008).

[37] Jacobs, K. Second law of thermodynamics and quantum feedback control: Maxwells demon with weak measurements. *Physical Review A* **80**, 012322 (2009).

[38] Morikuni, Y. & Tasaki, H. Quantum jarzynski-sagawa-ueda relations. *Journal of Statistical Physics* **143**, 1–10 (2011).

[39] Kim, K. H. & Qian, H. Fluctuation theorems for a molecular refrigerator. *Physical Review E* **75**, 022102 (2007).

[40] Lahiri, S., Rana, S. & Jayannavar, A. Fluctuation theorems in the presence of information gain and feedback. *Journal of Physics A: Mathematical and Theoretical* **45**, 065002 (2012).

[41] Ponmurugan, M. Generalized detailed fluctuation theorem under nonequilibrium feedback control. *Physical Review E* **82**, 031129 (2010).

[42] Horowitz, J. M. & Vaikuntanathan, S. Nonequilibrium detailed fluctuation theorem for repeated discrete feedback. *Physical Review E* **82**, 061120 (2010).

[43] Abreu, D. & Seifert, U. Extracting work from a single heat bath through feedback. *EPL (Europhysics Letters)* **94**, 10001 (2011).

[44] Ito, S. & Sano, M. Effects of error on fluctuations under feedback control. *Physical Review E* **84**, 021123 (2011).

[45] Ponmurugan, M. Tsallis statistics generalization of non-equilibrium work relations. *arXiv preprint arXiv:1110.5153* (2011).

List of Figures

List of Tables

Appendix A

Tables of Numerical Results

α_1	Average	Variance	Theoretical Variance
1.05	1.0000 ± 0.0014	0.0024 ± 0.0002	0.0024
1.20	1.0000 ± 0.0047	0.0340 ± 0.0042	0.0351
1.75	0.9972 ± 0.0204	0.4780 ± 0.2610	0.6730
2.00	1.0179 ± 0.0504	1.6800 ± 2.1379	2979.96
4.00	0.9636 ± 0.0801	8.0100 ± 9.4852	n/a

Table A.1: Numerical results for figures 2.5 and 2.6.

α_1	γ_E	Average	Variance
1.01	1.0018	1.0017 ± 0.0001	0.000023 ± 0.000004
1.05	1.0086	1.0086 ± 0.0008	0.000618 ± 0.000132
1.10	1.0171	1.0169 ± 0.0015	0.002503 ± 0.000602
1.20	1.0332	1.0336 ± 0.0036	0.044323 ± 0.016268
1.40	1.0630	1.0614 ± 0.0077	0.044323 ± 0.016268
1.75	1.1087	1.1096 ± 0.0160	0.222719 ± 0.132004
2.00	1.1376	1.1410 ± 0.0270	0.620550 ± 0.736162
4.00	1.2998	1.2639 ± 0.0878	8.152245 ± 14.769130
6.00	1.3964	1.2937 ± 0.0871	8.940321 ± 17.219530

Table A.2: Numerical results for figures 3.3, 3.4, 3.5, and 3.6.

α_1	γ_E	Average	Variance
1.01	1.0024	1.0022 ± 0.0002	0.000031 ± 0.000006
1.05	1.0118	1.0109 ± 0.0010	0.000877 ± 0.000206
1.10	1.0231	1.0198 ± 0.0013	0.003080 ± 0.000360
1.20	1.0441	1.0398 ± 0.0038	0.014460 ± 0.003024
1.40	1.0812	1.0745 ± 0.0077	0.067962 ± 0.022749
1.75	1.1345	1.1254 ± 0.0188	0.255385 ± 0.114132
2.00	1.1661	1.1517 ± 0.018879	0.400041 ± 0.133355
4.00	1.3227	1.3446 ± 0.1905	41.623230 ± 110.150557
6.00	1.4069	1.3156 ± 0.0902	13.580896 ± 16.938726

Table A.3: Numerical results for figures 3.7, 3.8, and 3.9.

$\Delta t'$	γ_E	Average	Variance
0.1	1.0088	1.0086 ± 0.0015	0.0017 ± 0.0002
0.2	1.0159	1.0157 ± 0.0011	0.0037 ± 0.0006
0.3	1.0216	1.0218 ± 0.0022	0.0054 ± 0.0006
0.4	1.0263	1.0259 ± 0.0026	0.0070 ± 0.0014
0.5	1.0300	1.0308 ± 0.0035	0.0097 ± 0.0015
0.6	1.0329	1.0335 ± 0.0031	0.0101 ± 0.0021
0.7	1.0353	1.0363 ± 0.0032	0.0118 ± 0.0020
0.8	1.0371	1.0374 ± 0.0052	0.0137 ± 0.0051
0.9	1.0386	1.0397 ± 0.0036	0.0130 ± 0.0022
1.0	1.0397	1.0403 ± 0.0034	0.0142 ± 0.0028

Table A.4: Numerical results for figures 3.10 and 3.11.

σ'	γ_E	Average	Variance
0.00	1.0441	1.0364 ± 0.0032	0.0119 ± 0.0018
0.25	1.0413	1.0370 ± 0.0031	0.0145 ± 0.0038
0.50	1.0346	1.0321 ± 0.0043	0.0162 ± 0.0045
0.75	1.0273	1.0254 ± 0.0048	0.0158 ± 0.0030
1.00	1.0211	1.0213 ± 0.0041	0.0193 ± 0.0043
1.25	1.0163	1.0142 ± 0.0032	0.0177 ± 0.0035
1.50	1.0127	1.0126 ± 0.0047	0.0188 ± 0.0027
1.75	1.0101	1.0087 ± 0.0032	0.0182 ± 0.0025
2.00	1.0082	1.0055 ± 0.0061	0.0193 ± 0.0061
2.25	1.0068	1.0047 ± 0.0034	0.0180 ± 0.0022

Table A.5: Numerical results for figures 3.12 and 3.13.

α_1	γ_E	Average	Variance
1.01	1.0019	1.0016 ± 0.0002	0.000032 ± 0.000005
1.05	1.0094	1.0080 ± 0.0009	0.000879 ± 0.000134
1.10	1.0183	1.0151 ± 0.0016	0.003183 ± 0.000494
1.20	1.0346	1.0310 ± 0.0022	0.014799 ± 0.002006
1.40	1.0627	1.0537 ± 0.0055	0.065590 ± 0.012462
1.75	1.1012	1.0960 ± 0.0138	0.242638 ± 0.091226
2.00	1.1229	1.1140 ± 0.0204	0.370506 ± 0.119840
4.00	1.2179	1.1911 ± 0.1072	15.351286 ± 34.661415
6.00	1.2594	1.1595 ± 0.1046	15.798225 ± 36.245776

Table A.6: Numerical results for figures 3.14, 3.15, and 3.16.

α_u	γ_E	Average	Variance
1.01	1.0564	1.0462 ± 0.0037	0.0255 ± 0.0053
1.05	1.0657	1.0557 ± 0.0071	0.0280 ± 0.0056
1.10	1.0770	1.0610 ± 0.0041	0.0242 ± 0.0027
1.20	1.0980	1.0844 ± 0.0060	0.0388 ± 0.0079
1.40	1.1352	1.1241 ± 0.0088	0.0925 ± 0.0170
1.75	1.1885	1.1798 ± 0.0266	0.7748 ± 1.0306
2.00	1.2200	1.1921 ± 0.0322	0.4695 ± 0.4164
4.00	1.3766	1.4240 ± 0.3804	125.3943 ± 384.2412
6.00	1.4608	1.3647 ± 0.0998	15.3772 ± 14.8081

Table A.7: Numerical results for figures 3.19, 3.20, and 3.21.

Appendix B

Important Code Used

All numerical results in this report were found from code written and compiled in Java version 7 update 17, through the Eclipse integrated development environment. All plots of the data were created using Wolfram Mathematica version 7.

The code used to model the langevin equation in section 2.4:

```
public class LangevinEquation {
       /**alpha is a variable proportional to the variable spring constant.
        */
double alpha;
/**alpha0 is the constant proportional to the constant spring constant.
 */
double alpha0;
/**dt is the discrete time increment.
 */
double dt;
/**x0 is the boundary value for x at t = 0.
 */
double x0;
/**max is the number of time increments to model.
 */
int max;

/**Contructor
 */
public LangevinEquation(){};
/**Constructor
 * @param a is the value of variable alpha.
 * @param a is the value of constant alpha.
 * @param t is the discrete time increment.
 * @param 0 is the boundary value for x.
 * @param m is the number of time increments to model.
 */
public LangevinEquation(double a, double a0, double t, double 0, int m)
{alpha = a;
alpha0 = a0;
dt = t;
x0 = 0;
max =m;
}

/**Numerically models the Langevin equation. Starting from a set
 * boundary value, updates the position over discrete time increments
 * according to the Langevin equation.
 * @return A HashMap of x values with keys determining the time increment multiple
 * they correspond to.
 * @throws Exception
 */
```

```
public HashMap<Integer,Double> numericalLangevin() throws Exception
{int i = 0;
double x = this.x0;
RandomVariable rand = new RandomVariable(0,Math.sqrt(2*this.alpha0));
HashMap<Integer,Double> sol = new HashMap<Integer,Double>();
sol.put(i, x);
while(i < this.max){
       x = (1 - this.alpha * this.dt)*x +
                     (rand.genRandVar() * Math.sqrt(this.dt));
       sol.put((1+i), x);
       i++;
}
return sol;
}
}


public class RandomVariable {
/**Member variable: mean is the chosen
* mean of the normal distribution.
*/
double mean;
/**Member variable: stDev is the chosen standard deviation of the
* normal distribution.
*/
double stDev;

/**Constructor
*/
public RandomVariable() {}
/**Constructor
* @param m is the desired mean of the distribution
* @param sd is the desired standard deviation of the
* distribution.
*/
public RandomVariable(double m,double sd)
{mean = m; stDev = sd;}

/**Generates a random double subject to the Gaussian distribution
* defined by the mean and stDev of the RandomVariable object.
* @return A random double subject to the Gaussian distribution.
* @throws Exception if stDev is less than or equal to 0.
*/
public double genRandVar() throws Exception
{if (this.stDev <= 0){
throw new Exception("Standard deviation of RandomVariable" +
"object must be greater than 0.");
}
double rand;
Random randNo = new Random();
rand = this.stDev * randNo.nextGaussian() + this.mean;
return rand;
}
}
```

The code used to model the Jarzynski equality in section 2.4:

```
/**Runs the Langevin update manually with the simple action of periodically changing the
    spring constant.
* Calculates the average of the exponentiated difference in work done by the system and work
    done on the system
* through the action over all cycles in the process, as well as the variance.
* Does this manually in an effort to make the process more efficient and quicker.
```

```
* @param alpha0 The lower value for the spring constant.
* @param alpha1 The upper value for the spring constant.
* @param dt The time increment value.
* @param x0 The boundary value of x at t = 0.
* @param actionNo The number of times the action is applied.
* @param deltat The number of time increments each cycle is run for.
* @return The average exponentiated value for the difference in work done over all cycles in a
    process, and the variance of these values.
* @throws Exception All arguments except x0 must be greater than 0.
*/
public static double[] averageAlwaysActionWithVarianceMk2(double alpha0, double alpha1, double
    dt, double x0,int actionNo,int deltat)
throws Exception{
if((alpha0<=0)&&(alpha1<=0)&&(dt<=0)&&(actionNo<=0)&&(deltat<=0)){
throw new Exception("All arguments except x0 must be greater than 0.");
}
double x = x0;
int i1 = 0;
while(i1 < deltat){
Random rand = new Random();
x = (1 - alpha0 * dt)*x + (((Math.sqrt(2*alpha0)) * rand.nextGaussian()) * Math.sqrt(dt));
i1++;
}
int i2 = 0;
double eSum = 0;
double evSum = 0;
while(i2<actionNo){
double w1 = ((alpha1 - alpha0)*Math.pow(x, 2))/(2*alpha0);
int i3 = 0;
while(i3 < Math.floor(deltat/2)){
Random rand1 = new Random();
x = (1 - alpha1 * dt)*x + (((Math.sqrt(2*alpha0)) * rand1.nextGaussian()) * Math.sqrt(dt));
i3++;
}
double w2 = ((alpha0 - alpha1)*Math.pow(x, 2))/(2*alpha0);
double w = w1 + w2;
double ew = Math.exp(- w);
double e2w = Math.exp(- 2*w);
eSum += ew;
evSum += e2w;
int i4 = (int) Math.floor(deltat/2);
while(i4 < deltat){
Random rand2 = new Random();
x = (1 - alpha0 * dt)*x + (((Math.sqrt(2*alpha0)) * rand2.nextGaussian()) * Math.sqrt(dt));
i4++;
}
i2++;
}
double averageWork = eSum / actionNo;
double varianceWork = (evSum / actionNo) - Math.pow(averageWork, 2);
double[] averageWithVariance = new double[2];
averageWithVariance[0] = averageWork;
averageWithVariance[1] = varianceWork;
return averageWithVariance;
}
```

The code used to model the Jarzynski-Sagawa-Ueda equality with range $x'_a = 0.5$ in section 3.3:

```
/**Runs the Langevin update manually with the simple action of periodically checking to see if
    the position
* is within a given range of the boundary value, then changing the spring constant if it is,
    and doing
* nothing if it isn't.
```

```
* Calculates the average of the exponentiated difference in work done by the system and work
    done on the system
* through the action over all cycles in the process, as well as the variance.
* @param alpha0 The lower value for the spring constant.
* @param alpha1 The upper value for the spring constant.
* @param dt The time increment value.
* @param x0 The boundary value of x at t = 0.
* @param xRange The value for which the action is applied if (x0 - xRange) < x < (x0 + xRange).
* @param actionNo The number of times the action is applied.
* @param deltat The number of time increments each cycle is run for.
* @return The average exponentiated value for the difference in work done over all cycles in a
    process, and the variance of these values.
* @throws Exception All arguments except x0 must be greater than 0.
*/
public static double[] averageSimpleActionWithVariance(double alpha0, double alpha1, double
    dt, double x0,double xRange,int actionNo,int deltat)
throws Exception{
if((alpha0<=0)&&(alpha1<=0)&&(dt<=0)&&(actionNo<=0)&&(deltat<=0)){
throw new Exception("All arguments except x0 must be greater than 0.");
}
double x = x0;
int i1 = 0;
while(i1 < deltat){
Random rand = new Random();
x = (1 - alpha0 * dt)*x + (((Math.sqrt(2*alpha0)) * rand.nextGaussian()) * Math.sqrt(dt));
i1++;
}
int i2 = 0;
double eSum = 0;
double evSum = 0;
while(i2<actionNo){
if((x < (x0 + xRange))&&(x > (x0 - xRange))){
double w1 = ((alpha1 - alpha0)*Math.pow(x, 2))/(2*alpha0);
int i3 = 0;
while(i3 < Math.floor(deltat/2)){
Random rand1 = new Random();
x = (1 - alpha1 * dt)*x + (((Math.sqrt(2*alpha0)) * rand1.nextGaussian()) * Math.sqrt(dt));
i3++;
}
double w2 = ((alpha0 - alpha1)*Math.pow(x, 2))/(2*alpha0);
double w = w1 + w2;
double ew = Math.exp(- w);
double e2w = Math.exp(- 2*w);
eSum += ew;
evSum += e2w;
int i4 = (int) Math.floor(deltat/2);
while(i4 < deltat){
Random rand2 = new Random();
x = (1 - alpha0 * dt)*x + (((Math.sqrt(2*alpha0)) * rand2.nextGaussian()) * Math.sqrt(dt));
i4++;
}
}
else{
int i5 = 0;
while(i5 < deltat){
Random rand3 = new Random();
x = (1 - alpha0 * dt)*x + (((Math.sqrt(2*alpha0)) * rand3.nextGaussian()) * Math.sqrt(dt));
i5++;
}
eSum++;
evSum++;
}
i2++;
```

```
}
double averageWork = eSum / actionNo;
double varianceWork = (evSum / actionNo) - Math.pow(averageWork, 2);
double[] averageWithVariance = new double[2];
averageWithVariance[0] = averageWork;
averageWithVariance[1] = varianceWork;
return averageWithVariance;
}
```

The code used to model the Jarzynski-Sagawa-Ueda equality with optimal range in section 3.3 and to model the time dependent case in section 3.4:

```
/**Runs the Langevin update manually with the simple action of periodically checking to see if
    the position
* is within a given range of the boundary value, then changing the spring constant if it is,
    and doing
* nothing if it isn't. Does this with the optimal range calculated
* Calculates the average of the exponentiated difference in work done by the system and work
    done on the system
* through the action over all cycles in the process, as well as the variance.
* @param alpha0 The lower value for the spring constant.
* @param alpha1 The upper value for the spring constant.
* @param dt The time increment value.
* @param x0 The boundary value of x at t = 0.
* @param cycleFraction The fraction which, when multiplied by deltat, gives the number of
    timesteps to go before returning the spring constant to its first value.
* @param actionNo The number of times the action is applied.
* @param deltat The number of time increments each cycle is run for.
* @return The average exponentiated value for the difference in work done over all cycles in a
    process, and the variance of these values.
* @throws Exception All arguments except x0 must be greater than 0.
*/
public static double[] averageOptimalRangeActionWithVariance(double alpha0, double alpha1,
    double dt, double x0,double cycleFraction,int actionNo,int deltat)
throws Exception{
if((alpha0<=0)&&(alpha1<=0)&&(dt<=0)&&(cycleFraction<=0)&&(actionNo<=0)&&(deltat<=0)){
throw new Exception("All arguments except x0 must be greater than 0.");
}
double xRange = Math.sqrt(Math.log(alpha1 / alpha0) / (alpha1 - alpha0));
double x = x0;
int i1 = 0;
while(i1 < deltat){
Random rand = new Random();
x = (1 - alpha0 * dt)*x + (((Math.sqrt(2*alpha0)) * rand.nextGaussian()) * Math.sqrt(dt));
i1++;
}
int i2 = 0;
double eSum = 0;
double evSum = 0;
while(i2<actionNo){
if((x < (x0 + xRange))&&(x > (x0 - xRange))){
double w1 = ((alpha1 - alpha0)*Math.pow(x, 2))/(2*alpha0);
int i3 = 0;
while(i3 < Math.floor(deltat * cycleFraction)){
Random rand1 = new Random();
x = (1 - alpha1 * dt)*x + (((Math.sqrt(2*alpha0)) * rand1.nextGaussian()) * Math.sqrt(dt));
i3++;
}
double w2 = ((alpha0 - alpha1)*Math.pow(x, 2))/(2*alpha0);
double w = w1 + w2;
double ew = Math.exp(- w);
double e2w = Math.exp(- 2*w);
eSum += ew;
```

```
evSum += e2w;
int i4 = (int) Math.floor(deltat * cycleFraction);
while(i4 < deltat){
Random rand2 = new Random();
x = (1 - alpha0 * dt)*x + (((Math.sqrt(2*alpha0)) * rand2.nextGaussian()) * Math.sqrt(dt));
i4++;
}
}
else{
int i5 = 0;
while(i5 < deltat){
Random rand3 = new Random();
x = (1 - alpha0 * dt)*x + (((Math.sqrt(2*alpha0)) * rand3.nextGaussian()) * Math.sqrt(dt));
i5++;
}
eSum++;
evSum++;
}
i2++;
}
double averageWork = eSum / actionNo;
double varianceWork = (evSum / actionNo) - Math.pow(averageWork, 2);
double[] averageWithVariance = new double[2];
averageWithVariance[0] = averageWork;
averageWithVariance[1] = varianceWork;
return averageWithVariance;
}
```

The code used to model the Jarzynski-Sagawa-Ueda equality with error in measurement in section 3.4:

```
/**Runs the Langevin update manually with the simple action of periodically checking to see if
    the position
* is within a given range of the boundary value, then changing the spring constant if it is,
    and doing
* nothing if it isn't. Does this with an error in the measurement. Does this with the optimal
    range calculated
* Calculates the average of the exponentiated difference in work done by the system and work
    done on the system
* through the action over all cycles in the process, as well as the variance.
* @param alpha0 The lower value for the spring constant.
* @param alpha1 The upper value for the spring constant.
* @param error The error associated with the measurement of the position at the start of each
    cycle.
* @param dt The time increment value.
* @param x0 The boundary value of x at t = 0.
* @param cycleFraction The fraction which, when multiplied by deltat, gives the number of
    timesteps to go before returning the spring constant to its first value.
* @param actionNo The number of times the action is applied.
* @param deltat The number of time increments each cycle is run for.
* @return The average exponentiated value for the difference in work done over all cycles in a
    process, and the variance of these values.
* @throws Exception All arguments except x0 must be greater than 0.
*/
public static double[] averageErrorActionWithVariance(double alpha0, double alpha1, double
    error, double dt, double x0,double cycleFraction,int actionNo,int deltat)
throws Exception{
if((alpha0<=0)&&(alpha1<=0)&&(error<0)&&(dt<=0)&&(cycleFraction<=0)&&(actionNo<=0)&&(deltat<=0)){
throw new Exception("All arguments except x0 must be greater than 0.");
}
double xRange = Math.sqrt((Math.log((Math.pow(error,2) + 1) / (Math.pow(error,2) + (alpha0 /
    alpha1)))*(Math.pow(error,2) + 1)*(Math.pow(error,2) + (alpha0 / alpha1))) / (1 - (alpha0
    / alpha1)));
```

```
double x = x0;
int i1 = 0;
while(i1 < deltat){
Random rand = new Random();
x = (1 - alpha0 * dt)*x + (((Math.sqrt(2*alpha0)) * rand.nextGaussian()) * Math.sqrt(dt));
i1++;
}
int i2 = 0;
double eSum = 0;
double evSum = 0;
while(i2<actionNo){
Random masterrand = new Random();
double y = error * masterrand.nextGaussian() + x;
if((y < (x0 + xRange))&&(y > (x0 - xRange))){
double w1 = ((alpha1 - alpha0)*Math.pow(x, 2))/(2*alpha0);
int i3 = 0;
while(i3 < Math.floor(deltat * cycleFraction)){
Random rand1 = new Random();
x = (1 - alpha1 * dt)*x + (((Math.sqrt(2*alpha0)) * rand1.nextGaussian()) * Math.sqrt(dt));
i3++;
}
double w2 = ((alpha0 - alpha1)*Math.pow(x, 2))/(2*alpha0);
double w = w1 + w2;
double ew = Math.exp(- w);
double e2w = Math.exp(- 2*w);
eSum += ew;
evSum += e2w;
int i4 = (int) Math.floor(deltat * cycleFraction);
while(i4 < deltat){
Random rand2 = new Random();
x = (1 - alpha0 * dt)*x + (((Math.sqrt(2*alpha0)) * rand2.nextGaussian()) * Math.sqrt(dt));
i4++;
}
}
else{
int i5 = 0;
while(i5 < deltat){
Random rand3 = new Random();
x = (1 - alpha0 * dt)*x + (((Math.sqrt(2*alpha0)) * rand3.nextGaussian()) * Math.sqrt(dt));
i5++;
}
eSum++;
evSum++;
}
i2++;
}
double averageWork = eSum / actionNo;
double varianceWork = (evSum / actionNo) - Math.pow(averageWork, 2);
double[] averageWithVariance = new double[2];
averageWithVariance[0] = averageWork;
averageWithVariance[1] = varianceWork;
return averageWithVariance;
}
```

The code used to model the Jarzynski-Sagawa-Ueda equality with the optimal change in spring constant in section 3.5:

```
/**Runs the Langevin update manually with the optimal action of periodically checking to see
    if the position
* is within a given range of the boundary value, then increasing the spring constant if it is,
    or to if the
* position is outside another given range of the boundary value, then decreasing the spring
    constant, and doing
```

```
* nothing if neither of those are true. Does this with the optimal ranges calculated.
* Calculates the average of the exponentiated difference in work done by the system and work
    done on the system
* through the action over all cycles in the process, as well as the variance.
* @param alpha0 The starting value for the spring constant.
* @param alphaU The upper value for the spring constant.
* @param alphaL The lower value for the spring constant.
* @param dt The time increment value.
* @param x0 The boundary value of x at t = 0.
* @param cycleFraction The fraction which, when multiplied by deltat, gives the number of
    timesteps to go before returning the spring constant to its first value.
* @param actionNo The number of times the action is applied.
* @param deltat The number of time increments each cycle is run for.
* @return The average exponentiated value for the difference in work done over all cycles in a
    process, and the variance of these values.
* @throws Exception All arguments except x0 must be greater than 0.
*/
public static double[] optimalActionWithVariance(double alpha0, double alphaL, double alphaU,
    double dt, double x0,double cycleFraction,int actionNo,int deltat)
throws Exception{
if((alpha0<=0)&&(alphaL<=0)&&(alphaU<=0)&&(dt<=0)&&(cycleFraction<=0)&&(actionNo<=0)&&(deltat<=0)){
throw new Exception("All arguments except x0 must be greater than 0.");
}
double xRangeI = Math.sqrt(Math.log(alphaU / alpha0) / (alphaU - alpha0));
double xRange0 = Math.sqrt(Math.log(alpha0 / alphaL) / (alpha0 - alphaL));
double x = x0;
int i1 = 0;
while(i1 < deltat){
Random rand = new Random();
x = (1 - alpha0 * dt)*x + (((Math.sqrt(2*alpha0)) * rand.nextGaussian()) * Math.sqrt(dt));
i1++;
}
int i2 = 0;
double eSum = 0;
double evSum = 0;
while(i2<actionNo){
if((x < (x0 + xRangeI))&&(x > (x0 - xRangeI))){
double w1 = ((alphaU - alpha0)*Math.pow(x, 2))/(2*alpha0);
int i3 = 0;
while(i3 < Math.floor(deltat * cycleFraction)){
Random rand1 = new Random();
x = (1 - alphaU * dt)*x + (((Math.sqrt(2*alpha0)) * rand1.nextGaussian()) * Math.sqrt(dt));
i3++;
}
double w2 = ((alpha0 - alphaU)*Math.pow(x, 2))/(2*alpha0);
double w = w1 + w2;
double ew = Math.exp(- w);
double e2w = Math.exp(- 2*w);
eSum += ew;
evSum += e2w;
int i4 = (int) Math.floor(deltat * cycleFraction);
while(i4 < deltat){
Random rand2 = new Random();
x = (1 - alpha0 * dt)*x + (((Math.sqrt(2*alpha0)) * rand2.nextGaussian()) * Math.sqrt(dt));
i4++;
}
}
else if((x > (x0 + xRange0))||(x < (x0 - xRange0))){
double w1 = ((alphaL - alpha0)*Math.pow(x, 2))/(2*alpha0);
int i5 = 0;
while(i5 < Math.floor(deltat * cycleFraction)){
Random rand3 = new Random();
x = (1 - alphaL * dt)*x + (((Math.sqrt(2*alpha0)) * rand3.nextGaussian()) * Math.sqrt(dt));
```

```
i5++;
}
double w2 = ((alpha0 - alphaL)*Math.pow(x, 2))/(2*alpha0);
double w = w1 + w2;
double ew = Math.exp(- w);
double e2w = Math.exp(- 2*w);
eSum += ew;
evSum += e2w;
int i6 = (int) Math.floor(deltat * cycleFraction);
while(i6 < deltat){
Random rand4 = new Random();
x = (1 - alpha0 * dt)*x + (((Math.sqrt(2*alpha0)) * rand4.nextGaussian()) * Math.sqrt(dt));
i6++;
}
}
else {
int i7 = 0;
while(i7 < deltat){
Random rand5 = new Random();
x = (1 - alpha0 * dt)*x + (((Math.sqrt(2*alpha0)) * rand5.nextGaussian()) * Math.sqrt(dt));
i7++;
}
eSum++;
evSum++;
}
i2++;
}
double averageWork = eSum / actionNo;
double varianceWork = (evSum / actionNo) - Math.pow(averageWork, 2);
double[] averageWithVariance = new double[2];
averageWithVariance[0] = averageWork;
averageWithVariance[1] = varianceWork;
return averageWithVariance;
}
```

The code used to model the Jarzynski-Tsallis equality in section 4.2:

```
/**Runs the non-isothermal Langevin update manually with the simple action of periodically
    changing the spring constant.
* Calculates the average of the Tsallis q-exponentiated difference in work done by the system
    and work done on the system
* through the action over all cycles in the process, as well as the variance.
* Does this manually in an effort to make the process more efficient and quicker.
* @param alpha0 The lower value for the spring constant.
* @param alpha1 The upper value for the spring constant.
* @param alphaT The constant spring constant parameter for the Tsallis q-exponential.
* @param dt The time increment value.
* @param x0 The boundary value of x at t = 0.
* @param actionNo The number of times the action is applied.
* @param deltat The number of time increments each cycle is run for.
* @return The average exponentiated value for the difference in work done over all cycles in a
    process, and the variance of these values.
* @throws Exception All arguments except x0 must be greater than 0.
*/
public static double[] averageAlwaysTsallisActionWithVariance(double alpha0, double alpha1,
    double alphaT, double dt, double x0,int actionNo,int deltat)
throws Exception{
if((alpha0<=0)&&(alpha1<=0)&&(alphaT<=0)&&(dt<=0)&&(actionNo<=0)&&(deltat<=0)){
throw new Exception("All arguments except x0 must be greater than 0.");
}
double x = x0;
int i1 = 0;
double q1 = 1 + (alphaT / (alpha1 - alpha0));
```

```
double q2 = 1 - (alphaT / (alpha1 - alpha0));
while(i1 < deltat){
Random rand = new Random();
x = (1 - alpha0 * dt)*x + (((Math.sqrt(2*alpha0 + alphaT*Math.pow(x,2))) *
    rand.nextGaussian()) * Math.sqrt(dt));
i1++;
}
int i2 = 0;
double eSum = 0;
double evSum = 0;
while(i2<actionNo){
double w1 = ((alpha1 - alpha0)*Math.pow(x, 2))/(2*alpha0);
double expq1 = Math.pow((1 + (1 - q1)*(- w1)),(1 / (1 - q1)));
int i3 = 0;
while(i3 < Math.floor(deltat/2)){
Random rand1 = new Random();
x = (1 - alpha1 * dt)*x + (((Math.sqrt(2*alpha0 + alphaT*Math.pow(x,2))) *
    rand1.nextGaussian()) * Math.sqrt(dt));
i3++;
}
double w2 = ((alpha0 - alpha1)*Math.pow(x, 2))/(2*alpha0);
double expq2 = Math.pow((1 + (1 - q2)*(- w2)),(1 / (1 - q2)));
double ew = expq1 * expq2;
double e2w = Math.pow(ew, 2);
eSum += ew;
evSum += e2w;
int i4 = (int) Math.floor(deltat/2);
while(i4 < deltat){
Random rand2 = new Random();
x = (1 - alpha0 * dt)*x + (((Math.sqrt(2*alpha0 + alphaT*Math.pow(x,2))) *
    rand2.nextGaussian()) * Math.sqrt(dt));
i4++;
}
i2++;
}
double averageWork = eSum / actionNo;
double varianceWork = (evSum / actionNo) - Math.pow(averageWork, 2);
double[] averageWithVariance = new double[2];
averageWithVariance[0] = averageWork;
averageWithVariance[1] = varianceWork;
return averageWithVariance;
}
```

The code used to model the position distribution in section 4.3:

```
/** A class to perform the non-isothermal langevin update for a set number of repeats,
* and then store the final position values in an ArrayList.
* @param alpha The spring constant value for the update.
* @param alphaT The parameter for the Tsallis statistics.
* @param dt The timestep value.
* @param x0 The initial position value.
* @param deltat The number of timesteps for the process.
* @param sample The number of repeats for the process.
* @return An ArrayList of final position values.
* @throws Exception All arguments except x0 must be greater than 0.
*/
public static ArrayList<Double> tsallisStatisticsTest(double alpha, double alphaT, double dt,
    double x0, int deltat, int sample)
throws Exception{
if((alpha<=0)&&(alphaT<=0)&&(dt<=0)&&(deltat<=0)&&(sample<=0)){
throw new Exception("All arguments except x0 must be greater than 0.");
}
ArrayList<Double> list = new ArrayList<Double>();
```

```
int i1 = 0;
while(i1 < sample){
double x = x0;
int i2 = 0;
while(i2 < deltat){
Random rand = new Random();
x = (1 - alpha * dt)*x + (((Math.sqrt(2*alpha + alphaT*Math.pow(x,2))) * rand.nextGaussian())
    * Math.sqrt(dt));
i2++;
}
list.add(x);
i1++;
}
return list;
}
```

The code used to model the work distributions in section 4.3:

```
/**Performs the non-isothermal langevin update at the lower spring constant value, and repeats
    this for a specified sample.
* Calculates the work values for a step up at the end of each sample and stores them in an
    ArrayList.
* @param alpha0 The lower spring constant value.
* @param alpha1 The higher spring constant value.
* @param alphaT The parameter for the Tsallis statistics.
* @param dt The timestep value.
* @param x0 The initial position value.
* @param deltat The number of timesteps in a cycle.
* @param actionNo The number of cycles in a process.
* @return An ArrayList of the work values from sample of updates.
* @throws Exception All arguments except x0 must be greater than 0.
*/
public static ArrayList<Double> stepUpWorkList(double alpha0, double alpha1, double alphaT,
    double dt, double x0, int deltat, int sample)
throws Exception{
if((alpha0<=0)&&(alpha1<=0)&&(alphaT<=0)&&(dt<=0)&&(deltat<=0)&&(sample<=0)){
throw new Exception("All arguments except x0 must be greater than 0.");
}
ArrayList<Double> list = new ArrayList<Double>();
int i1 = 0;
while(i1 < sample){
double x = x0;
int i2 = 0;
while(i2 < deltat){
Random rand = new Random();
x = (1 - alpha0 * dt)*x + (((Math.sqrt(2*alpha0 + alphaT*Math.pow(x,2))) *
    rand.nextGaussian()) * Math.sqrt(dt));
i2++;
}
double w = ((alpha1 - alpha0)*Math.pow(x, 2))/(2*alpha0);
list.add(w);
i1++;
}
return list;
}


/**Performs the non-isothermal langevin update at the higher spring constant, and repeats this
    for a specified sample.
* Calculates the work values for a step down at the end of each sample and stores them in an
    ArrayList.
* @param alpha0 The lower spring constant value.
* @param alpha1 The higher spring constant value.
```

```
* @param alphaT The parameter for the Tsallis statistics.
* @param dt The timestep value.
* @param x0 The initial position value.
* @param deltat The number of timesteps in a cycle.
* @param actionNo The number of cycles in a process.
* @return An ArrayList of the work values from sample of updates.
* @throws Exception All arguments except x0 must be greater than 0.
*/
public static ArrayList<Double> stepDownWorkList(double alpha0, double alpha1, double alphaT,
    double dt, double x0, int deltat, int sample)
throws Exception{
if((alpha0<=0)&&(alpha1<=0)&&(alphaT<=0)&&(dt<=0)&&(deltat<=0)&&(sample<=0)){
throw new Exception("All arguments except x0 must be greater than 0.");
}
ArrayList<Double> list = new ArrayList<Double>();
int i1 = 0;
while(i1 < sample){
double x = x0;
int i2 = 0;
while(i2 < deltat){
Random rand = new Random();
x = (1 - alpha1 * dt)*x + (((Math.sqrt(2*alpha0 + alphaT*Math.pow(x,2))) *
    rand.nextGaussian()) * Math.sqrt(dt));
i2++;
}
double w = ((alpha0 - alpha1)*Math.pow(x, 2))/(2*alpha0);
list.add(w);
i1++;
}
return list;
}
```